Queensland Government
Department of Natural Resources and Mines
Department of Emergency Services
Environmental Protection Agency

Queensland Climate Change and Community Vulnerability to Tropical Cyclones

OCEAN HAZARDS ASSESSMENT - Stage 2

Report

July 2004

Tropical Cyclone-Induced Water Levels and Waves: Hervey Bay and Sunshine Coast

Australian Government
Department of Transport and Regional Services

Australian Government
Bureau of Meteorology

SEA Systems Engineering Australia Pty Ltd
Numerical Modelling and Risk Assessment

In association with:

JCU James Cook University
Marine Modelling Unit

Queensland Climate Change and Community Vulnerability to Tropical Cyclones: Ocean Hazards Assessment

Stage 2

Tropical Cyclone-Induced Water Levels and Waves: Hervey Bay and Sunshine Coast

Professor Tom Hardy
Mr Luciano Mason
Mr Ashley Astorquia

Marine Modelling Unit
School of Engineering
James Cook University

Dr Bruce Harper

Systems Engineering Australia Pty Ltd
7 Mercury Court
Bridgeman Downs Q 4035

16 August 2004

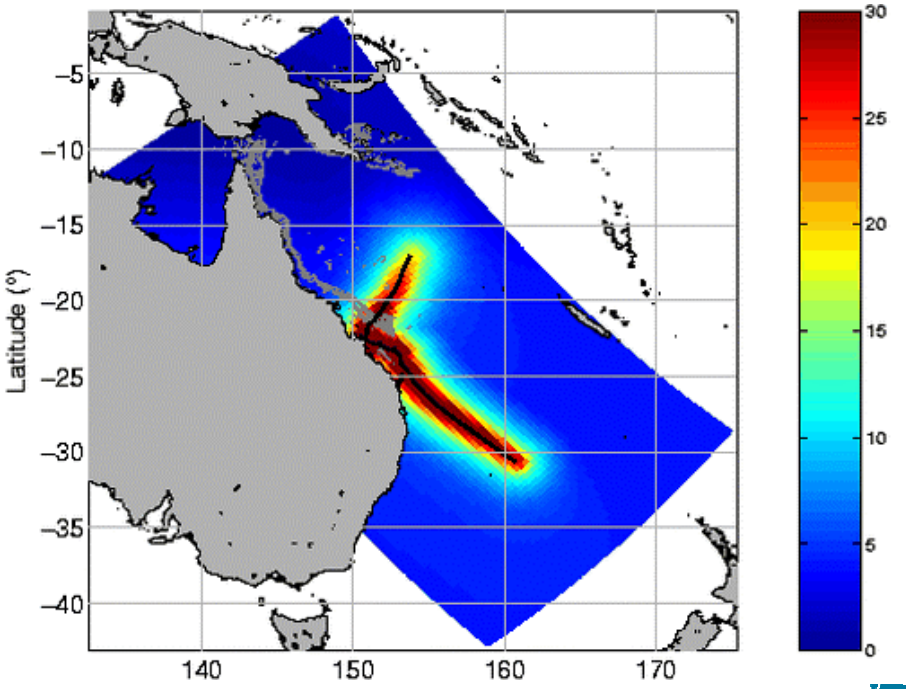

TABLE OF CONTENTS

EXECUTIVE SUMMARY

The frequencies of storm tide and waves during tropical cyclones were determined for the Hervey Bay and Sunshine Coast regions of southeast Queensland, Australia. The goal was to produce return period curves for storm tide (storm surge plus wave setup plus astronomical tide) and for significant wave height for return periods between 10 and 1000 years.

A series of sophisticated models was employed. First a tropical cyclone track and pressure model produced a synthetic dataset consisting of the time series of position and pressure for almost 10,000 storms. This represents 3000 years of data for the western Coral Sea. Numerical models with three nested grids with increasing spatial resolution for both storm surge and wave generation were established for the study areas. The storm surge model had been validated in Phase 1 of this overall study. The wave model was validated by comparing measurements and modelled significant wave heights during *T. C. Simon* (1980). It was computationally impossible to model all 10,000 storms to the needed resolution; therefore, a system was developed to determine which storms would contribute to returns periods above 10 years. This reduced the number of storms to be modelled from 10,000 to about 500 for each of the two study areas.

Wave setup was calculated as a function of wave height and peak wave period using an empirical formula. Wave setup is the most uncertain of all the components since the surf zone width during a severe tropical cyclone would be very much wider than those used to derive the empirical wave setup formula. Although all other components of this study received state-of-the-art treatment it was infeasible to do this for the wave setup. At locations such as the Sunshine Coast where wave setup is more important that storm surge, developing state-of-the-art wave setup calculations has much more importance than at Hervey Bay where storm surge is the dominant component.

It is important to note that water levels created by wave setup will not translate far inland after overtopping frontal dunes, flowing overland over low lying areas, or proceeding through inlets. Once flow starts wave setup reduces markedly; therefore, the storm tide curves that include wave setup should apply only to areas with direct wave attack. For areas more than a couple hundred metres landward of the shoreline during the storm, a better estimate of potential flood levels is obtained from the storm surge plus tide return period curves. An overland flooding study might be necessary to provide definitive results for inland locations, especially if the inland floodable area is large.

An astronomical tidal signal was created using tidal analyses. Each coupled set of storm surge and wave setup time series from a single storm were linearly added to 500 separate tidal time series. The tide series were randomly chosen (with a weighting to reflect the monthly change in cyclone frequency) from a long tidal record. The maximum water level and significant wave height during each storm-tide event were determined and these values were ranked by magnitude and return period curves were created.

Establishing a datum and a tidal range at the project output points caused considerable difficulty. Most of the output points were not at established tidal measurement stations. The elevations of the modelled storm tide time series were assigned relative to the official MSL and then the official MSL to AHD correction was used to transfer the results to AHD.

In general storm surge is much more important in Hervey Bay with its broader continental shelf and protection by Fraser Island from severe wave directions. In Hervey Bay storm surge is up to twice the magnitude of wave setup at the 100 year level. For the Sunshine Coast with its narrower and more open shelf, wave setup is more important than storm surge. Wave setup is more than twice the magnitude of storm surge at the 100 year level.

The effect of greenhouse-induced climate change was investigated. Three separate scenarios were tested. These were (A) combined effect of an increase in maximum intensity (MPI) of

10% and a poleward shift in tracks of 1.3°. (B) increase in frequency of tropical cyclones by 10%. (C) mean sea level rise of 300 mm. In general the mean sea level rise is the most important effect especially at lower return periods. The 10% increase in tropical cyclone frequency is insignificant. The combined increase in intensity and poleward shift in tracks becomes increasingly significant with larger return periods. This is more evident in Hervey Bay where storm surge is more important than at Sunshine Coast where depth limitation reduces the effect of increased wave setup. Both the magnitude and probability of greenhouse-induced mean sea level rise are more certain than greenhouse-induced changes in tropical cyclone frequency, central pressure, or track.

Note that the results in this study are for tropical cyclone-induced water levels. For return periods below about 100 years, extra tropical events will be increasingly important; therefore, the combined curve of tropical and extra-tropical storm tides will be higher than the cyclone-induced storm tide curves shown in this report.

There are several different non-cyclonic influences that affect water levels that are not considered in this study. These include not only non-cyclonic winds, low pressures and waves during storms, but non-storm events such as changes in oceanic currents and continental shelf waves which can also alter water levels.

For all project reporting locations, the occurrence of a tropical cyclone was defined as any that occurred in the western Coral Sea regardless of its distance from the location. This has the property of merging the return period curve for tropical cyclone-induced storm tide into the return period curve for astronomical tide at the lower end of the curves. This definition was used to avoid any misinterpretation of the frequency of water levels at return periods that may be dominated by non-cyclonic events.

A caution is necessary on the possibility of water levels much higher than the 1000 year levels that are presented in this report. The occurrence of the probable maximum water level could have devastating consequences for a nearby community. Although the probability of occurrence is very rare, a calculation of the risk (probability times consequences) is an important component of both disaster and longer term land use planning.

The probable maximum water level at a given location would be caused by a tropical cyclone and tide with the following characteristics. (1) landfall point at a distance equal to the radius of maximum winds to the north, (2) very severe central pressure, (3) large radius to maximum winds, (4) forward speed of the eye equal to the short wave speed offshore and the long wave speed over the shelf, and very importantly, (5) an astronomic tide level that is close to HAT at the time of maximum surge plus wave setup. The combination of these characteristics would be very rare, but not impossible.

An estimate of the probable maximum level could be calculated by adding the largest storm surge and wave setup from the 3000 years of simulations to the HAT level. For example, this would result in a storm tide of about 4.1 m (AHD) at Coolum, Sunshine Coast (see Figure 17) and 6.7 m (AHD) at Torquay, Hervey Bay (see Figure 18). These are approximately 1 and 2 m, respectively above the 1000 year water levels. It must be emphasised that these probable maximum figures are only a rough estimate. The 3000 year storm surges and wave setups are not necessarily the largest possible (i.e. they don't meet the first four of the above criteria).

Wave information at near coastal and offshore sites was generated in both study areas. Sheltering from southeasterly wave directions by large Islands to the south of Hervey Bay and Sunshine Coast (Fraser Island and Moreton Island, respectively) was evident at all near coastal sites. The offshore Hervey Bay location, had the widest spread of directions and the largest significant wave heights at the 500 year level (16.5 m) as compared with the Sunshine Coast (14 to 15 m). The more northerly position and the more northerly aspect of Hervey Bay is thought to allow larger waves from more frequent and more severe tropical cyclones.

1.0 INTRODUCTION

This study was commissioned by the Queensland Environmental Protection Agency (EPA) through the Natural Disasters Risk Management Studies Program (NDRMSP) with support from the Commonwealth Bureau of Meteorology (BoM) and the Greenhouse Special Treasury Initiative. The *Marine Modelling Unit* (*MMU*) of the School of Engineering at James Cook University working through the *Cooperative Research Centre for the Great Barrier Reef World Heritage Area* (*CRC Reef*) was commissioned to provide storm tide and wave statistics during tropical cyclones for two regions of the Queensland eastern coast: Hervey Bay and the Sunshine Coast (Figures 1 and 2). The impact of possible greenhouse climate change was to be assessed.

This study is Stage 2 of the *Queensland Climate Change and Community Vulnerability to Tropical Cyclones* project. Stage 1 was reported in Harper *et al.* (2001).

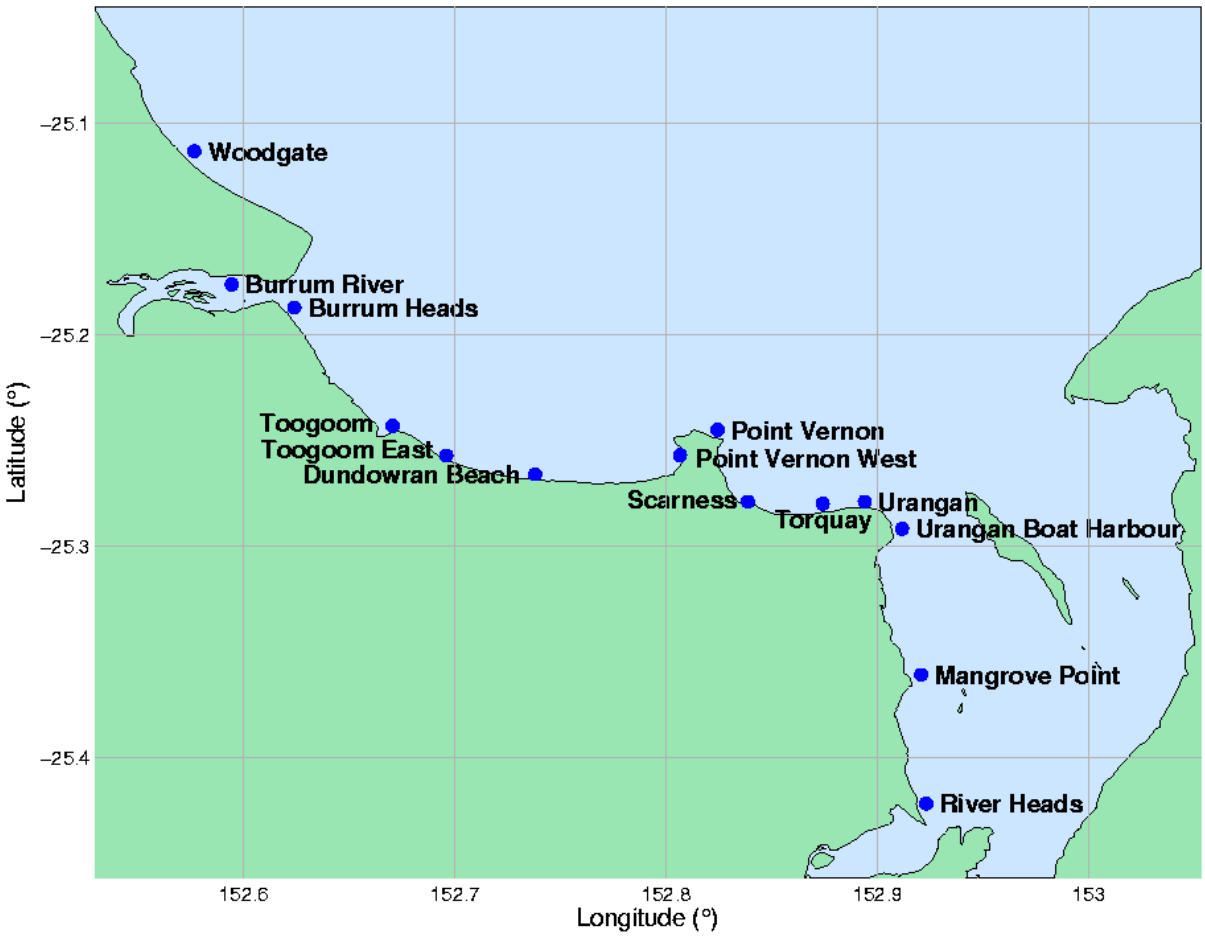

Figure 1. Hervey Bay study area and water level reporting locations

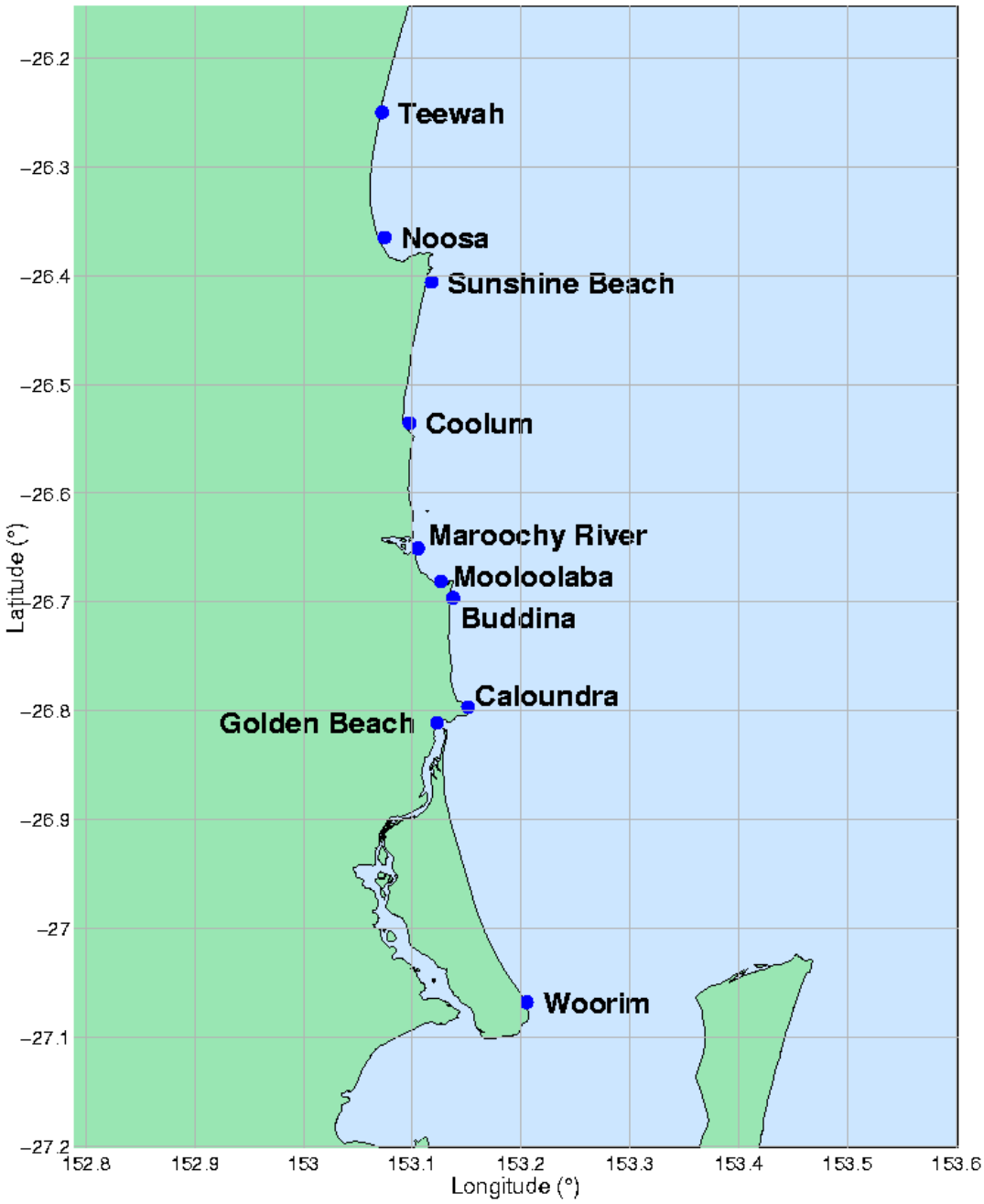

Figure 2. Sunshine Coast study area and water level reporting locations

1.1 Scope

The original scope derived from Harper et al. (2001) envisaged that parametric models of storm surge and wave setup developed by *BoM* and *SEA/MMU*, respectively would be used to develop the storm tide and wave statistics. However several developments required rethinking of the original proposal. The most important of these was a ten-fold increase in computational capability available to the *MMU* through upgrades to the JCU super computer. This increase in computing capability allowed the use of the numerical models *MMUSURGE* and *WAMGBR* in the direct simulation of the very large number of storms necessary to create the storm tide data necessary for the creation of return period and encounter probability curves. This is in contrast to the original proposal, which would have used these two more expensive primitive equation models only to create the cheaper-to-use parametric models. Nevertheless, the development of the parametric wave model was completed in order to provide *BoM* with

an economical and user-friendly means of forecasting waves during the approach of a tropical cyclone to the Queensland coast.

The scope of the project is as follows:

Wave Model Development:

1. An existing nested grid system (Hardy *et al.* 2003) for the wave model, *WAMGBR*, *(Hardy* et al. 2000) was adapted for the project. A single coarse resolution grid (*A* grid) was extended to the south by 5°. Two additional intermediate resolution grids (*B* grids) were established to provide boundary conditions for two additional fine resolution grids (*C* grids) that cover the study regions.
2. The implementation of *WAMGBR* was validated by simulating one historical cyclone. Model simulation was compared to buoy data.

Wave Parametric Model

3. An ensemble of more than 100 storms was chosen to represent the range of tropical cyclones that affect the region. In order to keep the number of simulated storms to a reasonable level, the parameters of the storms (central pressure, radius to maximum winds, forward speed, track angle, etc.) were held constant throughout the life of the storm.
4. The ensemble was simulated using *WAMGBR* on the nested numerical grid system.
5. The results of these simulations were used to develop a parametric model that creates time histories of H_s and T_p given inputs of cyclone parameters.

Storm Tide and Wave Simulations

6. A very large ensemble of synthetic tropical cyclones was created using the *MMU* track and pressure model, *CycSyn*, (James and Mason, 1999). This ensemble represents 3000 years of storms. The goal was to accurately define the 1000 year return periods.
7. This ensemble was simulated by *MMUSURGE* and *WAMGBR*.
8. Wave setup was included using the empirical technique recommended in Stage 1 (Harper *et al.* 2001) of this study (eqn. 8.19, p. 138).
9. The storm surge and wave setup time series were linearly combined with a large number of possible astronomical tides to create a very large set of storm tide events for each study area.
10. The final results are statistics (return period) of storm tide and waves (significant wave height) at open coast locations (i.e. overland flooding was not to be considered). Statistics for at most six points were generated for each study area.

Greenhouse Effects

11. The effects of greenhouse-induced sea level rise, as well as changes in the frequency and intensity of tropical cyclones were incorporated by either post-processing the simulation results or a re-simulation (at most one) of the ensemble.

2.0 PARAMETRIC MODEL OF WAVES DURING TROPICAL CYCLONES

The report on the parametric wave model is attached as Appendix G. As the speed of computers has increased over the last few years, the need for the use of expensive super computing capability for the numerical modelling of storm surge has diminished. It is now possible to economically run state-of-the-art storm surge models using affordable personal computers. However modelling waves is at least two orders of magnitude more computationally expensive. In other words, modelling the waves during a single storm requires about the same computational effort as modelling storm surges from 100 storms. Thus, for regions where wave setup is important, the parametric wave model will have good utility in the forecasting of wave setup during the assessment of emergency response during the approach of a tropical cyclone.

3.0 FREQUENCY OF TROPICAL CYCLONE STORM SURGE AND WAVES

Our goal is to provide a good estimate of the 500-year return period and a reasonable estimate of the 1000-year level, so an ensemble representing 3000 years was modelled. The results can be thought of as 1, 3 and 6 samples of the infinite number of possible 3000, 1000 and 500 year lengths of record. Since lower return periods are increasingly dominated by non-cyclonic events, the goal is to determine which tropical cyclones will contribute wave heights and storm tides greater than the 10-year level and to simulate only those storms.

The results of this modelling will be presented in terms of return period curves for the maximum storm tide and the maximum significant wave height that occur during a tropical cyclone. The return periods, R_η and R_H, of the *maximum* water level and *maximum* significant wave height that occur during a single storm are given as the inverse of the rates of occurrence, λ_η and λ_H, of water levels and wave heights that are *equal to or greater than* that given magnitude (η and H_s), or

$$\begin{aligned} R_\eta &= \frac{1}{\lambda_\eta} \\ R_H &= \frac{1}{\lambda_H} \end{aligned} \quad . \tag{1}$$

The values of the rates of occurrence, λ_η and λ_H, are determined by ranking the values of water level and wave height from largest to smallest over a known period of time and then dividing by the length of that time period. This is given by

$$\begin{aligned} \lambda_\eta &= \frac{m_\eta}{n} \\ \lambda_H &= \frac{m_H}{n} \end{aligned} \quad , \tag{2}$$

where m_η and m_H are the rank of the water level and wave height, respectively and n is the number of years of record. For example, if a simulated cyclone has a maximum water level of 3.2 m and this is the 6th largest in 3000 years of simulated record then the frequency of occurrence and return period of a water level equal to 3.2 m would be

$$\lambda_{\eta=3.2} = \frac{6}{3000} = 0.002$$
$$R_{\eta=3.2} = \frac{1}{0.002} = 500 \text{ years} \quad . \tag{3}$$

4.0 PRESENTATION OF THE MODELLING SYSTEMS

4.1 Synthetic Tropical Cyclone Track and Pressure Model – *CycSyn*

The availability of data for Coral Sea tropical cyclones is discussed in the Stage 1 report (Harper et al., 2001) and by Holland (1981). Although some satellite data is available from 1960, the record is not complete until 1969 when increased satellite coverage and improved analysis techniques began to provide a complete record of track position and central pressure. The creation of the synthetic database used in this project requires a complete data set. A complete and reliable set of historical data on the tracks and intensities of tropical cyclones affecting the western Coral Sea is limited to the relatively small number (approximately 108 which have occurred (1969-2001). The data are available from the BoM web site, ftp://ftp.bom.gov.au .

If just these tropical cyclones were modelled, this sample would give only one of an infinite number of possible renditions of 33 years of water levels and waves during tropical cyclones. This short record is much too small to define the 500 year or even the 100 year return period values. To overcome this lack of data, a model (*CycSyn*) capable of simulating synthetic time histories of tracks and central pressures of tropical cyclones in the Coral Sea was developed. Full details of the model are contained in James and Mason (1999 and submitted). A very brief description of the model is as follows.

Cyclone position and central pressure are determined by an autoregressive model that determines the change of longitude, latitude and central pressure based on the changes at the preceding time step. The model coefficients are estimated by multiple linear regression of historical cyclone data for a chosen sub-region of the Coral Sea.

Each simulation of a synthetic cyclone required initial values of position and pressure. Historical starting values could be used to generate a large number of synthetic tracks, but the small number of historical starting positions could bias these tracks. Therefore initial values were randomly selected from a six-dimensional data space based on the data set of historical initial values of each of the six parameters.

The box in Figure 3 indicates the boundary of data zone for both initial values and model coefficients. This region was selected, as opposed to the whole of the Coral Sea, since we desired the population of tropical cyclones that threatens the east coast of Queensland and storms that do not cross into this region pose little threat.

Radius of maximum winds is an important parameter for wave generation since larger radii increase both the available wind energy and the effective fetch over which the waves are generated. Almost no radius to maximum winds data are available for Coral Sea tropical cyclones and time series data are rare in other regions; therefore, an autoregressive model such as that described above for position and central pressure cannot be developed and an alternative procedure was necessary (Hardy *et al.* 2003).

The time histories of position (latitude, ϕ and longitude, λ), central pressure, p_o, and radius to maximum winds, R_m, were created for a 3000 year long record of cyclones or 9818 synthetic tropical cyclones. The statistics of this synthetic ensemble compares well with those of the measured data as is shown in Figure 4. In this figure the historical data fall within the 90% confidence limits about the model results obtained by applying a bootstrap technique (Efron, 1979) to the synthetic data.

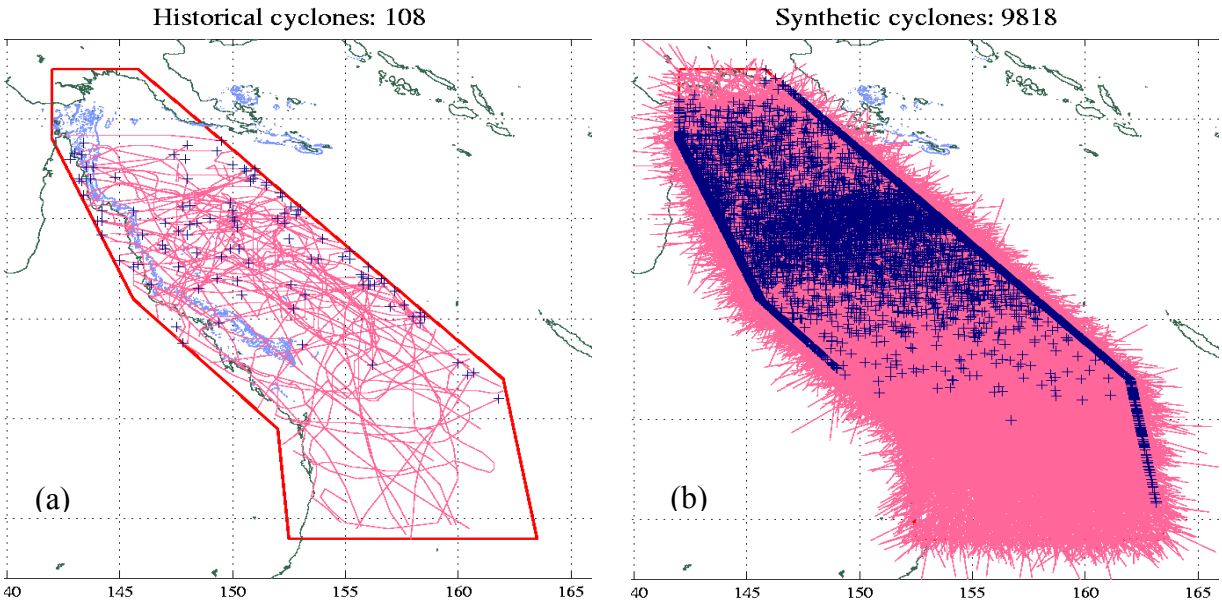

Figure 3. 3000 years of synthetic tropical cyclones tracks. (a) contains 108 historical tracks (1969-2002). (b) contains 9818 tracks (3000 year simulation). Dark blue crosses indicate starting positions. Light blue area in (a) is the Great Barrier Reef.

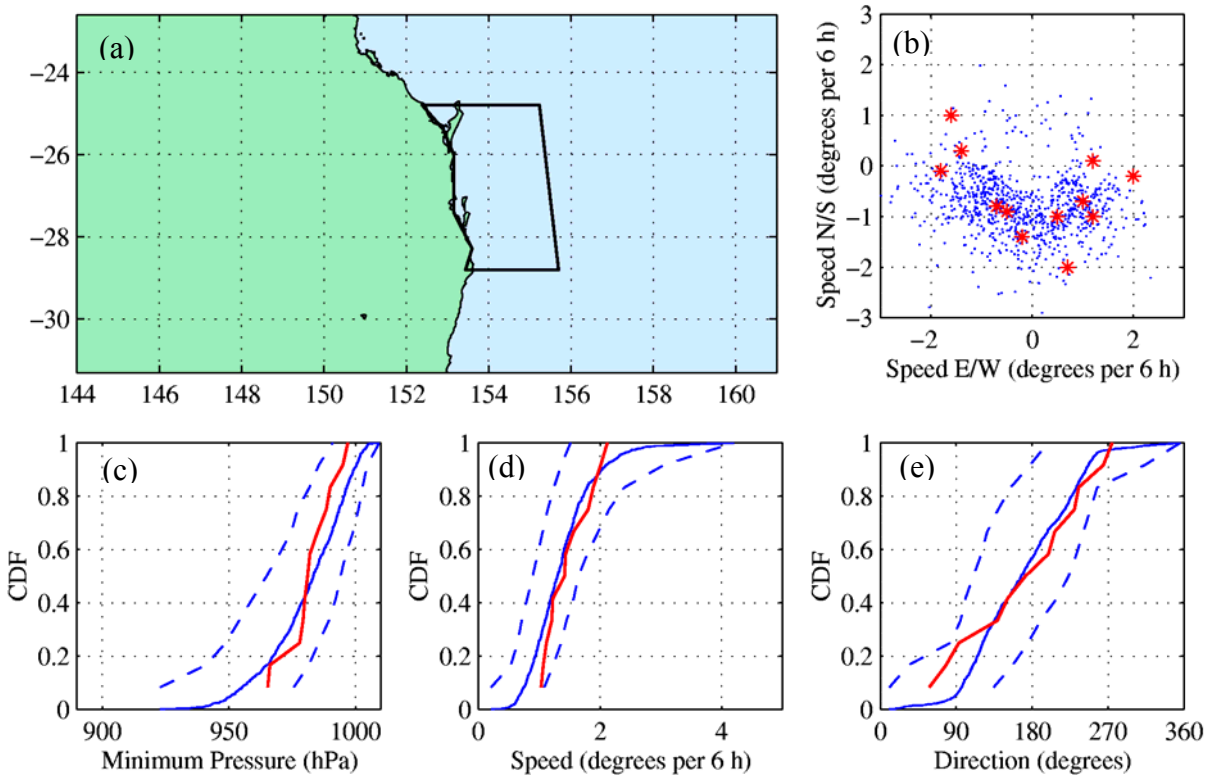

Figure 4. Statistical comparison between synthetic and measured data inside box in (a). Measurements are shown by * and numerical data by • in (b). The lines in (c), (d) and (e) are — historical data; — synthetic data; and - - 90% confidence limits about synthetic data.

4.2 Tropical Cyclone Windfield Model for the Coral Sea - *CycWind*

The *MMU* has developed a parametric model of the wind fields during tropical cyclones in the Coral Sea region. This model named *CycWind* is fully described in McConochie *et al.* (1999, in press). *CycWind* is based on the parametric model introduced by Holland (1980).

A secondary vortex is included in *CycWind*, following the work of Thompson and Cardone (1996). Willoughby *et al*. (1982) discussed the occurrence of multiple concentric eyewalls in tropical storms, typhoons and super typhoons for the western Pacific region. They found that the presence of two concentric eyewalls was a common occurrence in intense symmetric storms. The secondary eyewall has also been found in Coral Sea tropical cyclones such as *Justin*, (Callaghan, personal communication) and *Althea* (Callaghan, 1996). Although a second eyewall does not always occur in Coral Sea cyclones, tropical cyclones in this region are almost always embedded in the monsoon trough. Hence use of a secondary eyewall formulation, which creates an outer extended region of lower pressure, can also be used to represent the effect of the trough. The effect of the second eyewall is to reduce the wind speed in the vicinity of the primary eyewall and to increase it at distances greater than about three times the radius to maximum winds.

Full description of the wind field model is beyond the scope of this report and can be obtained from McConochie *et al.* (1999, in press). In brief, the wind field (speed and direction as a function of time and space) is determined as a function of nine parameters

$$\{\Delta p_1, \Delta p_2, R_{m1}, R_{m2}, B_1, B_2, K_m, U_s, \theta_s\}$$

for which the subscripts 1 and 2 indicate the primary and secondary vortices, respectively; Δp_i is the portion of the pressure deficit assigned to the vortex, R_{mi} is the radius to maximum winds of the vortex, B_i is a peakedness parameter that affects the shape of a special cross section of the wind profile, K_m converts the gradient winds to a 10 m elevation, U_s and θ_s are the speed and direction of the synoptic winds (see below).

For this study

$$\Delta p = p_\infty - p_o = \Delta p_1 + \Delta p_2 , \tag{4}$$

where p_o, the central pressure of the storm, is obtained from *CycSyn*, $p_\infty = 1010$ hPa is the ambient pressure.

Extensive testing (McConochie *et al.,* 1999, in press) has found that Coral Sea tropical cyclones are well represented by values of pressure deficit and radius for the secondary vortex of

$$\Delta p_2 = 8 + \frac{1}{20}(\Delta p - 8) \text{ hPa}, \tag{5}$$

$$R_{m2} = 250 \text{ km}. \tag{6}$$

Finally, the peakedness parameters were given values of

$$B_1 = 7.3 - \frac{p_o}{160}$$
$$B_2 = 7.2 - \frac{p_o}{160} \quad . \tag{7}$$

For example, if p_0 = 950 hPa (representative of the severest storm in the measurements in this region), then Δp = 60 hPa, Δp_2 = 10.6 hPa, B_1 = 1.3625 and B_2 = 1.2625.

The extended pressure field as described by Cardone et al. (1994) is calculated using

$$p = p_0 + \sum_{i=1}^{2} \Delta p_i \, e^{-(R_{mi}/r)^{B_i}}$$
$$\sum_{i=1}^{2} \Delta p_i = p_\infty - p_0 \quad , \tag{8}$$

where p is the pressure at radial distance r.

The gradient wind speed, V_{gc}, due to the cyclone, which is a balance between the pressure gradient force, the Coriolis force , f, and the centrifugal force, is calculated using

$$V_g = \sqrt{\sum_{i=1}^{2} V_{ci}^2 + \left(\frac{rf}{2}\right)^2} - \frac{r|f|}{2} \quad , \tag{9}$$

where, the cyclostrophic wind speed is given as

$$V_{ci} = \sqrt{\left(\frac{R_{mi}}{r}\right)^{B_i} \frac{B_i \Delta p_i}{\rho_a} e^{-\left(\frac{R_{mi}}{r}\right)^{B_i}}} \quad . \tag{10}$$

In order to obtain the surface winds, a boundary layer wind speed and direction (inflow) correction is applied to the gradient wind. The surface wind speed at a 10 m elevation is calculated using:

$$V_{10} = K_m V_g \quad . \tag{11}$$

The formulation adopted for the calculation of the parameter K_m is based on work reported in the Stage 1 study, Harper et al. (2001), in which

$$\begin{aligned}
K_m &= 0.81 && V_g < 6 \text{ m/s} \\
K_m &= 0.81 - 2.96\times10^{-3}\left(V_g - 6\right) && 6 \le V_g < 19.5 \text{ m/s} \\
K_m &= 0.77 - 4.31\times10^{-3}\left(V_g - 19.5\right) && 19.5 \le V_g < 45 \text{ m/s} \\
K_m &= 0.66 && 45 \le V_g \text{ m/s}
\end{aligned} \quad . \tag{12}$$

The inflow angle correction is applied to represent the cross-isobaric flow caused by surface friction and based on the work of Sobey et al (1977) is given as,

$$\begin{aligned} \beta &= 10\frac{r}{R_{m1}} && r < R_{m1} \\ \beta &= 75\frac{r}{R_{m1}} - 65 && R_{m1} \le r < 1.2R_{m1} \\ \beta &= 25 && 1.2R_{m1} \le r \end{aligned} \tag{13}$$

This wind profile is used to simulate not only concentric eye-wall cyclones (as in Cardone et al., 1994), but also to improve the fit of the model wind speeds to those measured more than $3R_{m1}$ from the centre of the cyclone. The adoption of the Cardone pressure profile formulation was motivated primarily by the existence of monsoon troughs in which cyclones in the Coral Sea are often embedded. The formulation has worked very well in enabling better fits in a wide range of tropical cyclones in both the Coral Sea and Australian Indian Ocean (McConochie et al., 2001, in press).

A representation of winds generated outside the cyclone vortex, herein called s*ynoptic* winds has been included in the wind model used in this project. During Coral Sea cyclones, large pressure gradients often occur between the cyclone and the mid-latitude high pressure cell, which can induce wind speeds up to 40 knots (Callaghan, 1996). Since waves generated by these winds can add considerable energy to the region during cyclones, a wind field based solely on a vortex model will under-estimate wave energy, especially more than about $8R_m$ to the south of the storm centre where the diminished effect of the main cyclone vortex makes synoptic winds relatively more important.

For each synthetic simulation a speed and direction for the synoptic component were randomly selected from historic data during tropical cyclones at weather stations in the south Coral Sea. These values are held constant throughout the simulation. Holding the synoptic winds constant will give a conservative result, since changes would invoke both duration and fetch limitations.

4.3 Tropical Cyclone Storm Surge Model – *MMUSURGE*

MMUSURGE is a numerical model that calculates water velocities (actually transports) and water surface elevation on a discrete grid by numerically solving the conservation of momentum and mass equations using finite difference techniques. *MMUSURGE* was validated in Stage 1 of this project (Harper *et al.*, 2001) for modelling storm surge along the Queensland coast. It is a 2-D version of the 3-D model *MMUHYDRO*, which has been under continuous development and use by the *MMU* over the last two decades.

The horizontal transports *U* and *V* are specified on a spatially staggered finite difference grid (the Arakawa *C* scheme). The governing equations are solved by a fully implicit splitting procedure, based originally on work by Wilders *et al.* (1988). Changes from this scheme of Wilders *et al.* are described in more detail in Bode & Mason (1994) and include the use of transport rather than velocity components as prognostic variables, implicit bottom friction, and an implicit method for treating the Coriolis terms on a staggered grid. Changes have also been made to the treatment of advective terms. A pre-conditioned version of the conjugate gradient squared method is used to invert the sparse matrices generated by the difference

scheme. Further modifications to the difference scheme have been implemented to accommodate the reef parameterisation algorithms.

Storm surge grid system

The main rationale behind the use of the nested grid system used in *MMUSURGE* is the need to overcome open boundary condition problems, which are commonly encountered in limited area, fine-scale modelling. By means of nesting, the finest-scale grid, which surrounds the area of interest, is linked to the dynamics of the continental shelf, so that open boundary problems are largely transferred further afield, where: (i) The extensive range of tidal data from the shelf region can be utilised for boundary conditions. (ii) Any inaccuracies in the specification of boundary conditions will have negligible influence on the evolution of model solutions in the region of interest. (iii) The essentially unknown boundary conditions associated with wind forcing are assumed to be zero.

Three nested grids are used for computational efficiency, so that accurate wind driven and tidal boundary conditions can be supplied to the finest grid. A standard 5:1 increase in resolution between successive grids was used to obtain a 550 m resolution in the study area. The *A*-grid (Figure 5) has a 7.5′ resolution. Note that 1.0′ of latitude (1.0 minute of arc) is equal to 1.0 nautical mile which is equal to 1852 m). The two *B* grids (Figure 6) have resolutions of 1.5′ (2800 m). The two *C* grids (Figure 7) increase the resolution to about 550 m roughly centred on the two study areas. The varying oblique orientations of the grids are achieved by using transformed spherical coordinate systems. The primary source of information for model bathymetry was navigational charts. This was supplemented by bathymetric surveys supplied by *EPA*.

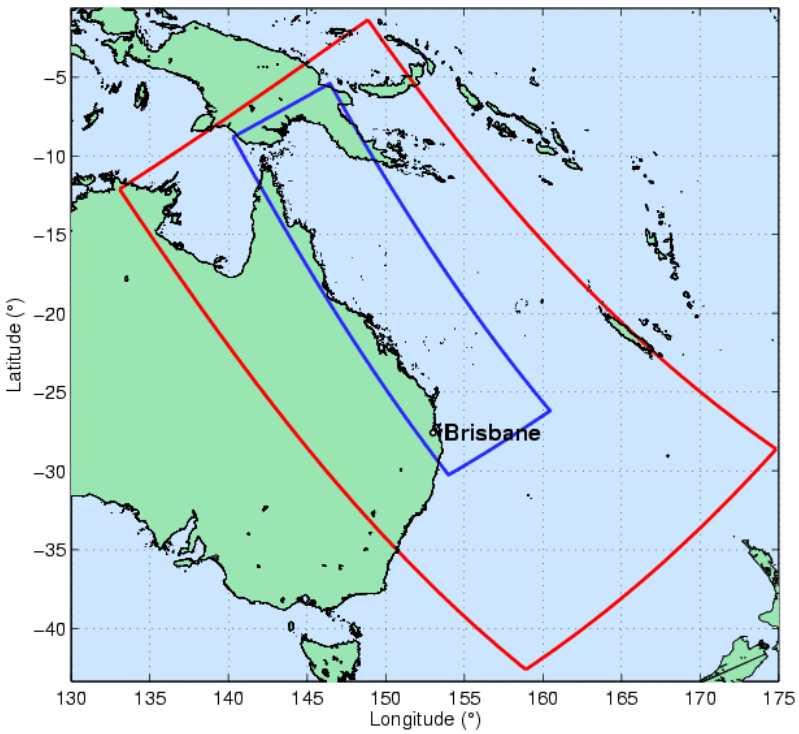

Figure 5. *A* grids: Surge (blue) resolution 7.5′ and Wave (red) resolution 20′.

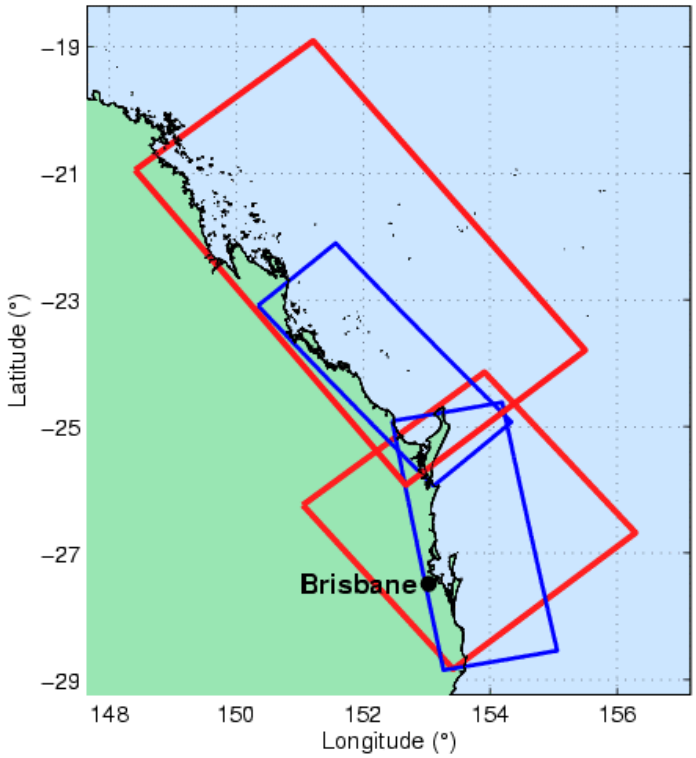

Figure 6. *B* grids: Surge (blue) resolution 1.5′ and Wave (red) resolution 4′.

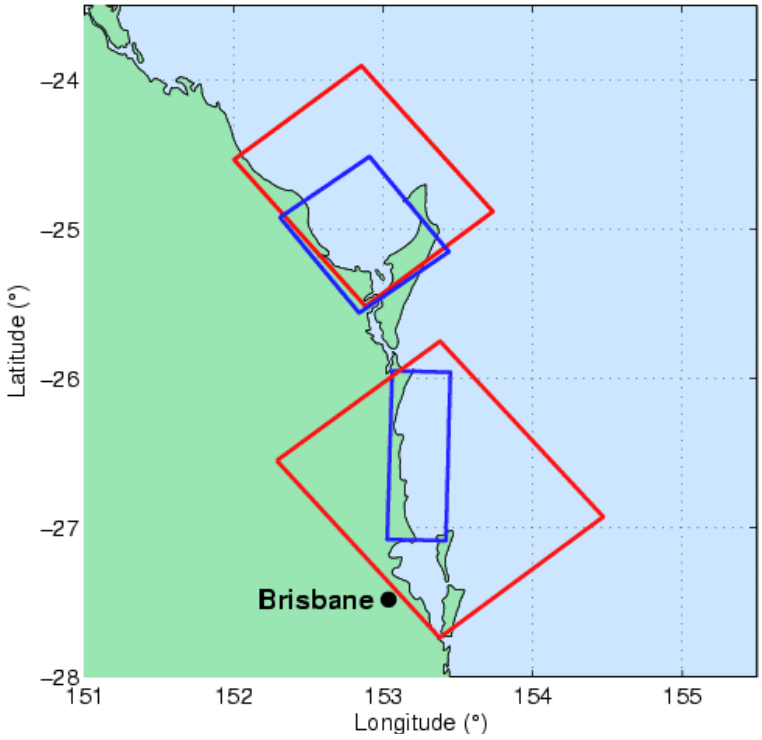

Figure **7**. *C* grids: Surge (blue) resolution 550 m; and Wave (red) resolution 1500 m

Validation of MMUSURGE

Extensive validation results for *MMUSURGE* were presented in the Stage 1 report (Harper *et al.*, 2001). This implementation of the model did not require changing the values of any calibration parameters.

4.4 Tropical Cyclone Wave Model - *WAMGBR*

The *MMU* has developed a wave generation model especially designed for use in the complicated GBR region (Hardy *et al.,* 2000). This model was used to model a very large ensemble of synthetic tropical cyclones to represent the population of tropical cyclones that threaten the GBR (Hardy *et al.*, 2003; http://mmu.jcu.edu.au).

WAMGBR is based on *WAM* (*WA*ve *M*odel) cycle *4* (Komen *et al.* 1994). Significant alterations and additions have been incorporated into *WAM* to adapt it for use in the complex GBR region. These alterations, presented in Hardy *et al.* (2000), include (i) numerical scheme with implicit capabilities; (ii) offset in discrete angle values; (iii) rotated spherical coordinates; and most significantly; (iv) a reef parameterization scheme that provides sub-grid scale dissipation.

Wave model grids

As with the storm surge model, multiple nested numerical grids in a spherical coordinate system have been established to cover the whole of the eastern Queensland coastal region. The current study will use one outside, two intermediate and two inner grids. The *A*-grid (Figure 5) has a 20′ (20 minute) resolution. The two *B* grids (Figure 6) have resolutions of 4′. The two *C* grids (Figure 7) increase the resolution to 0.8′ (1500 m) in the two study areas. The varying oblique orientations of the grids are achieved by using transformed spherical coordinate systems.

Validation of WAMGBR

Comparisons between modelled and measured data have shown that *WAMGBR* produces very good results in the difficult challenge of modelling tropical cyclone waves in the geographically complex environment of the Great Barrier Reef (Hardy *et al.* 2000). Here we will show comparisons for *T.C. Simon* using the wave model grids that were used for the ensemble simulations.

T.C. Simon was a significant cyclone that affected the Capricorn coast region of Queensland (Figure 8). It tracked south-westerly after forming in the middle of the Coral Sea and steadily intensified until reaching estimated maximum intensity of 950 hPa near the coastal town of Yeppoon. *Simon* then turned towards the south-east, tracking parallel to the coast, and began filling. It passed within 100 km of five automatic weather stations (*Marion Reef*, *Cape Capricorn Lighthouse*, *Heron Island*, *Lady Elliot Island*, and *Sandy Cape Lighthouse*).

The tropical cyclone windfield model, *CycWind* produced the time histories of wind speed and direction at each computational grid point of the numerical grids used for a *WAMGBR* simulation.

The *MMU* cyclone wind field calibration tool, *CyCal*, was used to develop these input values through a trial and error comparison of the calculated windfield with wind speed and direction data from several meteorological stations along the Queensland coast and throughout the Coral Sea (Figure 8). In Figure 8, only those stations with useful data are named. Using *CyCal*, input values of the tropical cyclone windfield model can be interactively changed with

instantaneous graphical comparisons of calculated and measured wind speed and direction at multiple stations. This tool greatly reduces the time needed to calibrate the windfield model.

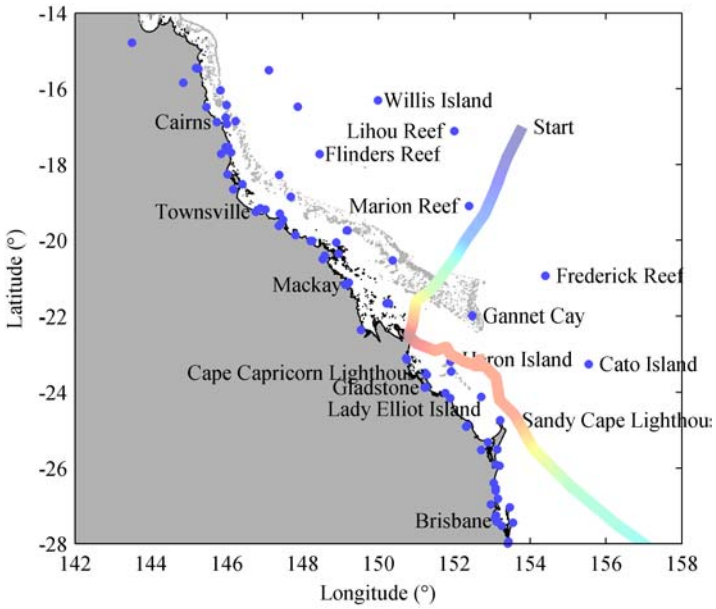

Figure 8. Track of Tropical Cyclone Simon occurred February 1980 with minimum central pressure of 950 hPa.

In our calibration technique, the data of track and central pressure from the BoM Tropical Cyclone database (ftp://ftp.bom.gov.au) are accepted without alteration. In the multidimensional parametric windfield model it is difficult to justify the alteration of these two important parameters. Instead the calibration consists of varying the parameter values of parameters for which little or no data exists. In general the order of importance of these parameters is R_{m1}, R_{m2}, Δp_2, p_∞, B_1, B_2, U_s, θ_s, although the order of this list varies from storm to storm and station to station during a single storm.

Measurements taken by stations close to the path of the storm play an important role in selecting R_{m1} (primary radius to maximum winds) and B_1 (primary Holland peakedness parameter). If a cyclone does not pass close to a measurement station, the fitting process for these two important parameters becomes more subjective.

The wind model input parameters were adjusted until the modelled values of wind speed, direction and pressure achieved the best match with the measured data. Of the more than 100 measurement sites only 22 stations measured data suitable for use in calibrating the wind field of *T.C. Simon*.

Time series comparisons of measured and modelled wind speed and pressure are shown in Figure 9 for the five stations that were within 100 km of the track of *T.C. Simon* sometime during the storm. One important issue with the measured data is evident in the comparisons; the measurements are often irregular and intermittent (e.g. *Heron Island Research Station*). Note also that only very few of the measurements in Figure 9 are taken when the centre of the cyclone was within 100 km of the station, in this case fewer than 40 individual samples.

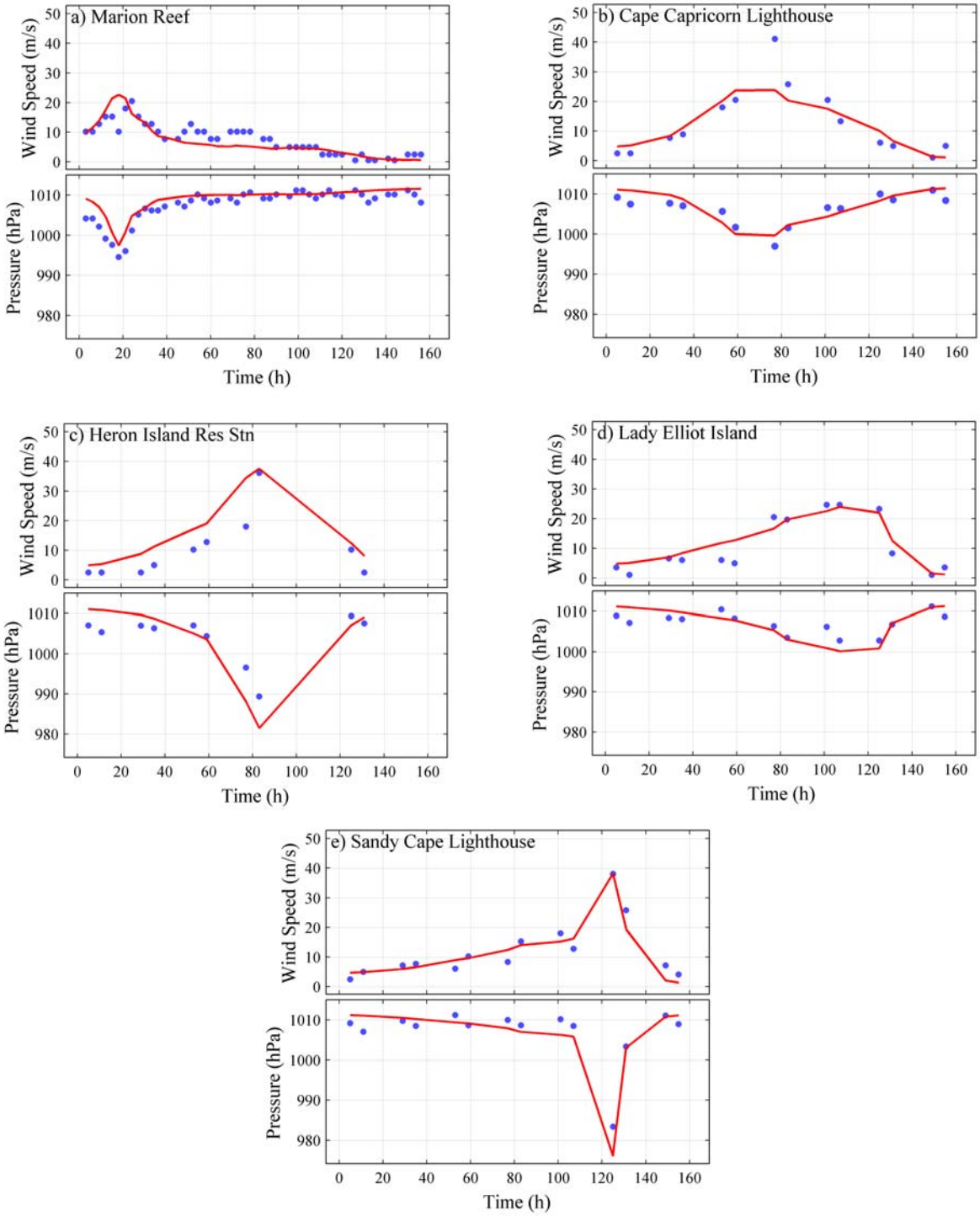

Figure 9. Comparison of modelled (——) and measured (•) time series of wind speed and pressure during *T.C. Simon*.

A good fit is obtained at *Sandy Cape Lighthouse* (Figure 9e) with the peak wind speed matching very closely (less than 1 m/s difference). The mean error (e_m) is less than 0.5 m/s and root mean squared error (e_{rms}) is less than 4 m/s. Similarly good fits are obtained at *Marion Reef* and *Lady Elliot Island*. However, results at *Cape Capricorn* and *Heron Island* indicate the model underestimates and over-estimates the wind speed, respectively. This is a common occurrence during calibrations and the best fit is often a subjective compromise (based on the experience of the user) sometimes favouring one station over another.

The calibrated wind field was used to force a *WAMGBR* simulation for *T.C. Simon*. Figure 10 shows scatter diagrams of modelled versus measured (synchronous) for: wind speed, wind direction and pressure at the five stations included in Figure 9.

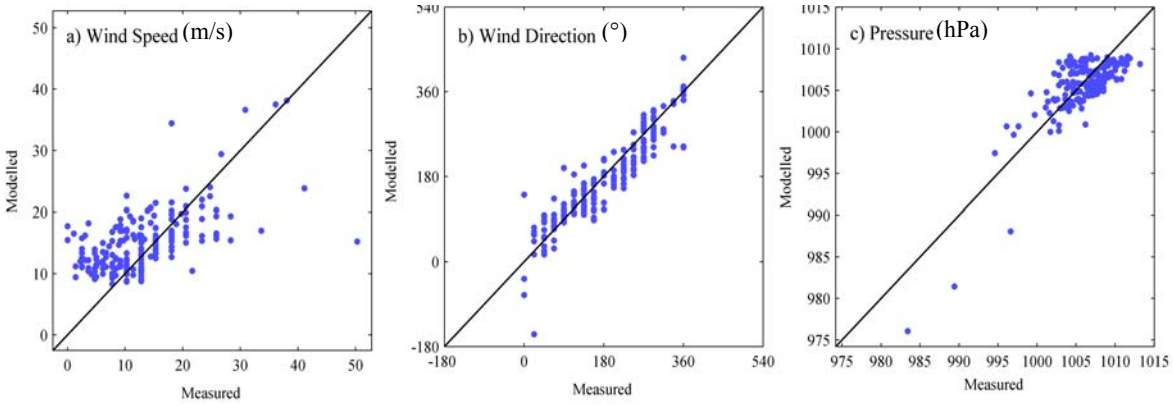

Figure 10. Comparison of modelled and measured a) Wind speed, b) Wind direction and c) Mean sea level pressure for the calibration of *T.C. Simon*. Wind speeds in m/s, direction in degrees from North and pressure in hPa. Data from stations shown in Figure 9.

Modelled and measured significant waves heights are compared in Figure 11. The location of the buoy is close to the position of the Burnett Heads Waverider buoy (see Figure 19a).

In general the modelled and measured wave heights match well in the vicinity of the largest waves when the storm is closest to the buoy. The model appears to over predict the wave height for 24-25 April during the approach of the storm. It is difficult to determine the cause of this over prediction and discovering the reason is made more difficult by the missing data points during the approach of the storm. In other hydrodynamic modelling (not shown here), a large eddy in the East Australian Current to the north of the study area may cause refraction that could reduce the wave energy of the waves travelling from the location of the cyclone to the study site. Such current-induced refraction is not included in the *WAMGBR* simulations.

It is important to note that this process of model validation shows how the model performs in *hindcast* mode. The historic wave field is determined by the historic wind field and, despite the availability of wind data at several field stations, the complex 3-D nature (2 spatial and 1 time) of the wind field is largely unknown. Thus, duplicating the historical windfield during a *hindcast* with all of its unrecorded individuality is a daunting challenge. Matching modelled and measured waves is as much a validation of the wind model as it is of the wave model. The wind field model (*CycWind*) has been shown (McConochie et al., 1999, in press) to do a good job providing representative tropical cyclone wind fields. The quality of the wave simulations demonstrated in Figure 11 indicates that the waves hindcast during Tropical Cyclone Simon match recorded data very well considering the uncertainties inherent in the process. Other excellent validation results using *CycWind* and *WAMGBR* to model tropical cyclone waves inside the complexity of the Great Barrier Reef are provided in Hardy *et al.* (2000).

The wind and wave models do not operate in *hindcast*, but rather in *prediction* mode, for this study. In other words, the wind field is specified and the wave model produces wave conditions forced by this *given* wind field. Although there can be no measured data with which to compare the wave model results, based on the results shown in Figure 11, the wave model should perform excellently in this far simpler prediction mode.

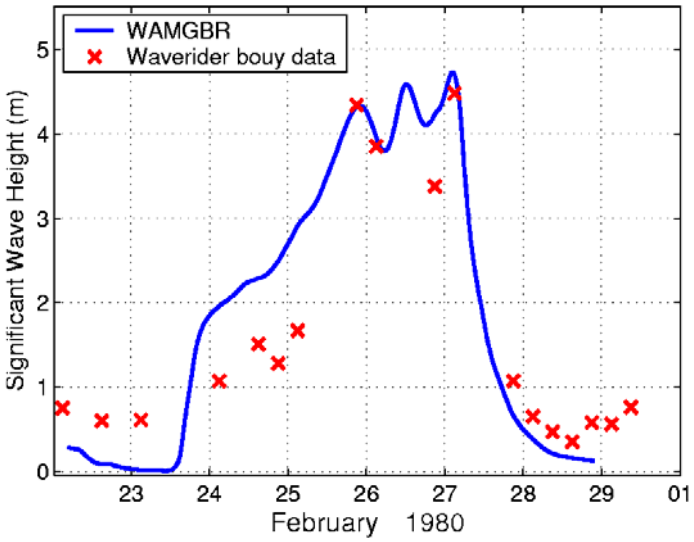

Figure 11. Wave model verification during *T.C. Simon*.

4.5 Wave Setup Model

The empirical wave setup of Hanslow & Nielsen (1993) was recommended in Stage 1 of this study (eqn. 8.19, p. 138, Harper *et al.*, 2001). This formula is given as

$$\bar{\eta}_w = 0.048\sqrt{H_{rms_o} L_o} \qquad \text{(Hanslow \& Nielsen)} \quad , \tag{14}$$

where $\bar{\eta}_w$ is the wave setup at the shoreline, H_{rms_o} is the deepwater *rms* wave height and L_o is the deepwater wave length, which is calculated by

$$L_o = \frac{gT_p^2}{2\pi} , \tag{15}$$

in which T_p is the peak wave period from the numerical wave model simulation at the selected output point.

Two other empirical setup formulae (Gourlay, 1992 – eqn 16; and Raubenheimer *et al.* 2001 – eqn 17) were also investigated for the calculation of wave setup at the shoreline. These are

$$\bar{\eta}_w = 0.35 H_{rms_o} \xi_o^{0.4} \qquad \text{(Gourlay)} \tag{16}$$

$$\bar{\eta}_w = H_{so}\left(0.019 + 0.003\beta_{av}^{-1}\right) \qquad \text{(Raubenheimer)} \quad , \tag{17}$$

In which H_{s0} is the deepwater significant wave height and the surf similarity parameter (ξ_o) is

$$\xi_o = \frac{\tan\alpha}{\sqrt{H_o / L_o}} , \tag{18}$$

in which tan α is the beach slope. Eqn. 17 uses an alternate method to determine beach slope (β_{av}) to account for non-planar beaches. It is given by

$$\beta_{av} = \frac{h_{av}}{\Delta x} \quad , \tag{19}$$

in which Δx is the width of the surf zone and the average water depth is

$$h_{av} = \frac{1}{\Delta x} \int (h + \eta)\, \mathrm{d}x \quad , \tag{20}$$

where h is the still water depth and η is the wave setup measured from the still water level. Note that, for a planar beach, β_{av} would be approximately equal to ½ the beach slope.

These empirical wave setup equations, were developed from field and laboratory data in which moderately sized deepwater waves impinge almost directly on the coastline. The surf zones during these conditions would vary with wave parameters but would be several hundreds of metres wide. These formulae then result from an assumption of steady state conditions during which wave-induced currents and water levels reach an equilibrium condition.

The situation during severe tropical cyclones will be very different from conditions during which these field and laboratory data were collected. Offshore significant wave heights and peak periods can be 15 m and 14 s (and larger) during tropical cyclones. For these very large and very long (L_0 = 305 m) waves, deepwater is h > 150 m and *shallow water* wave breaking begins at h = 30 m. Under these conditions *all* of Hervey Bay would be a surf zone, with breaking occurring more than 30 km offshore, and even at the more open and deeper Sunshine Coast inner shelf, the surf zone would be at least 4 kilometres wide and as wide as 10 km. A calculation of wave setup (Eqn. 14) using values of H_{s0} = 14 m and L_0 = 305 m gives a setup of 2.6 m at the shoreline. This value is most likely too large for surf zones that are very much wider than those of the field measurements that formed the basis for the empirical setup formula.

All across these very wide surf zones local wave breaking will cause local wave-induced water levels and currents. However, since some of this action occurs several kilometres offshore, it will have a much reduced effect on the magnitudes of wave setup at the shoreline. Some of the contribution to shoreline setup that would be created far offshore will be dissipated by bottom friction from currents generated during the unsteady and non-uniform conditions.

The best modelling solution to determine the value of wave setup at shoreline during extreme events would be to couple wave and storm surge models at a very fine scale. The wave model must not only have a very good wave breaking component, but also should be a phase-resolved rather than a phased-averaged model. This is needed in order to simulate short crested waves necessary to predict the non-uniform and unsteady effects that wave breaking has on the currents and water levels. A phase resolved wave model such as a Bousinesq model (e.g. Madsen et al. 1996) would be ideal. Unfortunately the Sunshine Coast is at least two orders of magnitude too large for even one simulation, let alone the simulation of a large ensemble of storms. Hervey Bay with its much larger surf zone is more difficult.

Several methods were investigated to solve this problem with the calculation of wave setup. We decided to select wave model output points closest to the shoreline to represent the waves

that more directly attack the beach. These points will be inside the surf zone for more severe conditions, but the assumption here (as discussed above) is that the wave breaking far from shore does not significantly affect shoreline water levels. The wave energy at these inshore points is reduced by sheltering, refraction, bottom friction and breaking. In the development of the wave model depth grid, we chose to assign depths, at the points closest to the coastline, so that they represented a location 750 m offshore (half a grid space). Since the wave model does not allow water depth to change with time, the depth at these points was set at highest astronomical tide (HAT). For all of these points the wave height will be depth limited by wave breaking during more severe events; therefore, the deepwater wave height that is calculated by de-shoaling output at these inshore points will also be depth limited. Since all of the wave setup formula (eqns. 14, 16 and 17) are functions of wave height, this depth limitation of wave height tends to limit severely the increase in setup with increase in return period (i.e. more severe conditions).

In order to obtain the deepwater wave heights needed for eqns. 14, 16 and 17, the procedure was as follows: First the significant wave height at the inshore model output point is de-shoaled to a deepwater value to obtain

$$H_{s0} = \sqrt{\frac{c_g}{c_{go}}} H_s \quad , \tag{21}$$

where c_g and c_{go} are the wave group speeds at the wave output point and deepwater, respectively, given as

$$c_g = \frac{1}{2}\left[1 + \frac{4\pi h/L_p}{\sinh\left(4\pi h/L_p\right)}\right]\left[\frac{gT_p}{2\pi}\tan\left(\frac{2\pi h}{L_p}\right)\right] \tag{22}$$

$$c_{go} = \frac{gT}{4\pi} \ , \tag{23}$$

in which L_p is the wavelength of the peak frequency of the spectrum given as.

$$L_p = \frac{gT_p^2}{2\pi}\tan\left(\frac{2\pi h}{L_p}\right) \quad . \tag{24}$$

This deepwater significant wave height was used in eqn. 17. For eqns. 14 and 16 the significant wave height is converted to an rms value using

$$H_{rms0} = \frac{1}{\sqrt{2}} H_{s0} \quad . \tag{25}$$

Figure 12 contains the wave setup return period curves for the three formula (eqns, 14, 16, and 17) at *Coolum* on the Sunshine Coast. Note how both the curves for eqns 16 and 17 (Gourlay, 1992 and Raubenheimer *et al.*, 2001) are severely truncated above about the 20 year levels. The results for eqn 14 (Hanslow & Nielsen (1993)) continue to increase despite the depth-limited wave height, since this formula is more strongly dependant on increasing the wavelength and, in general, wavelength increases with storm severity.

Figure 12 is shown here for comparison purposes. The techniques for creating the return period curves will be described below. Eqn. 14 (Hanslow and Nielsen, 1993) was chosen for the calculation of wave setup at the shoreline. This equation resulted from the most extensive set of field measurements, and we could not justify the severe depth limitation shown if the other two equations (eqns. 6 and 7) were used.

Wave setup was calculated using eqn. 14 at each time step of the simulation of each tropical cyclone in order to produce a time series of wave setup values.

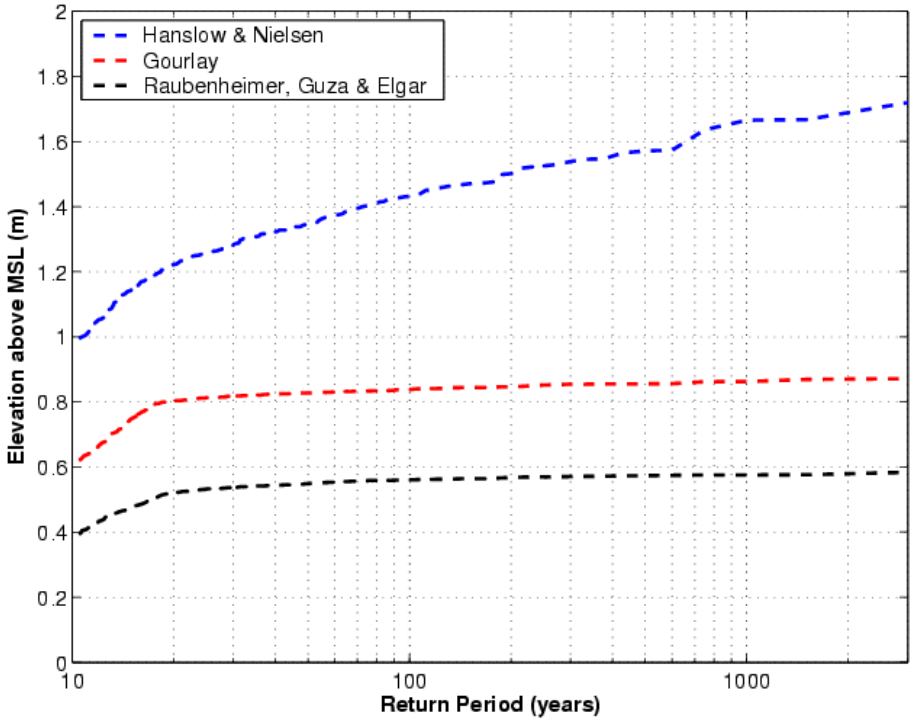

Figure 12. Comparison of Hanslow and Nielsen (1993) (eqn. 14), Gourlay (1992) (eqn. 16) and Raubenheimer *et al.* (2001) (eqn. 17) empirical setup formula at *Coolum* on the Sunshine coast.

5.0 MODELLING STORM TIDE OF THE TROPICAL CYCLONE POPULATION

5.1 Synthetic Ensemble of Tropical Cyclones for the East Coast of Queensland

The tropical cyclone data were analysed to separate the tropical cyclones that threatened the eastern Queensland coast (defined as entering the area delineated by the box in Figure 3). Thus a rate of cyclone occurrence of λ_C = 3.273 tropical cyclones per year (108 tropical cyclones in 33 years: 1969 to 2001) was determined from this data. We choose to conduct a Monte-Carlo simulation of 3000 years of tropical cyclones, so that three renditions of a 1000 year record would improve the estimates of the 1000 year return periods. To achieve this target, 9818 tropical cyclones (3000 years) × (3.273 T.C. per year) were modelled.

The first step in this process was to create the time series of position, pressure and radius to maximum winds for 9818 tropical cyclones using *CycSyn*. The model was calibrated using historical tropical cyclones that started or passed through the area shown by the box in Figure 3. These tropical cyclones represent the population of tropical cyclones that threaten the eastern coastline of Queensland, so not all of these will cause a severe impact in the study areas of this project. Statistics from this synthetic ensemble are compared to the historical data in Figure 4.

5.2 Selecting the Tropical Cyclones to be Modelled by *MMUSURGE* and *WAMGBR*

Surge, tide and wave setup, the components of storm tide, are nonlinearly related, as they all both affect and are affected by changes in water level. As will be seen in the following presentation, developing the frequency relationships will require a large number of simulations and this makes it infeasible to model these in a coupled, nonlinear fashion. Therefore storm surge, astronomical tide, and waves (wave setup) will be independently modelled and the storm tide will be determined by a linear superposition of the resulting time series.

The procedure to determine the ensemble of storms that defined return periods above 10 years is as follows: First, all 9818 storms (3000 years) were simulated by both *MMUSURGE* and *WAMGBR* on their respective *A* grids. Simulations on these coarse grids are much less computationally expensive than on *B* or *C* grids. Computational points from the *A* grid, which are inside the area of the *C* grid were used to represent the study area. These representative *A*-grid points were chosen to be the first two rows of points along the coastline in each of the two study area grids (Figures 13 and 14).

For each storm in the ensemble, the maximum surge and maximum significant wave height that occurred at each representative *A*-grid point were identified. After the complete storm ensemble was simulated, these maxima were ranked by size at each *A*-grid point. These ranks are the values of m_η and m_H (see eqn. 2). After substituting eqn. 2 into eqn. 1, the value of the rank at R = 10 years becomes

$$m_\eta = m_H = \frac{n}{R} = \frac{3000}{10} = 300 \quad . \tag{26}$$

Storm surges and wave heights greater than or equal to the 10 year level are determined by the storms with the 300 largest values of maximum storm surge and maximum significant wave height. Thus each location would require simulation of only a very small subset of the ensemble of 9818 storms in order to define the return period curve above 10 years.

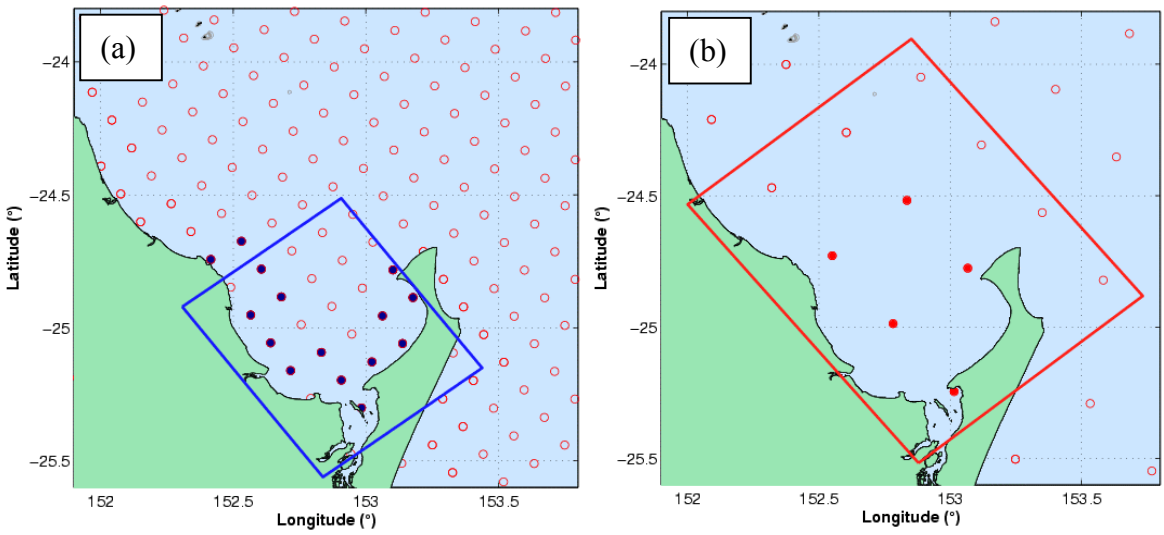

Figure 13. *A*-grid output points (solid circles) chosen to select storms that cause storm surge (a) and significant wave heights (b) greater than the 10 year return period at Hervey Bay. Boundaries of the storm surge and wave *C*-grids are shown.

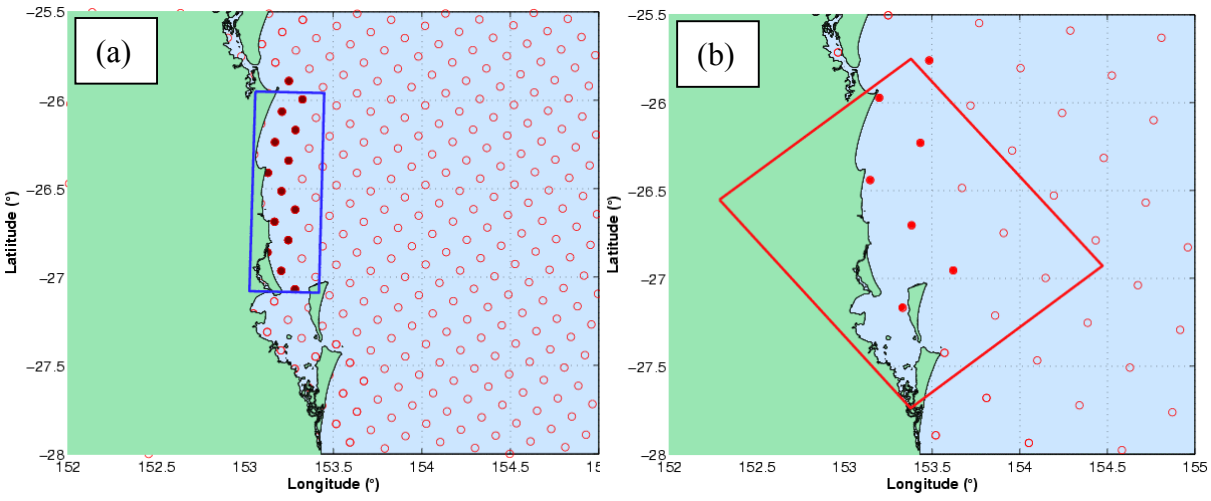

Figure 14. *A*-grid output points (solid circles) chosen to select storms that cause storm surge (a) and significant wave heights (b) greater than the 10 year return period at Sunshine Coast. Boundaries of the storm surge and wave *C*-grids are shown.

Of course, each representative *A*-grid point could have a unique set of the most severe 300 storms. Although the variation of these lists inside the relatively small geographical region of a single *C* grid would be limited, it is unlikely that the largest waves or storm surge at *all* locations in the area covered by the *C* grid would come from the same 300 tropical cyclones.

Also the list of tropical cyclones that produces the 300 largest storm surges in a region will be similar but not identical to the list that produces the 300 largest wave heights. For example Figure 15 shows the tracks of the storms that caused the largest 20 storm surges (Figure 15a) and the largest 20 significant wave heights (Figure 15b) at *Coolum* on the Sunshine Coast. The magnitude of storm surge at the coast is far more dependent on the characteristic of the cyclone at closest approach than is the magnitude of wave height. Thus the tracks for the largest 20 storm surges are in general grouped just to the north of the calculation point, (shown blue dot in Figure 15a) whereas the tracks for the waves (Figure 15b) are more diffuse.

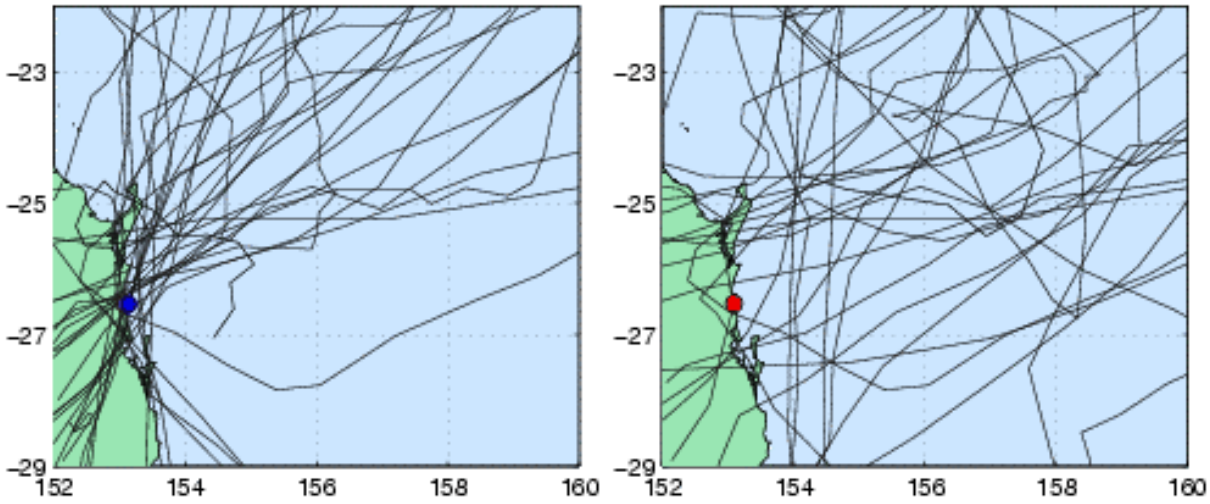

(a) Storm Surge (b) Waves

Figure 15. Tracks of the synthetic tropical cyclones that caused the 20 largest storm surges and 20 largest significant wave heights at the indicated point (*Coolum,* Sunshine Coast).

To account for the variation inside a C-grid, we decided to simulate all tropical cyclones that caused the largest 300 values in *either* wave height *or* storm surge at *any* of the representative *A*-grid points. These tropical cyclones were simulated by *both WAMGBR* and *MMUSURGE*. The number of tropical cyclones simulated is shown in Table 1. The rows labelled *Waves* and *Storm Surge* give the number of unique (i.e. a storm was not counted more than once) tropical cyclones that caused the 300 largest values for *at least one* of the representative points. The row labelled *Combined* gives the number of unique tropical cyclones that cause the 300 largest values for *either* wave height or storm surge for *at least one* representative point. This row gives the total number of tropical cyclones modelled by the system of models. For example if the *same* 300 synthetic tropical cyclones produced the largest waves and storm surge at *each* of the representative points then all numbers in Table 1 would be 300.

This selection procedure determined that only 540 (Hervey Bay) and 506 (Sunshine Coast) storms out of the 9818 storms contributed maximum storm surges *or* maximum significant wave heights larger than the 10 year return period at *A*-grid points that are chosen to represent the Hervey Bay and Sunshine Coast *C* grids, respectively. These storms were simulated on the respective grid systems (*A*, *B* and *C*) for Hervey Bay and the Sunshine Coast. The results were two data sets (one for storm surge and one for waves) that contain the time histories of storm surge and significant wave height during each storm at each of the *C*-grid output points.

Table 1. Number of tropical cyclones needed to provide the 300 largest significant wave heights and 300 largest storm surges at each *A*-grid point representing the *C* grid.

	Hervey Bay	**Sunshine Coast**
Waves	385	390
Storm Surge	427	385
Combined	540	506

Since over 500 of the severest storms are simulated instead of only the 300 most severe that are needed to define the 10 year return period, it is instructive to see how much lower this defines the return period curve. An analysis showed that at least the largest 320 (R = 9.4 years) storm surges and waves at every point were simulated and approximately 370 out of the largest 400 (R = 7.5 years) were simulated. This means that tropical cyclones that produce surge and waves with magnitudes larger than that of the 7.5 year return period are well represented.

The final outputs of this study are return period curves of *storm tide* (surge plus tide plus wave setup). The storm-tide events that contribute *water levels* above the 10-year level do not include solely those storms with *storm surges* and *wave setups* above the 10 year level. A storm with surge and wave setup smaller than 10 years could contribute to the storm tide curve above 10 years, if the maximum surge and waves during the storm combine with higher tides. Therefore simulating only the largest 300 storm surges and waves may slightly underestimate the level of the *storm tide* return period curve between 10 and, say, 100 years. This problem would disappear if the whole ensemble were simulated. However it is infeasible to model 9818 storms with both surge and wave models and, even it were feasible, a problem arises with the definition of when a tropical cyclone occurs.

The purpose of this project is to produce results *during tropical cyclones*. At the lower end of the return period curve a definition of *tropical cyclone* is necessary. Recall that the storm ensemble represents the western Coral Sea (Figure 3), so that surges and waves with lower rank (perhaps the bottom 90%), at any one location, occur during storms that do not pass close to that location. For many of these storms, the waves and storm surge may well be lower than those that occur during more frequent non-cyclonic events. Should a tropical cyclone that is located in the far northern Coral Sea be considered a tropical cyclone occurrence for the southern coast of Queensland, which might be more than 1500 km distant? For example, the value of tropical cyclone storm surge at the 10-year level is only about 0.3 m (300th largest out of almost 10,000 storms in 3000 years of simulation) for *Torquay* in Hervey Bay. The vast majority of storms in the whole ensemble (over 9500) have maximum surges at *Torquay* less than that, i.e. the maximum surges with ranks 1000, 5000 and 9000 at *Torquay* are less than 0.3 m and in the narrow range between 0.3 and 0.0m. The storm tide during such a storm is largely determined by the maximum tide that occurs during the duration of the storm. Is this truly a “storm tide” and should it be included in the set of storm tides “during tropical cyclones”? Certainly the magnitude of storm surge and wave setup during remote tropical

cyclones would occur much more commonly during the much more frequent non-cyclonic events.

Various definitions of what constitutes a tropical cyclone for a given location have been used. These definitions have included an approach with a set distance of the study area, say within 500 km; or the occurrence of strong winds, say above 40 knots; or the occurrence of storm surge above a set level, say 0.3 m. Many other similar definitions are possible, but any such definition is arbitrary. The first attempt at a definition for this project was the occurrence of storm surge or wave height above the 10 year return period (nominally the 7.5 year return period as discussed above). This definition is defendable as this project was to produce statistics of severe storm tides, and surges and waves at and below the 10-year level are increasingly dominated by events other than tropical cyclones. However, at lower return periods the resulting return period curve dips below highest tide levels and thus below the curve that would result from combining tropical cyclone storm tides with non-cyclonic storm tides. This result may be misinterpreted by inexperienced users.

After additional consideration, a definition of tropical cyclone has been adopted that includes the whole ensemble of tropical cyclones in the western Coral Sea, regardless of the proximity or effect at a project output location. The inclusion of all storms, the vast majority of which cause very small values of storm surge, creates storm tide return period curves that will asymptote at lower return periods to a return period curve of tidal height. Since it was infeasible to model the whole ensemble down to *C*-grid resolution by both storm surge and wave models, a method was developed to model a small number of representative storms.

An *A*-grid point was chosen to represent each output location. Recall that the largest storm surges are densely covered (all of the top 300 and most of the top 500). Weaker storms were chosen so that the gap between the rankings of selected representative storms (based on *A*-grid results) was reduced to at most 680 storms.

In order to represent these lower ranked storm tides 26 and 23 additional tropical cyclones were modelled for Hervey Bay and Sunshine Coast areas, respectively.

5.3 Astronomical Tides

A twenty-one year tidal prediction at a 15 minute interval was produced at each of the project output locations using the best available set of tidal constituents obtained from the analysis of a time series of tide gauge measurements. Few of the output locations are co-located with tidal measurement stations; therefore, a subjective judgement of the best nearby stations was necessary. Tables 2 and 3 show the information on the official station and datum (provided by EPA) and the station and data record length used to produce the project tidal signal. The acronyms HAT, LAT, MSL and AHD mean Highest Astronomical Tide, Lowest Astronomical Tide, Mean Sea Level and Australian Height Datum, respectively. The official and project tidal stations differ for several reasons. In some cases neither measurement time series nor tidal constituents were available at the official stations for the determination of tidal constituents needed to produce the time series of tidal heights. In some cases data were available at locations better representative of the output location. At most of the Project Tide stations, the length of the data time series was longer than one year. For those stations with records shorter than 1 year, semi-annual and annual constituents, from the nearest, long term analysis, were added to those obtained from tidal analysis.

The project tide, storm surge and wave setup time series were assumed to oscillate about the official values of MSL and then the official difference between AHD and MSL (Tables 2 and 3) were used to adjust the storm tide signal from a MSL to an AHD datum.

Table 2. Tidal Information: Hervey Bay. Official Data supplied by Maritime Safety Queensland. Project tides are the location and record length of the tidal measurements used to produce the tidal constituents.

	Official Data (m, LAT)					**Project Tides**	
Location (Fig. 1)	**Tide Station**	**HAT**	**MSL**	**AHD**	**MSL-AHD**	**Tide Station**	**Series Length**
Woodgate	Woodgate	3.78	1.78	1.77	0.0100	Burrum Heads	43 days
Point Vernon West	Point Vernon	4.01	1.90	1.89	0.0100	Urangan Boat Harbour	22.43 yrs
Dundowran Beach	Point Vernon	4.01	1.90	1.89	0.0100	Burrum Heads	43 days
Toogoom East	Point Vernon	4.01	1.90	1.89	0.0100	Burrum Heads	43 days
Toogoom	Point Vernon	4.01	1.90	1.89	0.0100	Burrum Heads	43 days
Burrum Heads	Burrum Heads	3.81	1.78	1.82	-0.0400	Burrum Heads	43 days
Burrum River	Burrum Heads	3.81	1.78	1.82	-0.0400	Burrum Heads	43 days
Urangan	Urangan	4.19	2.07	2.04	0.0300	Urangan Boat Harbour	22.43 yrs
Torquay	Urangan	4.19	2.07	2.04	0.0300	Urangan Boat Harbour	22.43 yrs
Scarness	Urangan	4.19	2.07	2.04	0.0300	Urangan Boat Harbour	22.43 yrs
Point Vernon	Point Vernon	4.01	1.90	1.89	0.0100	Urangan Boat Harbour	22.43 yrs
Urangan Boat Hr.	Urangan	4.19	2.07	2.04	0.0300	Urangan Boat Harbour	22.43 yrs
Mangrove Point	Bingham	4.80	2.17	2.17	0.0000	Bingham	39 days
River Head	Bingham	4.80	2.17	2.17	0.0000	Bingham	39 days

5.4 Combining Surge, Tide and Wave Setup to Produce Storm Tide Time Series.

The surge and wave setup time series during a single tropical cyclone are correlated, since they are both produced by the sae wind and pressure fields. In this project the nonlinear interactions between surge and waves were ignored. The storm surge and waves were simulated on a constant “tide” of MSL, and HAT, respectively. This result will be slightly conservative as the same storm with its peak coinciding with high tide will create slightly smaller storm surge than if it hit at low tide. Using a water depth based on HAT will also create slightly conservative wave setup results since offshore wave dissipation will be reduced.

The time series of storm surge and wave setup during each of the synthetic tropical cyclones that was chosen for simulation on the fine resolution *C*-grids (566 storms – Hervey Bay and 529 storms – Sunshine Coast) were linearly added to produce a time series of surge plus wave setup. Since the *timing* of a tropical cyclone is not dependant on the tidal signal (i.e., the cyclone can hit the coast at any phase of the tide), each of the surge plus wave setup time series was linearly added to multiple separate tide time series creating multiple storm tide events for each synthetic storm. This was done to model the range of possible storm tide combinations. The starting point in the tidal time series was randomly selected from the tidal signal. A weighting was used that favoured months with more cyclonic activity (e.g.

February) over months with fewer storms (e.g. November). The values of the weights, which are based on the historical occurrence of tropical cyclones in the region, are shown in Figure 16. Tests showed that combining each of the simulated synthetic tropical cyclone surge plus wave setup time series with 50 randomly selected tide time series produced excellent results. Since this process is inexpensive, the number of tides was increased to 500 in order to produce smoother curves, especially at the higher levels where fewer storms contribute.

Table 3. Tidal Information: Sunshine Coast. Official Data supplied by Maritime Safety Queensland. Project tides are the location and record length of the tidal measurements used to produce the tidal constituents.

	Official Data (m, LAT)					**Tidal Analysis**	
Location (Fig. 2)	**Tide Station**	**HAT**	**MSL**	**AHD**	**MSL-AHD**	**Tide Station**	**Series Length**
Teewah	Teewah Sands	2.18	1.00	1.06	-0.0600	Noosa Head	2.92 yrs
Noosa	Noosa Head	2.18	1.00	1.06	-0.0600	Noosa Head	2.92 yrs
Sunshine Beach	Noosa Head	2.18	1.00	1.06	-0.0600	Mooloolaba	18.5 yrs
Coolum	Coolum	2.13	0.97	0.99	0.0200	Mooloolaba	18.5 yrs
Maroochy River	Maroochy Bch	2.13	0.97	0.99	0.0200	Mooloolaba	18.5 yrs
Mooloolaba	Mooloolaba	2.13	0.97	0.99	0.0200	Mooloolaba	18.5 yrs
Buddina	Mooloolaba	2.13	0.97	0.99	0.0200	Mooloolaba	18.5 yrs
Caloundra	Caloundra Head	2.04	0.95	0.99	-0.0400	Caloundra Head	16.72 yrs
Golden Beach	Golden Beach	1.51	0.77	0.66	0.1100	Golden Beach	40 days
Woorim	Woorim	2.14	0.93	NA	NA	Tangalooma	5.4 yrs

This process can be thought of as repeating the 3000 year tropical cyclone ensemble 500 times, approximating a 1,500,000 year record. The maximum water level was determined for each of these more than 283,000 = 566 storms × 500 tides (Hervey Bay) and 264,500 (Sunshine Coast) storm tides. It is important to emphasise that we are *not* attempting to accurately produce the 1,500,000 year event. The process would not be accurate at that level since a 1,500,000 year record may include more severe storms than in the 3000 year record. However, this process is used to estimate the 1000 year event with 3000 years of storms.

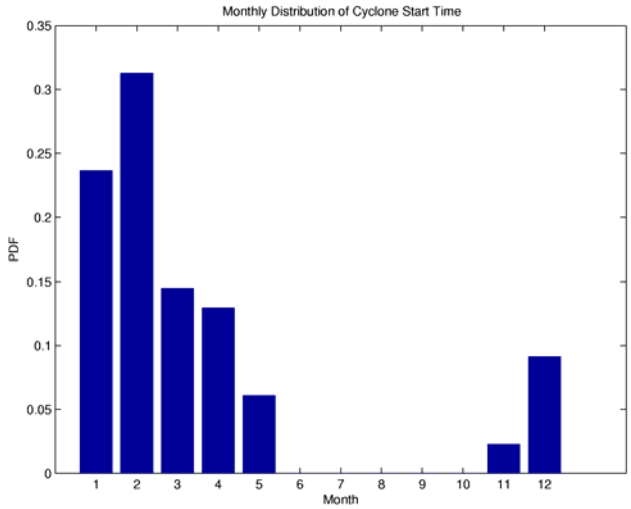

Figure 16. Probability distribution used to weight selection of tidal time series to match with surge plus wave setup time series.

6.0 RETURN PERIOD CURVES OF STORM TIDE AND WAVES

6.1 Creating Return Period Curves

Substituting eqn. 2 into eqn. 1 gives the formula for return period for storm tide, R_η, and significant wave height, R_H, which for this project becomes

$$R_\eta = \frac{n}{m_\eta} = \frac{1{,}500{,}000}{m_\eta} \qquad R_H = \frac{n}{m_H} = \frac{3000}{m_H} \qquad (27)$$

The nominal record length for the storm tide is n = (3000)(500) = 1,500,000 years. The record length for the waves (also for storm surge alone) remains at n = 3000 years since the waves were not combined with multiple tidal sets. The ranks, m_η = 1 and m_H = 1, are assigned to the largest storm tide and significant wave height, and these values are the 1,500,000 and 3000 year return period values (eqn. 1), respectively. Values of storm tide and wave height that rank m_η = 150,000 and m_H = 300 have return periods of 10 years.

6.2 Results: Storm Tide During Tropical Cyclones

The return period curves are formed by plotting points with (x, y) coordinate values of (return period, magnitude). An example, storm tide (surge plus wave setup plus tide) return period curve (*Coolum*, Sunshine Coast) is shown in Figure 17. The datum for water levels is Australian Height Datum (AHD), which is approximately mean sea level throughout the study area (see Tables 2 and 3). In order to show the range in values of the separate components of each plotted point, (i) storm surge (ii) surge plus tide and (iii) wave setup are also plotted in Figure 17a. A very large number of modelled events have formed the storm tide curves. There are 148,500 storm-tide events that make up the curve between 10 and 1000 years. The density of the events increases rapidly toward lower return periods. For example, only 1000 storm tide events make up the higher end of the curve (not plotted here) between the 1000 and 1,500,000 year return periods; 13,500 events are between 100 and 1000 years; and 135,000 are between 10 and 100 years. Because of the very large number of events, the results have been decimated to better distinguish the points, and only 14,850 are plotted in Figure 17a; 1/10 the number of events between 10 and 1000 year return periods).

For an explanation of Figure 17a, let us look at the storm tide curve in the vicinity of the 100-year level, which is a water level of approximately 2.4 m. The storm surge component of the storm tides near to the 100 year level varies by more than 1 m (from almost 0.0 to about 1.2 m) and the wave setup component varies about 0.5 m. The tidal component (not shown) will have variations approaching the tidal range. Although a 100 year storm tide can be assigned a single value, there is no single value to assign to any of its components. An infinite number of combinations of storm surge, tide and wave setup are possible that add together to produce a given value of storm tide.

Note that wave setup (blue squares in Figure 17a) is usually the largest component of storm tide level for the Sunshine Coast open coast locations. Wave setup is always positive at the shoreline. However, note that at the lower end of the curve, a few of the storm events have a storm surge component (black circles in Figure 17a) that is negative (wind blowing offshore) at the time of maximum storm tide (surge + tide + wave setup). For these cases a high tide has

combined with the wave setup to produce the maximum water level during the storm-tide event at a time when the surge was negative. As was discussed in the preceding paragraph, these maximum storm tides for which the surge component is negative are just a few of the infinite number of possible combinations that could cause the corresponding storm tide level. As return period increases, the storm tide level approaches and then surpasses the largest possible levels of tide plus wave setup, therefore, the lowest possible storm surge component increases with increasing higher water levels. (See also Figure 18a, below.)

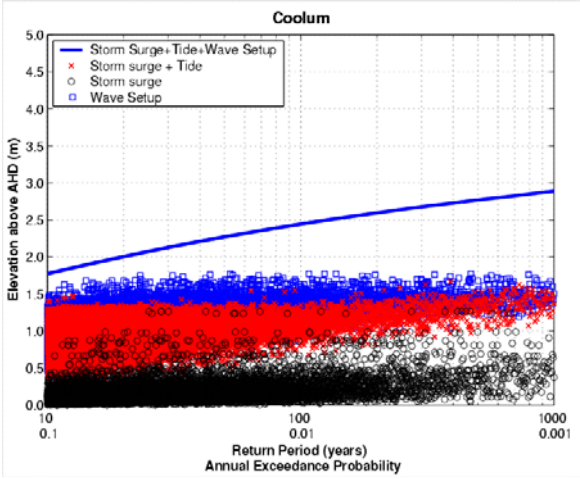

Figure 17a. Components of the storm tide return period curve at *Coolum*, Sunshine Coast

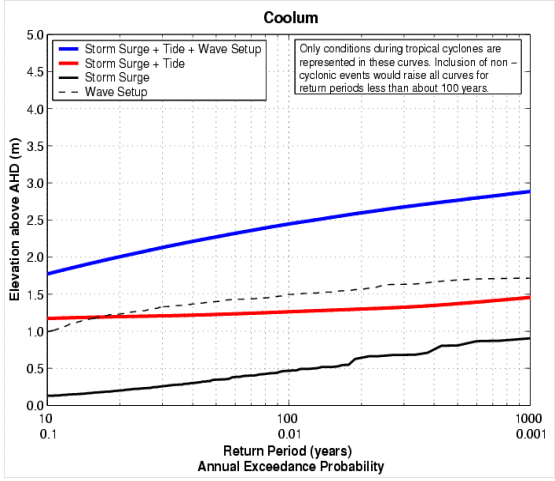

Figure17b. Return period of storm tide, storm surge + tide, storm surge, and wave setup at *Coolum*, Sunshine Coast

In Figure 17b, in addition to the storm tide curve (blue), three separate return period curves are shown for (i) storm surge plus tide (red), (ii) storm surge (solid black) and (iii) wave setup (dashed black). Note that the separate curves (surge plus tide and wave setup) do not add, at a given return period, to produce the storm tide curve. The maximum wave setup and maximum storm surge of a single storm do not necessarily have the same return period, and the maximum storm tide during a storm is the maximum of the sum of the tide, surge and wave setup. This is not the same as the sum of the maximums, which may occur at different times during the storm. Figure 17b highlights again that wave setup is more important than storm surge at the Sunshine Coast. The open coast and relatively narrow continental shelf of the Sunshine Coast allow larger waves but reduce storm surge. The storm surge and wave setup curves are less smooth than are the storm tide or surge plus tide curves, since only three points exist above the 500 year level in the storm surge and wave setup curves as compared with the 1500 points in the surge plus tide and storm tide curves.

Figures 18a and 18b show the same information as Figures 17a and 17b, but this time for *Torquay* at Hervey Bay. The protection provided by Fraser Island from the commonly occurring southeasterly wave directions and the wider continental shelf reduce the wave energy inside the bay and thus reduce the wave setup in comparison with Sunshine Coast locations. In Hervey Bay the wider continental shelf supports larger storm surge compared with that of Sunshine Coast locations. In Hervey Bay storm surge is more important than wave setup.

Return Period curves for storm tide, surge plus tide, surge and wave setup for the output points in Hervey Bay are presented in *Appendix A*, and for the output points at Sunshine Coast

in *Appendix B*. These same curves are also displayed in the *Atlas of Physical Processes in the Great Barrier Reef World Heritage Area* that is located on the *MMU* web site (http://mmu.jcu.edu.au).

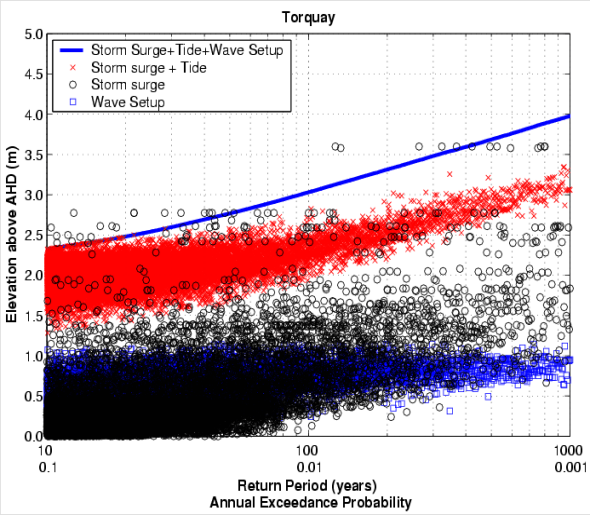

Figure 18a. Components of the storm tide return period curve at *Torquay*, Hervey Bay

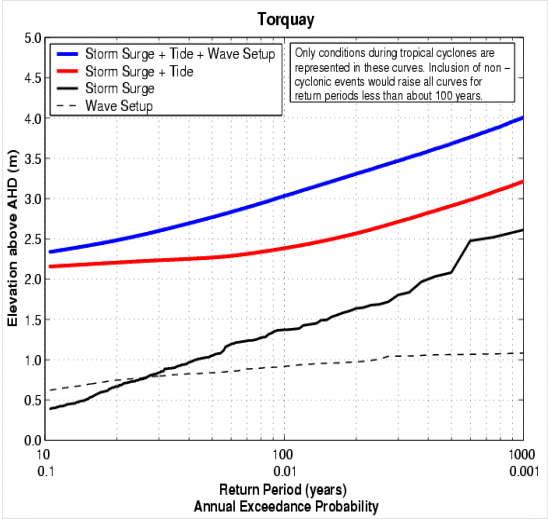

Figure18b. Return period of storm tide, storm surge + tide, storm surge, and wave setup at *Torquay*, Hervey Bay

Tables 4 and 5 summarise the results shown in *Appendices A* and *B* for storm tide return periods for output locations (Figures 1 and 2) at Hervey Bay and Sunshine Coast, respectively. Note that wave setup is not included for locations that are in highly sheltered locations. These include *Burrum River, Mangrove Point* and *River Heads* in Hervey Bay and *Golden Beach* at Sunshine Coast. The resolution of the wave modelling used in this project cannot accurately predict waves in these highly protected locations. Also, wave energy will be very much reduced in these areas; therefore, wave setup will be an insignificant component of the storm tide.

Recall that this study produces results *during tropical cyclones* and these are relatively rare in the southeast corner of Queensland. Non-cyclonic events will dominate the return period curve at lower return periods; therefore, a curve that included non-cyclonic events would be higher than those shown in this report for return periods less than about 100 years.

Table 4. Return periods of storm tide: 2004 and combined greenhouse scenarios: Hervey Bay

	Storm Tide (m, AHD) for three return periods:					
	100 year		500 year		1000 year	
Location	2004	Green house	2004	Green house	2004	Green house
Burrum Heads	2.79	3.29	3.46	4.17	3.73	4.55
Burrum River *	2.24*	2.82*	2.87*	3.62*	3.16*	4.01*
Dundowran Beach	2.96	3.54	3.69	4.45	4.03	4.85
Mangrove Point *	2.54*	2.91*	3.12*	3.65	3.36*	4.02*
Point Vernon West	2.98	3.55	3.66	4.39	4.00	4.81
Point Vernon	3.02	3.56	3.68	4.36	3.99	4.73
River Heads *	2.62*	3.08*	3.30*	3.93*	3.58*	4.32*
Scarness	3.11	3.68	3.82	4.55	4.15	4.95
Toogoom East	3.00	3.57	3.75	4.50	4.07	4.90
Toogoom	2.88	3.59	3.58	4.52	3.88	4.89
Torquay	3.03	3.59	3.68	4.38	4.01	4.77
Urangan Boat Hr.	2.93	3.46	3.51	4.18	3.75	4.52
Urangan	2.98	3.50	3.58	4.23	3.83	4.57
Woodgate	2.95	3.45	3.55	4.22	3.79	4.56

*Storm surge plus tide levels only. Wave setup not included

Table 5. Return periods of storm tide: 2004 and combined greenhouse scenarios: Sunshine Coast

	Storm Tide (m, AHD) for three return periods:					
	100 year		500 year		1000 year	
Location	2004	Green house	2004	Green house	2004	Green house
Buddina	2.55	3.02	2.90	3.40	3.02	3.53
Caloundra	2.55	3.07	2.98	3.52	3.10	3.66
Coolum	2.44	2.88	2.76	3.21	2.88	3.33
Golden Beach *	1.05*	1.50*	1.29*	1.88*	1.41*	2.03*
Maroochy River	2.50	2.96	2.86	3.33	2.98	3.47
Mooloolaba	2.37	2.80	2.63	3.11	2.74	3.23
Noosa	2.29	2.71	2.61	3.03	2.68	3.16
Sunshine Beach	2.61	3.09	3.01	3.49	3.15	3.62
Teewah	2.61	3.08	3.05	3.49	3.19	3.64
Woorim	2.29	2.78	2.61	3.18	2.75	3.34

*Storm surge plus tide levels only. Wave setup not included

6.3 Results: Waves During Tropical Cyclones

Data sheets for wave reporting points (Figures 19a and b) are provided in *Appendix C* (Hervey Bay) and *D* (Sunshine Coast), respectively. The data sheets have a location map and five data plots: (a) return period of H_s, (b) encounter probability of H_s, (c) polar plot of H_s as a function of direction, (d) polar plot of T_p as a function of direction, and (e) scatter plot of H_s vs T_p. Sample data sheets to illustrate the model output are presented in Figure 20 (*Burnett Heads Waverider Buoy* – Hervey Bay) and Figure 21 (*Mooloolaba Waverider Buoy* – Sunshine Coast).

The *encounter probability* P_E of a given wave height, H_s, is defined as the probability that an *equal or greater* wave height occurs *within a given length of time*, L, which for design is often selected to be the *design life* of the facility. The formula for encounter probability for a given value of significant wave height is a function of return period (R) and time period (L) is

$$P_E(H,L) = 1 - e^{-\frac{L}{R}}. \tag{28}$$

In Figures 20b and 21b and in *Appendices C* and *D* encounter probability is plotted as a function of significant wave height. Four encounter probability curves are presented, one each for L = 10, 20, 50 and 100 years. For example in Figure 20, a significant wave height of H_s = 8 m has probabilities of approximately 0.62 and 0.18 of being exceeded at least once during 50 and 10 years, respectively. The probability of exceeding any level increases as the time period lengthens.

Wave directions in Figures 20(c) and (d) and 21(c) and (d) are specified as the direction *from which* the waves are coming.

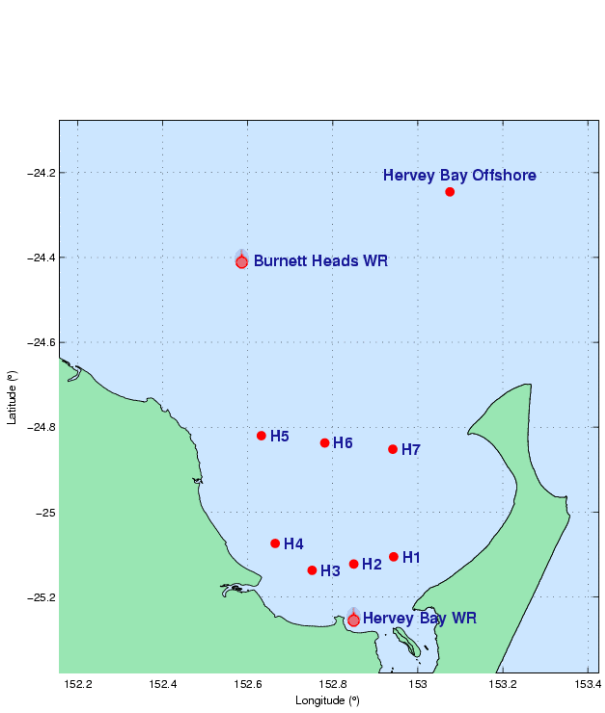

a) Hervey Bay

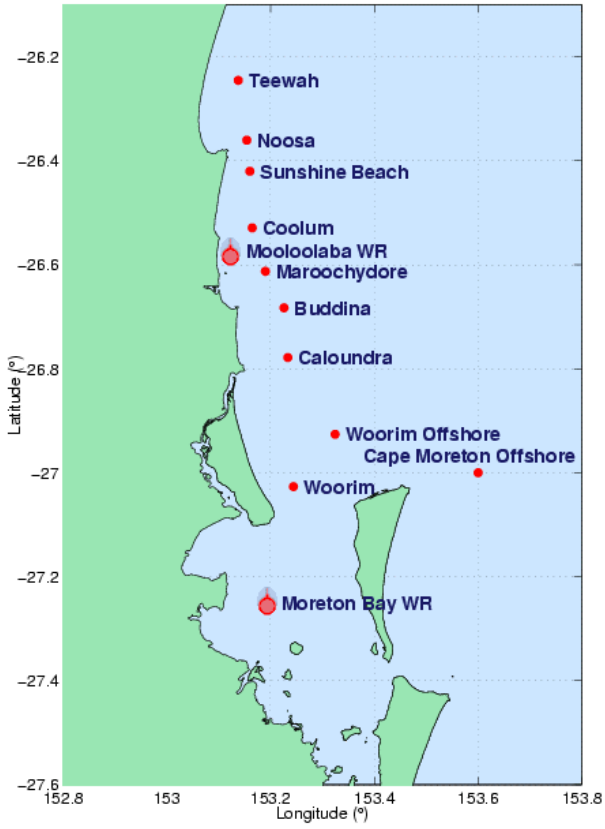

b) Sunshine Coast

Figure 19. Locations for wave information: Hervey Bay and Sunshine Coast

For *Burnett Heads WR* at Hervey Bay (Figure 20), note that depth-limitation of wave energy from shallow water wave breaking begins at about H_s = 12 m (Figure 20a). (Wave breaking begins if the significant wave height is larger than ½ the water depth.) Also the sheltering of this location by Fraser Island is evident as none of the more severe wave conditions are from the southeast (Figures 20c and d). The wave directions are widely spread from about 330° to about 90°. The orientation of the coastline north of Fraser Island allows wave energy to come from northerly directions. The largest waves come from between 30° and 90°. The locations farther inside Hervey Bay (see wave data sheets in *Appendix C*) are more sheltered than the *Burnett Heads WR*; and therefore, have reduced wave energy. Location *Hervey Bay Offshore*

(Figure C11), which is the farthest offshore and more out of the lee of Fraser Island, has the largest modelled significant wave height in this project (Hs = 27 m) and the widest spread of directions, 330° to 120°. The wave energy here is greater than that for the Sunshine Coast offshore locations (see below) since this site is both more open to the north and more northerly, both of which are conducive to a higher frequency of stronger tropical cyclones.

Results of significant wave height and peak period for return periods of 100 and 500 years are presented in Tables 6 and 7 for Hervey Bay and Sunshine Coast, respectively.

Table 6. Significant wave height and peak period for selected return periods: Hervey Bay

				100 years		**500 years**	
Location (Fig. 20a)	**Lat (°)**	**Long (°)**	**Depth (m)**	H_s **(m)**	T_p **(s)**	H_s **(m)**	T_p **(s)**
Burnett Heads WR	153.0756	-24.2451	24	9.63	12 – 16	12.01	15 – 18
Hervey Bay WR	152.8500	-25.2500	9	3.28	7 – 13	3.45	7 – 17
H1	152.9432	-25.1057	16	5.61	9 – 11	7.18	11 – 13
H2	152.8494	-25.1228	15	5.68	9 – 11	7.42	11 – 15
H3	152.7514	-25.1377	16	5.50	9 – 11	7.33	11 – 15
H4	152.6646	-25.0741	16	5.92	10 – 15	7.99	12 – 18
H5	152.6320	-24.8200	24	7.07	10 – 14	9.67	15 – 17
H6	152.7812	-24.3271	26	6.27	9 – 15	8.00	11 – 17
H7	152.9411	-25.852	24	6.40	11 – 15	8.60	14 – 18
Hervey Bay Offshore	152.5917	-24.4066	24	11.3	12 - 18	16.47	8 - 15

As expected the wave periods near to a given level of significant wave height have a wide range of values as can be seen in Figure 20e and in Table 6. At *Burnett Heads WR* the peak periods range from about 15s to about 18 s. The range of periods increases as wave height decreases.

The results at the *Mooloolaba WR* – Sunshine Coast (Figure 21) have many similarities with those at *Burnett Heads WR*. The wave directions along the Sunshine Coast are in a tighter band than those at Hervey Bay. Like Hervey Bay, most of the Sunshine Coast locations are also protected from the southeast (by Moreton Island). But unlike Hervey Bay no large waves come from the north due to the orientation of the coastline. The locations at the Sunshine Coast farthest away from Moreton Island (e.g., *Teewah* south to *Caloundra*) have wave directions from 60° to 90°. However directions swing to the North and the wave energy decreases for locations in the lee of Moreton Island (*Woorim Offshore, Woorim*, and *Moreton Bay*). Waves at the *Cape Moreton Offshore* location (Figure D12) display the most unsheltered energy for Sunshine Coast locations, similar to *Hervey Bay Offshore* in directions (spread from 0° to 150°), but reduced in wave height for reasons discussed above.

In the vicinity of the 500 year level, the storm tide return period curve has a much higher density of points than does the wave height curve. For storm tide, multiple events were created from each simulated storm by combining with 500 tides. This was not needed for wave height. So for storm tide, the 500 year level is the 3000th largest at each location, whereas the 500 year return period wave heights are only the 6th largest. Thus the results at the top end of the significant wave height return period curves (500 to 1000 years) have much more random variation than do the results for storm tide. Note in Table 7 that *Cape Moreton*

Offshore, as expected by its less sheltered location, has the largest 100 year significant wave heights for the Sunshine Coast region, but other more northerly points (*Teewah*, *Sunshine Beach,* and *Noosa* have larger waves at the 500 year return period. This may be a result of this random variation. However the frequency of more severe storms will also increase in a northerly direction, and this could also have more of an effect at the top end of the return period curves.

Table 7. Significant wave height and peak period for selected return periods: Sunshine Coast.

				100 years		**500 years**	
Location (Fig. 20b)	**Lat (°)**	**Long (°)**	**Depth (m)**	H_s **(m)**	T_p **(s)**	H_s **(m)**	T_p **(s)**
Mooloolaba WR	153.1318	-26.5724	27	9.01	12 - 19	13.08	14 – 19
Moreton Bay WR	153.2	-27.2500	14	2.48	7 - 10	3.00	8 – 10
Buddina	153.2259	-26.6828	34	9.28	11 - 19	12.71	14 - 19
Caloundra	153.2334	-26.7784	30	8.94	11 - 16	12.01	13 – 19
Coolum	153.1647	-26.5291	34	9.64	12 - 19	13.67	15 – 19
Maroochydore	153.1901	-26.6127	32	9.22	11 - 19	12.98	14 – 19
Noosa	153.1542	-26.3604	35	9.66	12 - 19	15.11	16 – 19
Sunshine Beach	153.1602	-26.4201	34	9.84	12 - 19	14.91	16 – 19
Teewah	153.1378	-26.5724	36	9.49	12 - 19	15.68	14 – 19
Woorim	153.2438	-27.0277	18	4.53	9 – 14	4.90	9 – 12
Woorim Offshore	153.3244	-26.9262	31	7.93	11 - 17	10.49	13 - 19
Cape Moreton Offshore	153.6000	-27.000	147	10.41	12 - 19	13.91	14 - 19

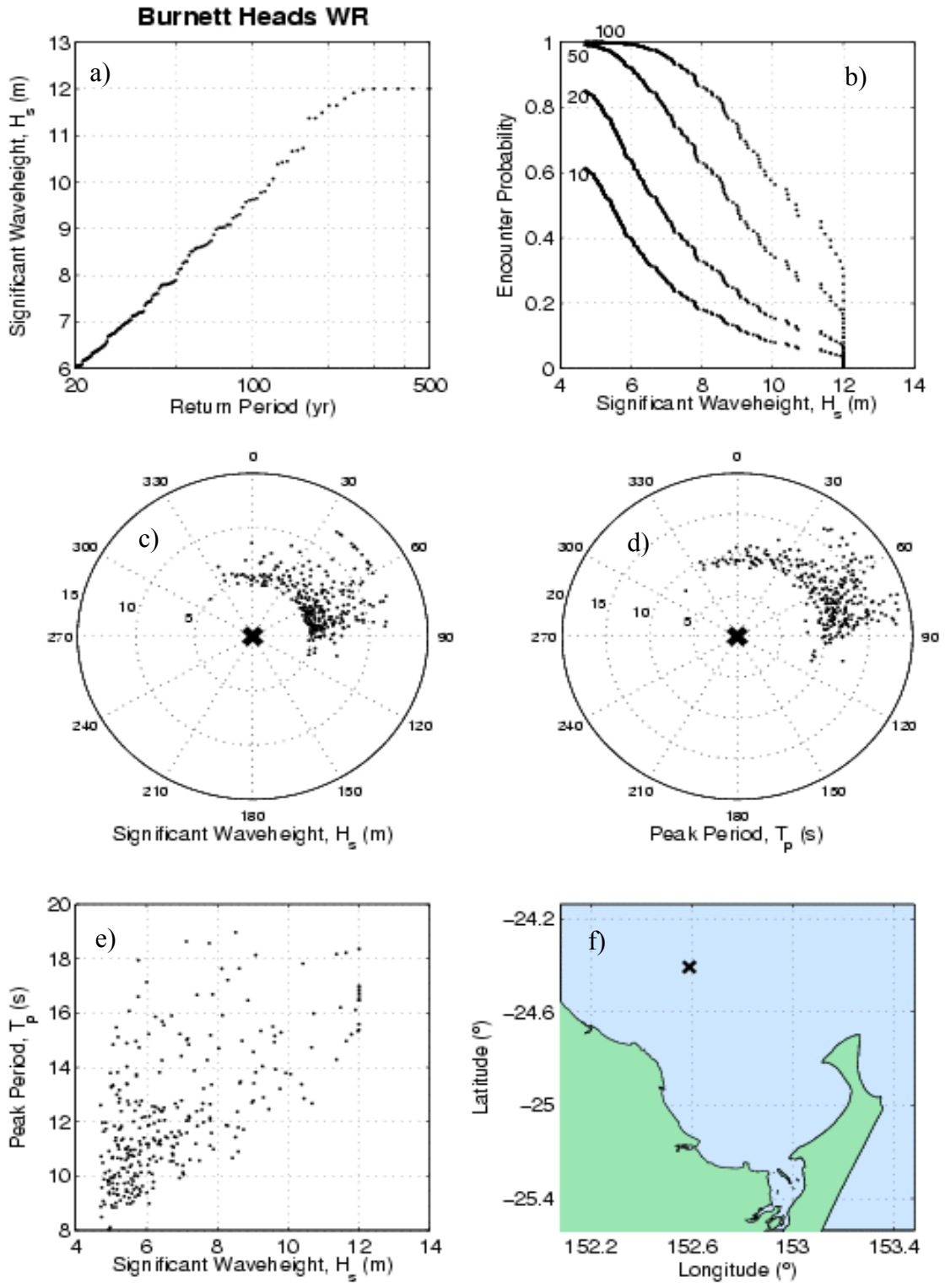

Figure 20. Sample data sheet for wave modelling output- *Burnett Heads WR*– Hervey Bay. (a) return period of H_s, (b) encounter probability of H_s for L = 10, 20, 50 and 100 years (c) polar plot of H_s as a function of direction, (d) polar plot of T_p as a function of direction, (e) scatter plot of H_s vs T_p, (f) location map

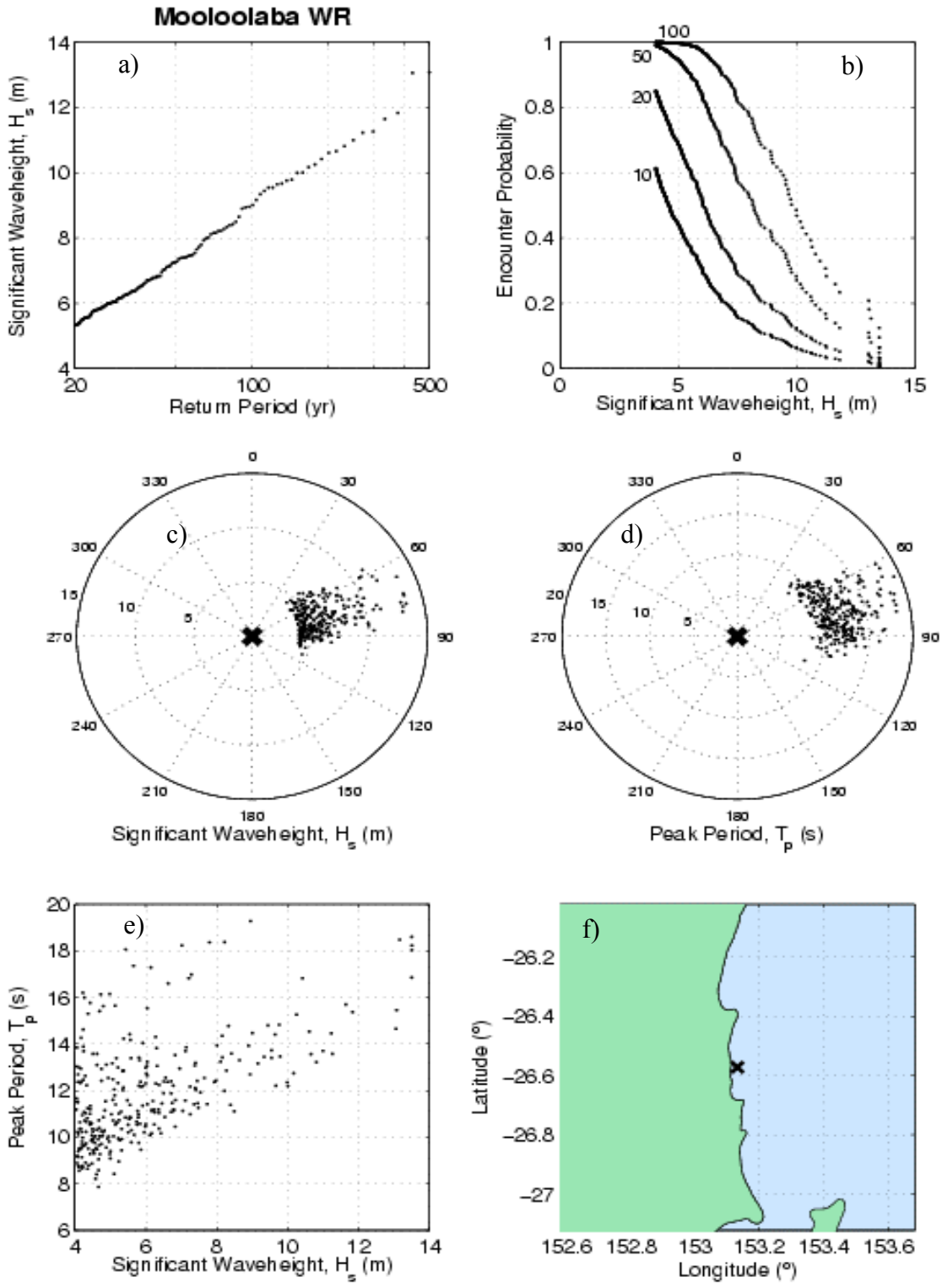

Figure 21. Sample data sheet for wave modelling output-*Mooloolaba WR* - Sunshine Coast. (a) return period of H_s, (b) encounter probability of H_s for L = 10, 20, 50 and 100 years (c) polar plot of H_s as a function of direction, (d) polar plot of T_p as a function of direction, (e) scatter plot of H_s vs T_p, (f) location map..

7.0 GREENHOUSE SCENARIOS

It is well established that changes in atmospheric concentrations of the so-called greenhouse gasses will change climate patterns. Both magnitude and frequency of waves and storm tides may be significantly affected by any changes in climate; therefore one of the tasks of this study is to simulate changes in wave and storm surge statistics for a few specified greenhouse scenarios. These are

A. Combined effect of an increase in Maximum Potential Intensity (MPI) of 10% and a poleward shift in tracks of 1.3°.

B. Increase in frequency of tropical cyclones of 10%.

C. Mean Sea Level rise of 300 mm.

It is very important to emphasise here that we are *not* endorsing these chosen values, although care has been taken to propose reasonable values. Rather the intention is to demonstrate the sensitivity of the wave and storm tide frequency curves to these climate change scenarios.

7.1 Increase in Intensity and Poleward Shift of Tracks: Scenario A

Unlike a change in MSL or a change in frequency of tropical cyclones, changes in either intensity or track imply changes in the ensemble of storms; therefore, these changes require the re-simulation of the ensemble. Since re-simulation of almost 10,000 storms on both wave and storm surge models is an expensive exercise, these two Greenhouse enhancements were combined and simulated together.

An increase of 10% in the Maximum Potential Intensity (MPI) was chosen for simulation following the advice from the IWTC-V (International Workshop on Tropical Cyclones, Cairns December 2002) (B. Harper, personal communication). As with the changes in frequency of tropical cyclones, an increase in intensity of tropical cyclones is uncertain. Although theoretical models (Emanuel, 1988; and Holland, 1997) indicate intensification with a warmer climate, other considerations (e.g. vertical shear) may temper the magnitude of any intensification (Walsh and Ryan, 2000). The 10% value is considered an upper estimate.

This assumed increase in MPI was simplified to a generalised 10% increase of intensity for our tests by the following formulas, which alter the central pressure of the synthetic tropical cyclones. The greenhouse-induced central pressures became

$$p_{0*} = p_{\infty} - \Delta p_{*}\,, \tag{29}$$

where

$$\Delta p_{*} = 1.1\left(p_{\infty} - p_{0}\right). \tag{30}$$

This transformation was applied at each time step of the time series of central pressures of the synthetic tropical cyclone ensemble.

Walsh and Katzfey (2000) used a regional climate model to simulate the response of the tropical cyclone formation and movement under a doubling of the CO_2 concentration. They found a slight poleward shift in genesis points and a slight poleward shift in track and these could be approximated with a 1.3° poleward shift in track.

7.2 Increase in Frequency of Tropical Cyclones: Scenario B

A Greenhouse induced increase in the frequency of tropical cyclones was assumed to be 10% based on discussions at the recent International Workshop on Tropical Cyclones (IWTC-V) held in December 2002 in Cairns (B. Harper, personal communication). Of the four Greenhouse enhancements tested the change in frequency has the least certainty. As with the change in MSL, the effects of changes in the frequency of tropical cyclones can be posted-processed, i.e. there is no need to re-simulate either waves or storm surge. The Greenhouse enhanced frequency of tropical cyclones, given a 10% increase is

$$\begin{aligned} \lambda_{c+} &= 1.10\lambda_c \\ &= (1.10)(3.2727) \\ &= 3.6 \text{ T. C. per year} \end{aligned} \tag{31}$$

This higher frequency translates into a period (n_+) shorter than 3000 years in which the M = 9818 tropical cyclones occur. The new record length becomes

$$\begin{aligned} n_+ &= \frac{M}{\lambda_{c+}} \\ &= \frac{9818}{3.6} = 2727 \text{ years} \end{aligned} \tag{32}$$

Thus for a given magnitude of either wave height or water level, the rank (value of m) does not change, but the return period of that magnitude does change. The Greenhouse enhanced return period is given as (for the example of water level, η)

$$\begin{aligned} R_{\eta+} &= \frac{1}{\lambda_{\eta+}} \\ &= \frac{1}{m/n_+} = \frac{1}{m/2727} \end{aligned} \tag{33}$$

The frequency and return period under the Greenhouse enhanced tropical cyclone frequency of 10%, as a function of existing frequency and return period, become

$$\begin{aligned} \lambda_{\eta+} &= 1.10\lambda_\eta \\ R_{\eta+} &= 0.909R_\eta \end{aligned} \tag{34}$$

Therefore, at a given water level, the return period curve for enhanced Greenhouse conditions is shifted towards lower return periods.

7.3 Mean Sea Level Rise: Scenario C.

A MSL rise of 300 mm is assumed. This is predicted to be the upper envelope of the rise in MSL by 2050 (IPCC, 2001). For this level of mean sea level rise, the effect on magnitudes of storm tide at the coast will be approximated as a linear addition to the return period curve that has been developed for present conditions. In other words the water level, at all return periods, increases by an amount equal to the chosen value of sea level rise. Other MSL rise scenarios can be easily adopted by the linear addition of the chosen value.

Of course, changes in MSL will have some nonlinear affects on storm tide levels. Holding all other thing constant, deeper water reduces storm surge, since the slope of the water surface caused by wind stress is inversely proportional to the water depth. The effect on wave setup is more complex and deeper water could actually result in higher setup levels. Nevertheless

these nonlinear effects are assumed to be much smaller than the linear effect of a sea level rise. The likely significant changes in beach slope and shoreline position (recession) that would result from a rise in sea level were not considered.

7.4 Greenhouse Storm Tide Results

Examples of return period curves for storm tide for the greenhouse scenarios are given in Figures 22 and 23 for *Torquay* and *Coolum*. The full set of results of the greenhouse simulations of storm tide are shown in *Appendix E* and *Appendix F* for Hervey Bay and Sunshine Coast, respectively.

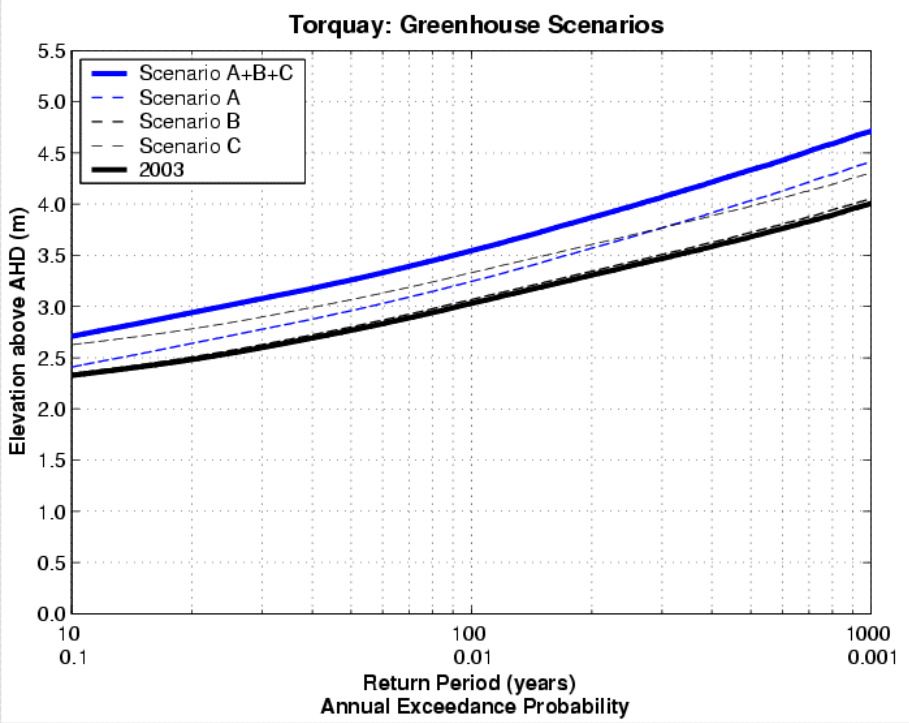

Figure 22. Storm tide for greenhouse scenarios – *Torquay*, Hervey Bay. (A) Combined effect of an increase in Maximum Potential Intensity (MPI) of 10% and a poleward shift in tracks of 1.3°. (B) Increase in frequency of tropical cyclones of 10%. (C) Mean Sea Level rise of 300 mm.

The 10% increase in the frequency of tropical cyclones (Scenario *B*) elevates the curve only an inconsequential amount at all locations in both study areas. At low to medium return periods, mean sea level rise (Scenario *C*) has the most significant effect of the three scenarios at all locations. For locations where wave setup is more important than storm surge (e.g. the open coast Sunshine Coast locations) mean sea level change remains the most important even at higher return periods. Note that at Caloundra on the Sunshine Coast, which has a wider inner shelf and storm surge is larger than at northern Sunshine Coast locations with a narrower shelf), the curves for mean sea level rise (Scenario *C*) and combined poleward shift and increase in intensity (Scenario *A*) merge at higher return periods.

In Hervey Bay the wider shelf and protection from waves means that surge is much larger than wave setup. The curve for combined poleward shift and increase in intensity (Scenario *B*) becomes higher than the mean sea level rise (Scenario *C*) curve at about $R = 300$ years as the *increase* in storm surge becomes larger than the *increase* in mean sea level. At first one would think that both storm surge and wave setup would increase with increasing return period (storm intensity). This is true, however, wave setup increases much more slowly with

increasing storm intensity as depth-limited wave breaking moves much of the hydrodynamic action farther offshore.

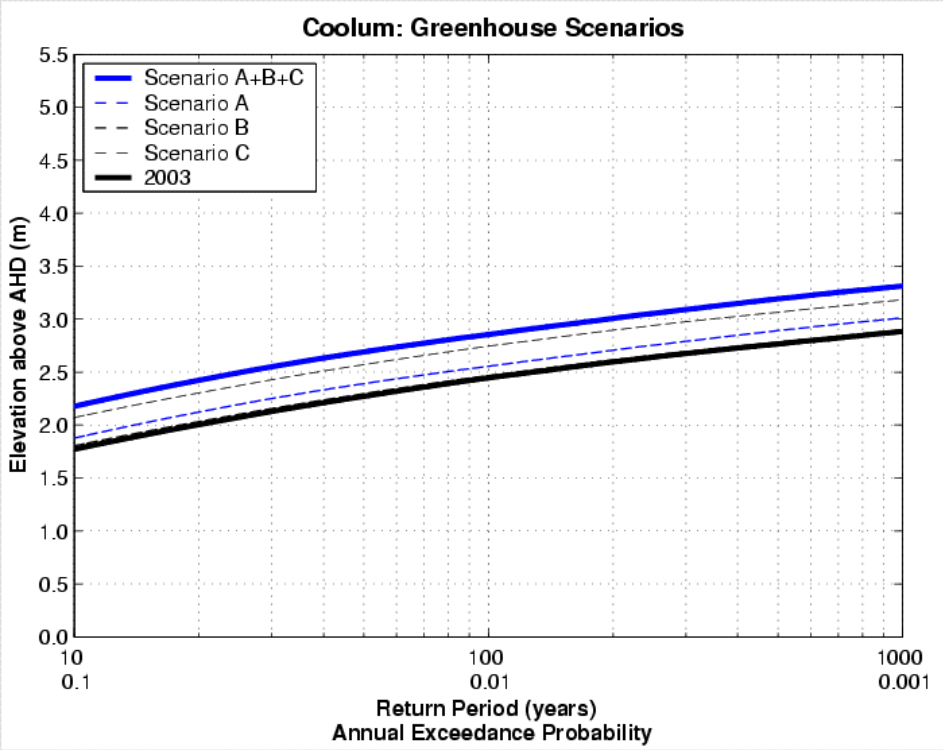

Figure 23. Storm tide for greenhouse scenarios – *Coolum*, Sunshine Coast. A) Combined effect of an increase in Maximum Potential Intensity (MPI) of 10% and a poleward shift in tracks of 1.3°. (B) Increase in frequency of tropical cyclones of 10%. (C) Mean Sea Level rise of 300 mm.

In general, the greenhouse curves formed from the combinations of all three scenarios increase the storm tide curve at Hervey Bay from about 0.5 to 0.6 m at R = 10 years to 0.8 to 0.9 m at R = 3000 years. For the Sunshine coast greenhouse and 2003 curves are more parallel with a greenhouse increase of about 0.5 m at all return periods.

Again it must be emphasised that these greenhouse tests are not meant to be a prediction of what is expected, but rather to provide some insight to the relative magnitudes of the most commonly cited greenhouse induced water level changes.

8.0 CONCLUSIONS AND DISCUSSION

The frequencies of storm tide and waves during tropical cyclones were determined for the Hervey Bay and Sunshine Coast regions of southeast Queensland, Australia. The goal was to produce return period curves for storm tide (storm surge plus wave setup plus astronomical tide) and for significant wave height for return periods between 10 and 1000 years.

A series of sophisticated models was employed. First a tropical cyclone track and pressure model produced a synthetic dataset consisting of the time series of position and pressure for almost 10,000 storms. This represents 3000 years of data for the western Coral Sea. Numerical models with three nested grids with increasing spatial resolution for both storm surge and wave generation were established for the study areas. The storm surge model had been validated in Phase 1 of this overall study. The wave model was validated by comparing measurements and modelled significant wave heights during *T. C. Simon* (1980). It was computationally impossible to model all 10,000 storms to the needed resolution; therefore, a system was developed to determine which storms would contribute to returns periods above 10 years. To do this all storms were modelled on the less computationally expensive coarse grids for both storm surge and waves. The most severe results on these coarse simulations were used to cull the number of storms to be modelled on the finer resolution grids from 10,000 to about 500 for each of the two study areas.

Wave setup was calculated as a function of wave height and peak wave period using an empirical formula. Wave setup is the most uncertain of all the components since the surf zone width during a severe tropical cyclone would be very much wider than those used to derive the empirical wave setup formula. Although all other components of this study received state-of-the-art treatment it was infeasible to do this for the wave setup. The physical scale over which bathymetry can affect wave setup is on the order of metres. At the same time the width (onshore – offshore) of surf zones during severe tropical cyclone events can be larger than ten kilometres and the length of the each of the two study areas was tens of kilometres. State-of-the-art techniques would require phase-resolved numerical models and computer speeds are still several orders of magnitude too slow to use these techniques. At locations such as the Sunshine Coast where wave setup is more important that storm surge, developing state-of-the-art wave setup calculations has much more importance than at Hervey Bay where storm surge is the dominant component.

> **It is important to note that water levels created by wave setup will not translate far inland after overtopping frontal dunes, flowing overland over low lying areas, or proceeding through inlets. Once flow starts wave setup reduces markedly; therefore, the storm tide curves that include wave setup should apply only to areas with direct wave attack. For areas more than a couple hundred metres landward of the shoreline during the storm, a better estimate of potential flood levels is obtained from the storm surge plus tide return period curves. An overland flooding study might be necessary to provide definitive results for inland locations, especially if the inland floodable area is large.**

An astronomical tidal signal was created using tidal analyses. Each coupled set of storm surge and wave setup time series from a single storm were linearly added to 500 separate tidal time series. The tide series were randomly chosen (with a weighting to reflect the monthly change in cyclone frequency) from a long tidal record. The maximum water level and significant wave height during each storm-tide event were determined and these values were ranked by magnitude and return period curves were created.

Establishing a datum and a tidal range at the project output points caused considerable difficulty. Most of the output points were not at established tidal measurement stations. Hence the datum at a location was often transferred from the nearest tide station and these official values (that were provided to us) did not always provide the best tidal information at that location. Considerable time and energy was expended to check and recheck values of MSL, AHD and HAT. Some official values were updated during the project in consultation with Maritime Safety Queensland. In the end the decision was reached to model storm surge relative to the official MSL and use the official transfer from MSL to AHD.

In general storm surge is much more important in Hervey Bay with its broader continental shelf and protection by Fraser Island from severe wave directions. In Hervey Bay storm surge is up to twice the magnitude of wave setup at the 100 year level. For the Sunshine Coast with its narrower and more open shelf, wave setup is more important than storm surge. Wave setup is more than twice the magnitude of storm surge at the 100 year level.

The effect of greenhouse-induced climate change was investigated. Three separate scenarios were tested. These were (A) combined effect of an increase in maximum intensity (MPI) by 10% and a poleward shift in tracks of 1.3°. (B) increase in frequency of tropical cyclones of 10%. (C) mean sea level rise of 300 mm. In general the mean sea level rise is the most important effect especially at lower return periods. The 10% increase in tropical cyclone frequency is insignificant. The combined increase in intensity and poleward shift in tracks becomes increasingly significant with larger return periods. This is more evident in Hervey Bay where storm surge is more important than at Sunshine Coast where depth limitation reduces the effect of increased wave setup. Both the magnitude and probability of greenhouse-induced mean sea level rise are more certain than greenhouse-induced changes in tropical cyclone frequency, central pressure, or track.

Note that the results in this study are for tropical cyclone-induced water levels. For return periods below about 100 years, extra tropical events will be increasingly important; therefore, the combined curve of tropical and extra-tropical storm tides will be higher than the cyclone-induced storm tide curves shown in this report.

There are several different non-cyclonic influences that affect water levels that are not considered in this study. These include not only non-cyclonic winds, low pressures and waves during storms, but non-storm events such as changes in oceanic currents and continental shelf waves which can also alter water levels.

For all project reporting locations, the occurrence of a tropical cyclone was defined as any that occurred in the western Coral Sea regardless of its distance from the location. This has the property of merging the return period curve for tropical cyclone-induced storm tide into the return period curve for astronomical tide at the lower end of the curves. A more selective definition of tropical cyclone occurrence would have caused the return period curve of storm tide to decrease rapidly (sometimes below HAT) at the lower end of the curve. This definition was used to avoid any misinterpretation of the frequency of water levels at return periods that may be dominated by non-cyclonic events.

A caution is necessary on the possibility of water levels much higher than the 1000 year levels that are presented in this report. The occurrence of the probable maximum water level could have devastating consequences for a nearby community. Although the probability of occurrence is very rare, a calculation of the risk (probability times consequences) is an important component of both disaster and longer term land use planning.

The probable maximum water level at a given location would be caused by a tropical cyclone and tide with the following characteristics. (1) landfall point at a distance equal to the radius of maximum winds to the north, (2) very severe central pressure, (3) large radius to maximum winds, (4) forward speed of the eye equal to the short wave speed offshore and the long wave speed over the shelf, and very importantly, (5) an astronomic tide level that is close to HAT at the time of maximum surge plus wave setup. The combination of these characteristics would be very rare, but not impossible.

An estimate of the probable maximum level could be calculated by adding the largest storm surge and wave setup from the 3000 years of simulations to the HAT level. For example, this would result in a storm tide of about 4.1 m (AHD) at *Coolum*, Sunshine Coast (see Figure 17) and 6.7 m (AHD) at *Torquay*, Hervey Bay (see Figure 18). These are approximately 1 and 2 m, respectively above the 1000 year water levels. It must be emphasised that these probable maximum figures are only a rough estimate. The 3000 year storm surges and wave setups are not necessarily the largest possible (i.e. they don't meet the first four of the above criteria).

Wave information at near coastal and offshore sites was generated in both study areas. Sheltering from southeasterly wave directions by large Islands to the south of Hervey Bay and Sunshine Coast (Fraser Island and Moreton Island, respectively) was evident at all near coastal sites. The offshore Hervey Bay location, had the widest spread of directions and the largest significant wave heights at the 500 year level (16.5 m) as compared with the Sunshine Coast (14 to 15 m). The more northerly position and the more northerly aspect of the waters offshore from Hervey Bay is thought to allow larger waves from more frequent and more severe tropical cyclones.

9.0 **REFERENCES**

Bode, L. and Mason, L.B. 1994. Application of an implicit hydrodynamic model over a range of spatial scales, *Proc. 6th Comp. Tech. Applications Conf.* (CTAC93) D. Stewart *e tal.,* eds, World Scientific, River Edge, N.J., pp. 112-121.

Callaghan, J. 1996. Tropical Cyclone-Analyses of the Destructive Wind Zone. *Conference on Natural Disaster Reduction*, Surfers Paradise.

Cardone, V.J., Cox, A.T., Greenwood, J.A., Thompson, E.F., (1994) Upgrade of tropical cyclone surface wind field model, *Miscellaneous Paper CERC-94-14*, US Army Corps of Engineers, Waterways Experiment Station, 101pp.

Eanes, R.J. 1994. Diurnal and semidiurnal tides from TOPEX/POSEIDON altimetry. *Eos Trans. AGU*, Vol. 75 No. 16, pp. 108.

Efron, B. 1979. Bootstrap methods; another look at the jackknife, *The Annuals of Statistics*, Vol. 7, pp. 1-26.

Emanuel, K.A. 1988. The maximum intensity of hurricanes, *J .Atmospheric Science*, Vol. 45, pp. 1143-1155.

Gourlay, M.R. 1992. Wave setup, run-up and beach water table: Interaction between surf zone hydraulics and groundwater hydraulics, *Coastal Engineering,* Vol. 17, pp. 93-144.

Hanslow, D.J. and Nielsen, 1993. Shoreline setup on natural beaches. *J. Coastal Research, Special Issue* 15, pp. 1-10.

Hardy, TA, McConochie, JD, and Mason, LB. 2003. Modeling tropical cyclone wave population of the Great Barrier Reef, *Journal of Waterway, Port, Coastal and Ocean Engineering, Am. Soc. Civil Eng.*, Vol. 129, No. 2, pp. 104-113.

Hardy, TA, Mason, LB, and McConochie, JD. 2000. A wave model for the Great Barrier Reef, *Ocean Engineering*, Vol. 28, pp. 45-70.

Harper, B.A., Hardy, T.A., Mason, L.B. and McConochie, J.D. 2001. Cyclone *Althea* Revisited. *Coast & Ports 2001*, IEAust, pp. 140-145.

Harper, B.A., Hardy, T.A., Mason, L.B., Bode, L., Young, I.R. and Nielsen, P 2001. Queensland Climate Change and Community Vulnerability to Tropical Cyclones: Ocean Hazzards Assessment – Stage 1, Queensland Department of Natural Resources and Mines. P. 318.

Holland, G.J. 1980. An analytical model of the wind and pressure profiles in hurricanes, *Mon. Weath. Rev.*, Vol. 108, pp. 1212-1218.

Holland, G.J. 1981. On the quality of the Australian tropical cyclone database, *Aust.Met. Mag.* Vol. 29, pp. 169-81.

Holland, G.J. 1997. The maximum potential intensity of tropical cyclones, *J .Atmospheric Science*, Vol. 54, pp. 2519-2541.

IPCC 2001. Technical Summary, Climate Change 2001: Impacts, Adaptation and Vulnerability, a Report of Working Group II of the Intergovernmental Panel on Climate Change, Geneva, Switzerland.

James, M.K., and Mason, L.B. 1999. Generation of a synthetic tropical cyclone database. *Coasts and Ports '99*, IEAust, 407-412.

Komen, G.J., Cavaleri, L., Donelan, M., Hasselmann, H., Hasselmann, S., and Janssen, P., 1994. *Dynamics and Modeling of Ocean Waves*, Cambridge University Press, p. 532.

Madsen, P.A., Banijamali, B. Schjaffer, H.A., Sorensen, O. 1996. Boussinesq type equations with high accuracy in dispersion and nonlinearity, Proc. 25th Int. Conf. Coastal Eng, ASCE.

McConochie, J.D., Mason, L.B., and Hardy, T.A. 1999. A Coral Sea cyclone wind model intended for wave modelling, *Proc. Coasts & Ports '99*. IEAust, pp. 413-418.

McConochie, J.D., Hardy, T.A. and Mason, L.B. in press. Modelling Tropical Cyclone Over-Water Wind and Pressure Fields. *Ocean Engineering*, to appear.

Raubenheimer, B., Guza, R.T. and Elgar, S. 2001. Field observations of wave-driven setdown and setup, *J. Geophysical Research,* Vol. 106, No. C3, pp. 4629-4638.

Sobey, R.J., Harper, B.A., Stark, K.P., (1977) Numerical simulation of tropical cyclone storm surge along the Queensland Coast, *Research Bulletin CS14, Dept. Civil and Systems Engineer, James Cook University*.

Thompson, E.F. and Cardone, V.J. 1996. Practical modeling of hurricane surface wind fields, *J. Waterway, Port, Coastal ,and Ocean Eng.*, Vol. 122, No. 4, pp. 195-205.

Walsh, K.J.E and Katzfey, J.J. 2000. The Impact of Climate Change on the Poleward Movement of Tropcial Cyclone-Like Vortices in a Regional Climate Model, *J.* of *Climate*, American Meteorological Society, Vol. 13, pp. 1116-32.

Walsh, K.J.E. and Ryan, B.F. 2000. Tropical cyclone intensity increase near Australia as a result of climate change, *J. of Climate*, American Meterorolical Society, vol 13. no. 16, pp. 3029-36.

Wilders, P., van Stijn, Th.L., Stelling, G.S. and Fokkema, G.A. 1988. A fully implicit splitting method for accurate tidal computations. *International Journal for Numerical Methods in Engineering*, 26, 2707-2721.

Willoughby, H.E., Clos, J.A., and Shoreibah, M.G. 1982. Concentric eye walls, secondary wind maxima and the evolution of the hurricane vortex, *J. Atmospheric Science*, Vol. 39, pp. 395-411.

APPENDIX A

STORM TIDE RETURN PERIOD CURVES: HERVEY BAY

Return Period curves for storm tide, surge plus tide, surge and wave setup for the output points in Hervey Bay (Figure A1) are presented. These same curves are also displayed in the *Atlas of Physical Processes in the Great Barrier Reef World Heritage Area* which is located on the *MMU* web site (http://mmu.jcu.edu.au).

These curves are valid for water levels produced during tropical cyclones. Extra-topical storms and other meteorological and oceanic causes of water level change (not modelled here) will contribute to the return period of water levels at lower return periods.

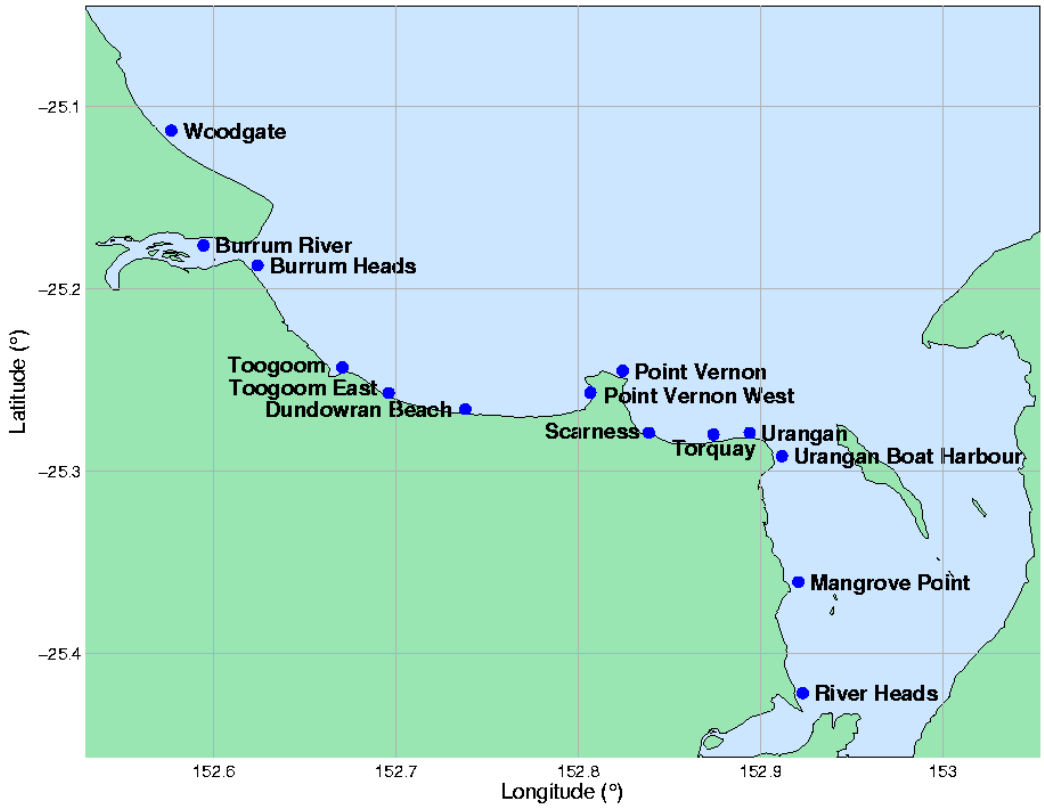

Figure A1. Hervey Bay study area and water level reporting locations

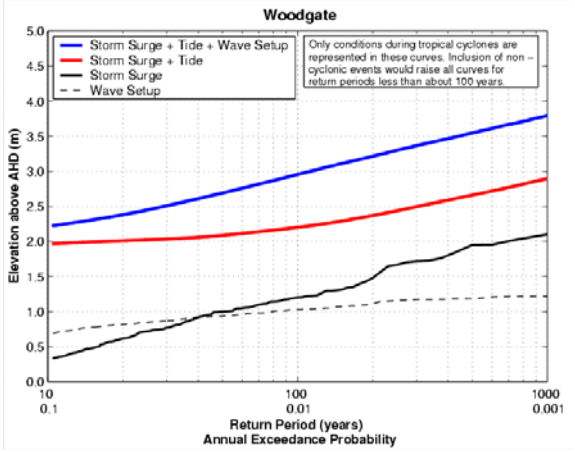

Figure A2. Water level frequency: Woodgate
HAT = 2.02

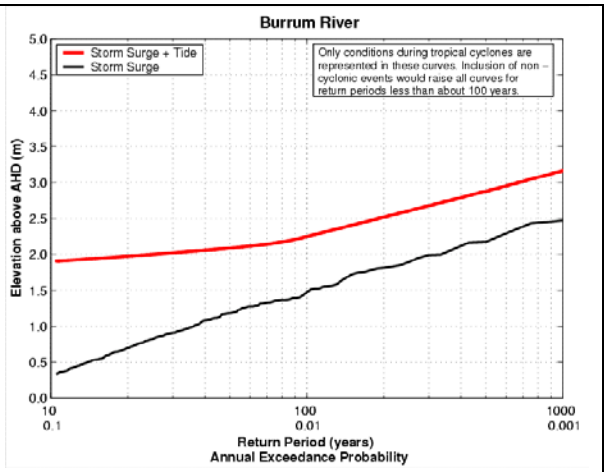

Figure A3. Water level frequency: Burrum River
HAT = 1.99 m

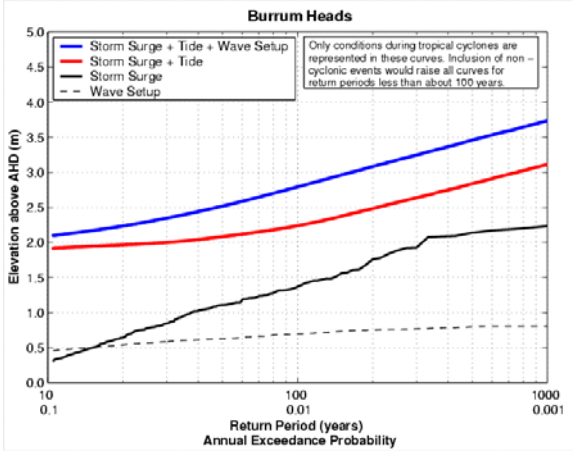

Figure A4. Water level frequency: Burrum Heads
HAT = 1.99 m

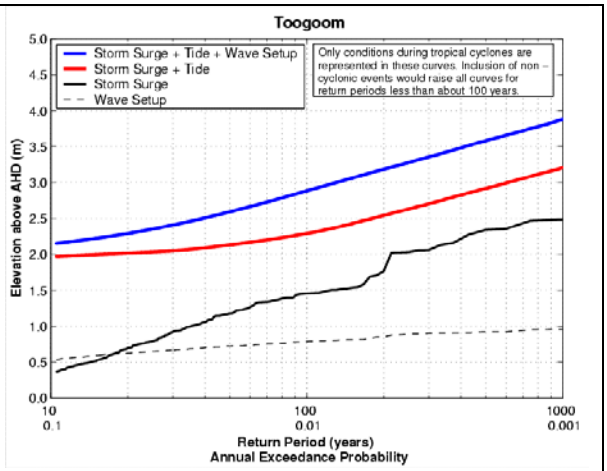

Figure A5. Water level frequency: Toogoom
HAT = 2.12 m

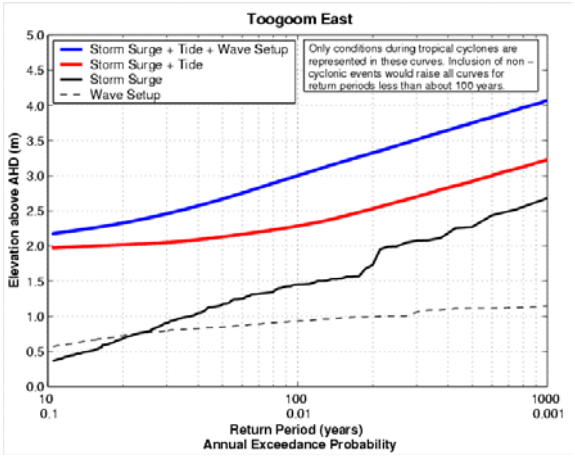

Figure A6. Water level frequency: Toogoom East
HAT =2.12

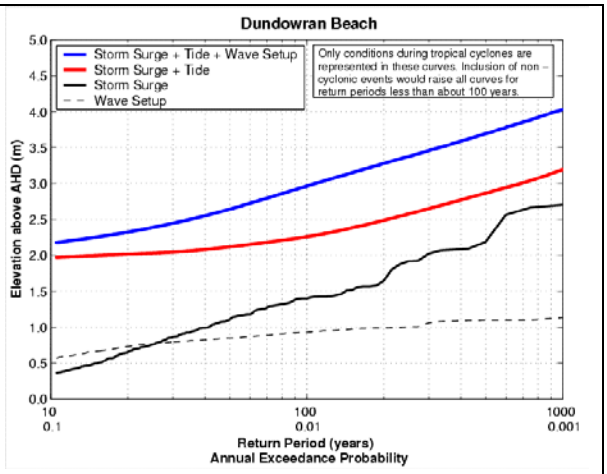

Figure A7. Water level frequency: Dundowran Beach
HAT = 2.12 m

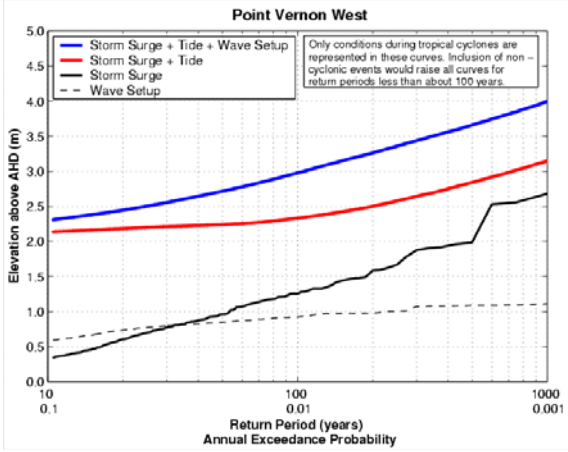

Figure A8. Water level frequency: Point Vernon West HAT = 2.12 m

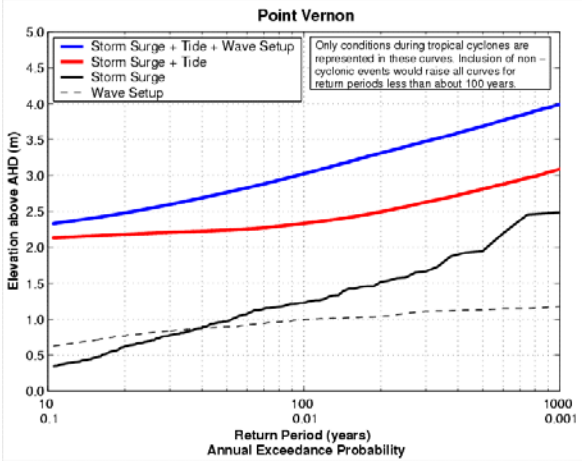

Figure A9. Water level frequency: Point Vernon HAT = 2.12 m

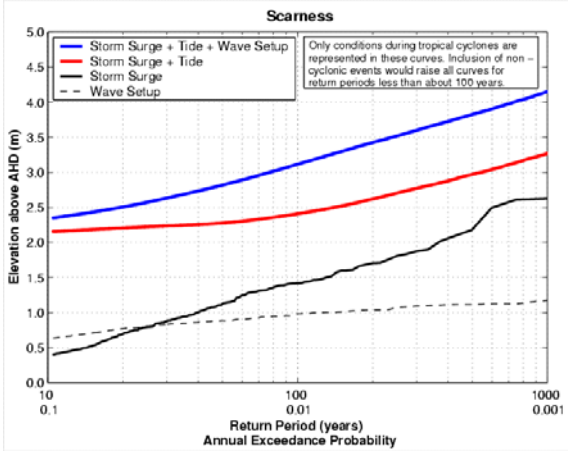

Figure A10. Water level frequency: Scarness HAT = 2.15 m

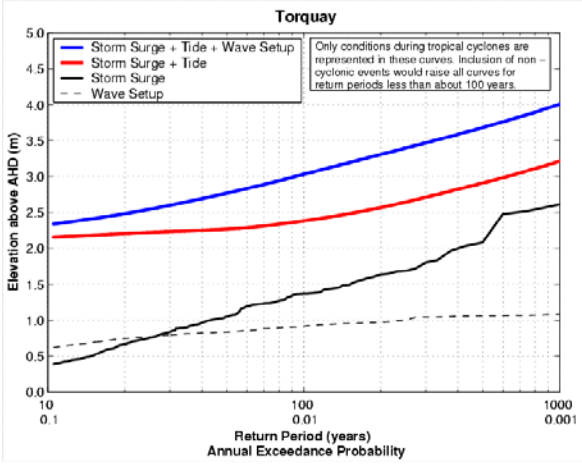

Figure A11. Water level frequency: Torquay HAT = 2.15 m

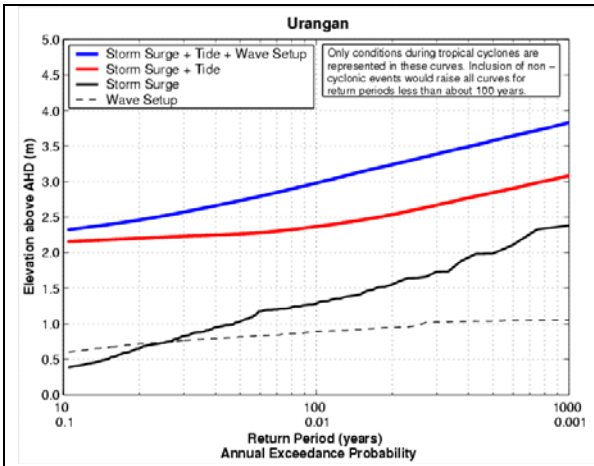

Figure A12. Water level frequency: Urangan HAT = 2.15 m

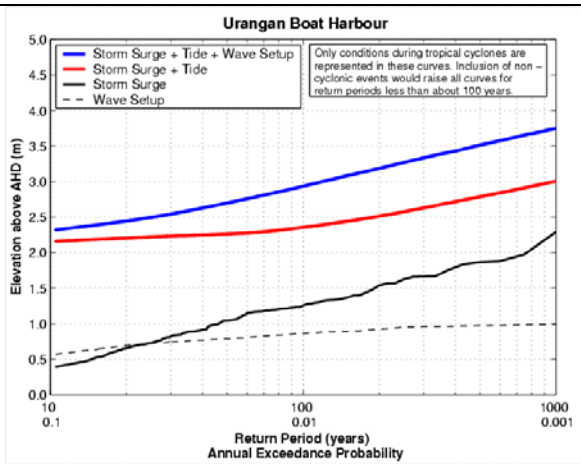

Figure A13. Water level frequency: Urangan Boat Hr. HAT = 2.15 m

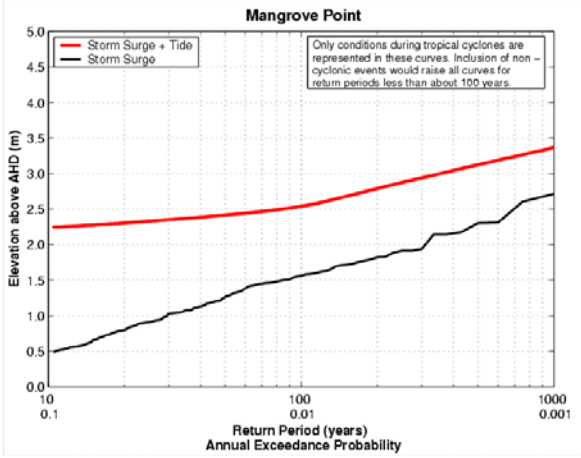

Figure A14. Water level frequency: Mangrove Point HAT = 2.63 m

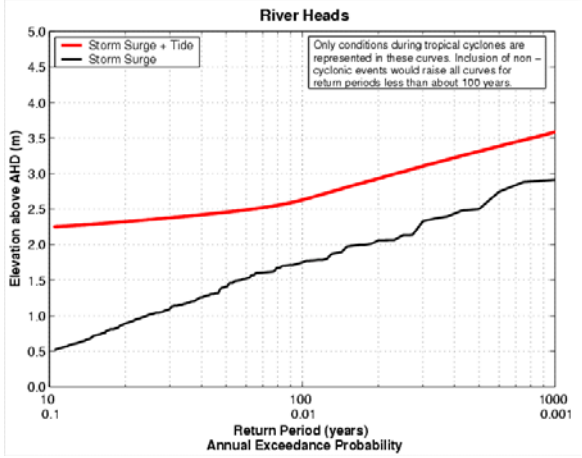

Figure A15. Water level frequency: River Heads HAT = 2.63 m

APPENDIX B

STORM TIDE RETURN PERIOD CURVES: SUNSHINE COAST

Return Period curves for storm tide, surge plus tide, surge and wave setup for the output points at Sunshine Coast (Figure B1) are presented. These same curves are also displayed in the *Atlas of Physical Processes in the Great Barrier Reef World Heritage Area* which is located on the *MMU* web site (http://mmu.jcu.edu.au).

These curves are valid for water levels produced during tropical cyclones. Extra-topical storms and other meteorological and oceanic causes of water level change (not modelled here) will contribute to the return period of water levels at lower return periods.

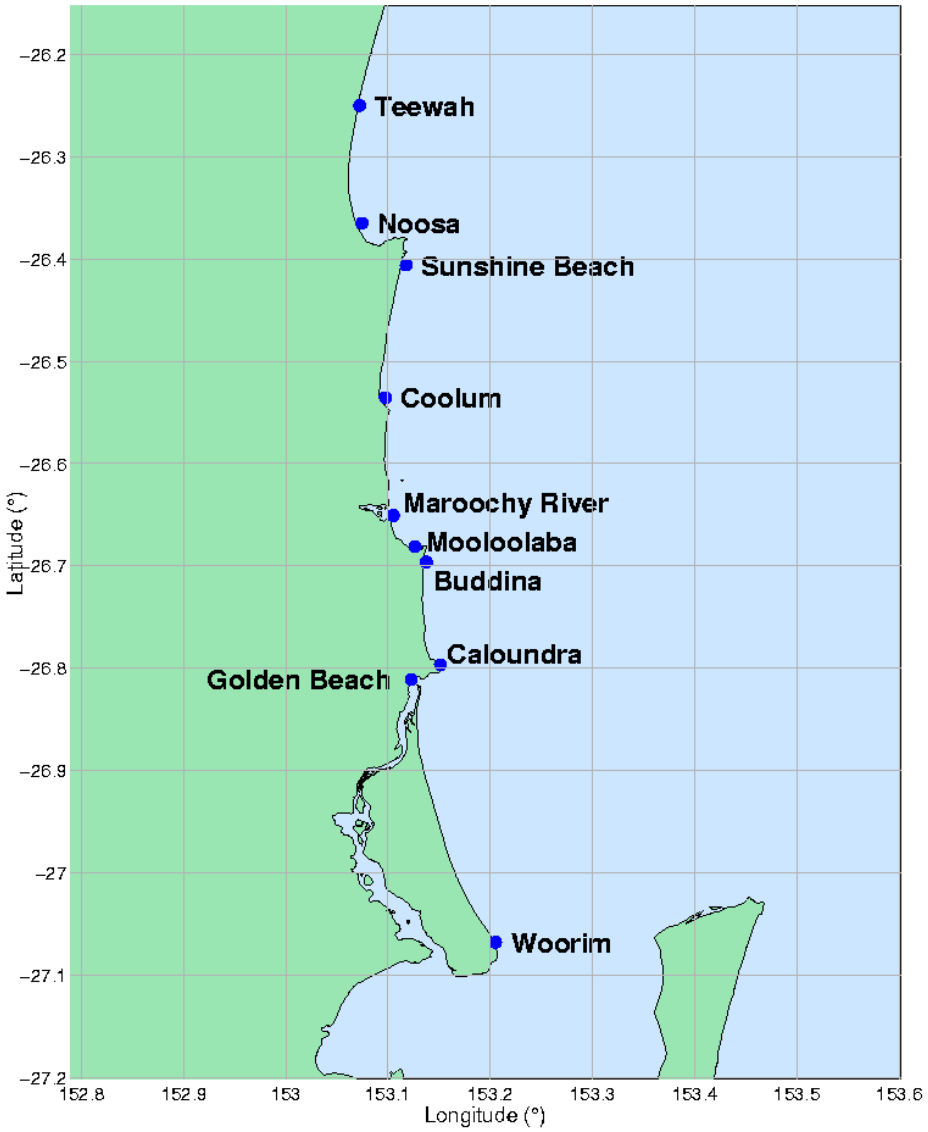

Figure B1. Sunshine Coast study area and water level reporting locations

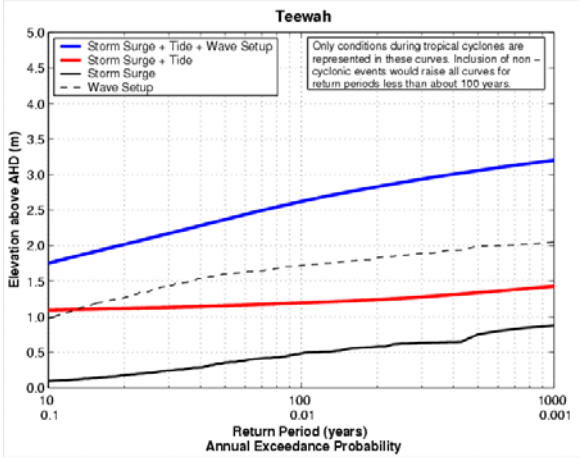

Figure B2. Water level frequency: Teewah
HAT = 1.12 m

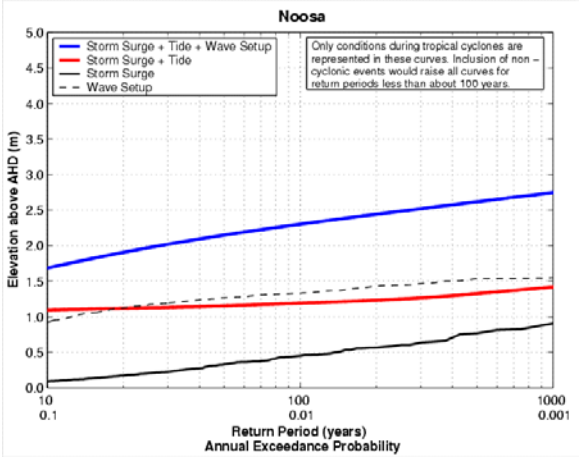

Figure B3. Water level frequency: Noosa
HAT = 1.12 m

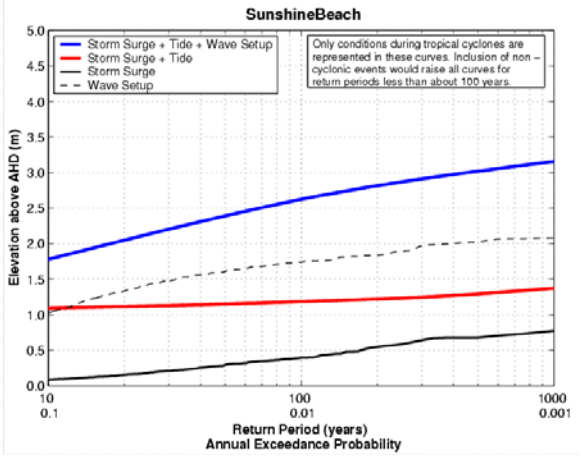

Figure B4. Water level frequency: Sunshine Beach
HAT = 1.12 m

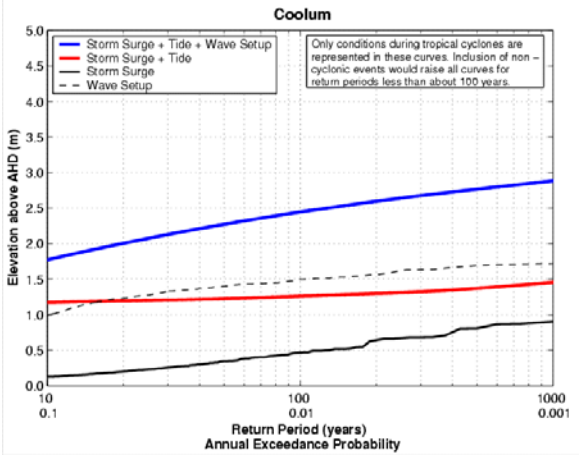

Figure B5. Water level frequency: Coolum
HAT = 1.14 m

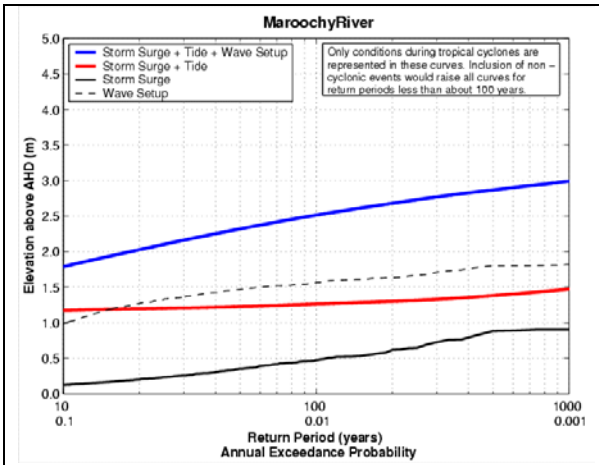

Figure B6. Water level frequency: Maroochy River
HAT = 1.14 m

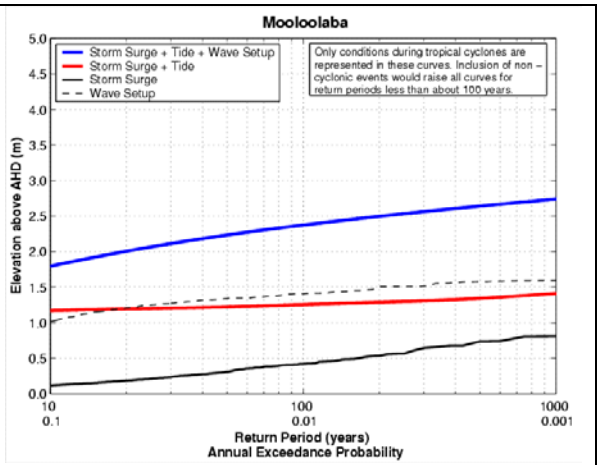

Figure B7. Water level frequency: Moolooaba
HAT = 1.14 m

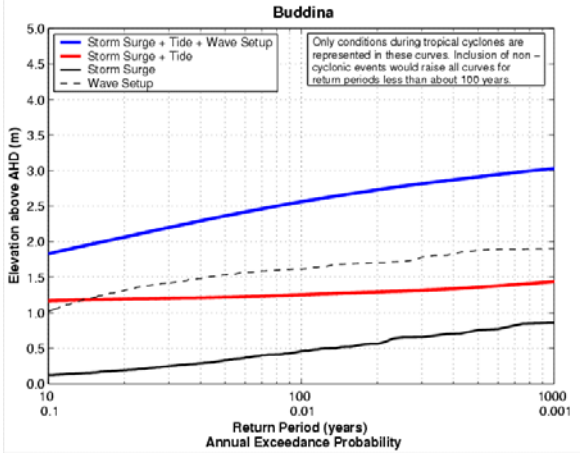

Figure B8. Water level frequency: Buddina
HAT = 1.14 m

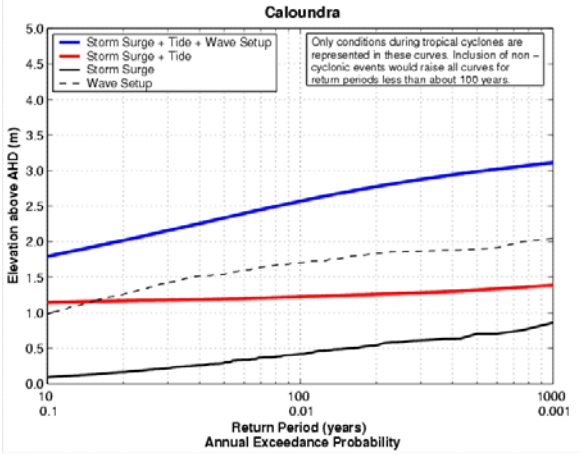

Figure B9. Water level frequency: Caloundra
HAT = 1.05 m

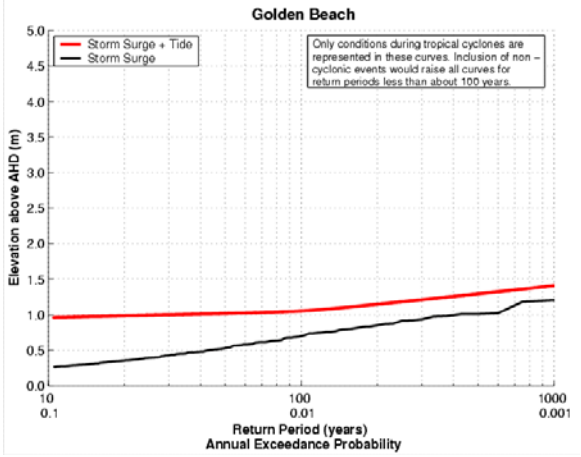

Figure B10. Water level frequency: Golden Beach
HAT = 0.85 m

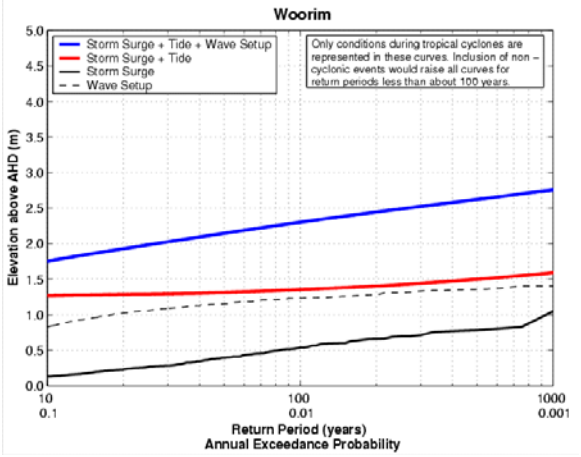

Figure B11. Water level frequency: Woorim
HAT = 1.21 m

APPENDIX C

WAVE DATA SHEETS: HERVEY BAY

Wave data sheets, a sample of which was presented and discussed in the main body of the report (Figure 21), are presented here for Hervey Bay.

These data are valid for waves produced during tropical cyclones. Extra-topical storms and other meteorological and oceanic causes of water level change (not modelled here) will contribute waves at lower return periods.

The following data sheets are for the locations indicated in Figure C1.

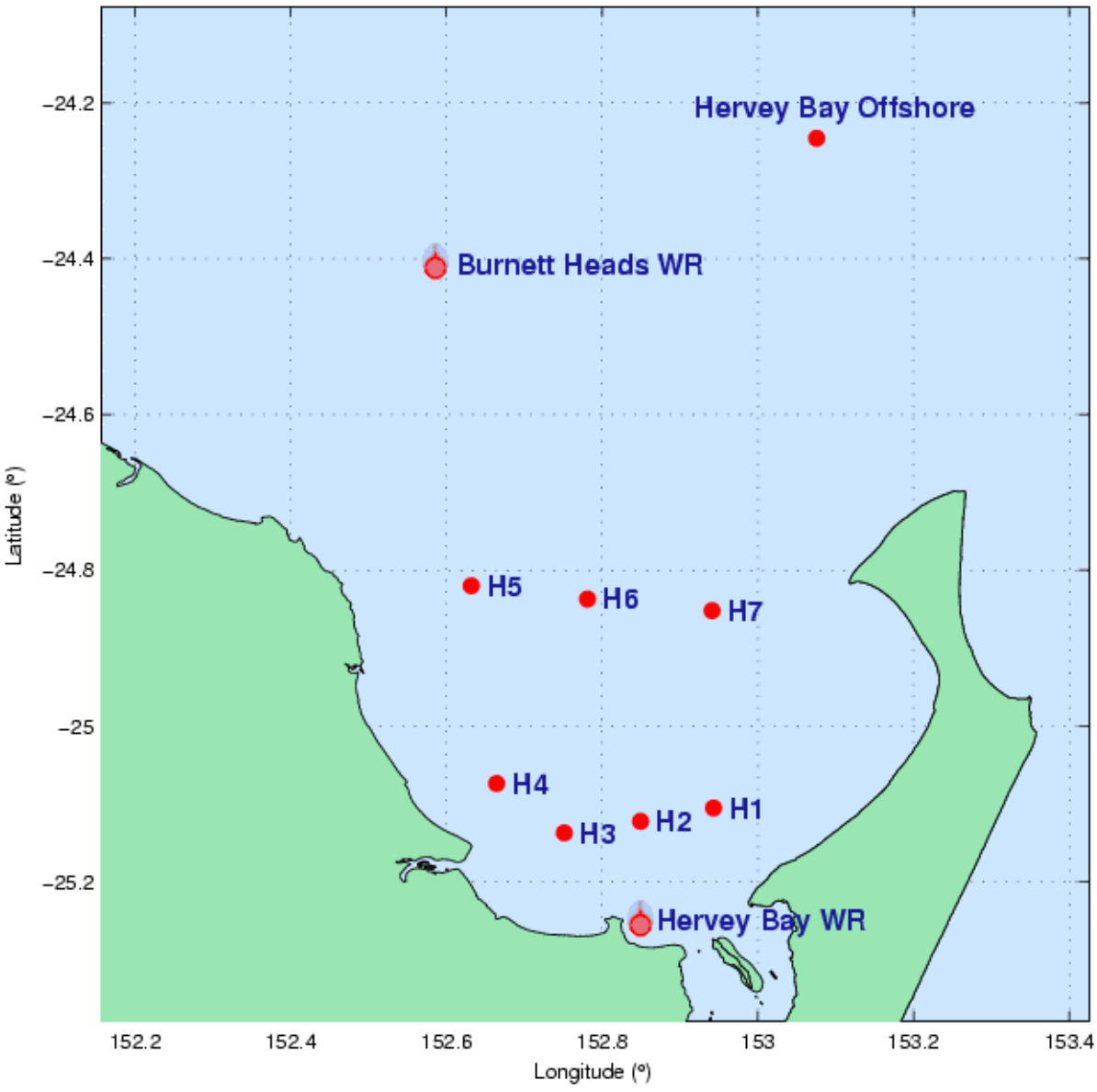

Figure C1. Locations for wave information: Hervey Bay

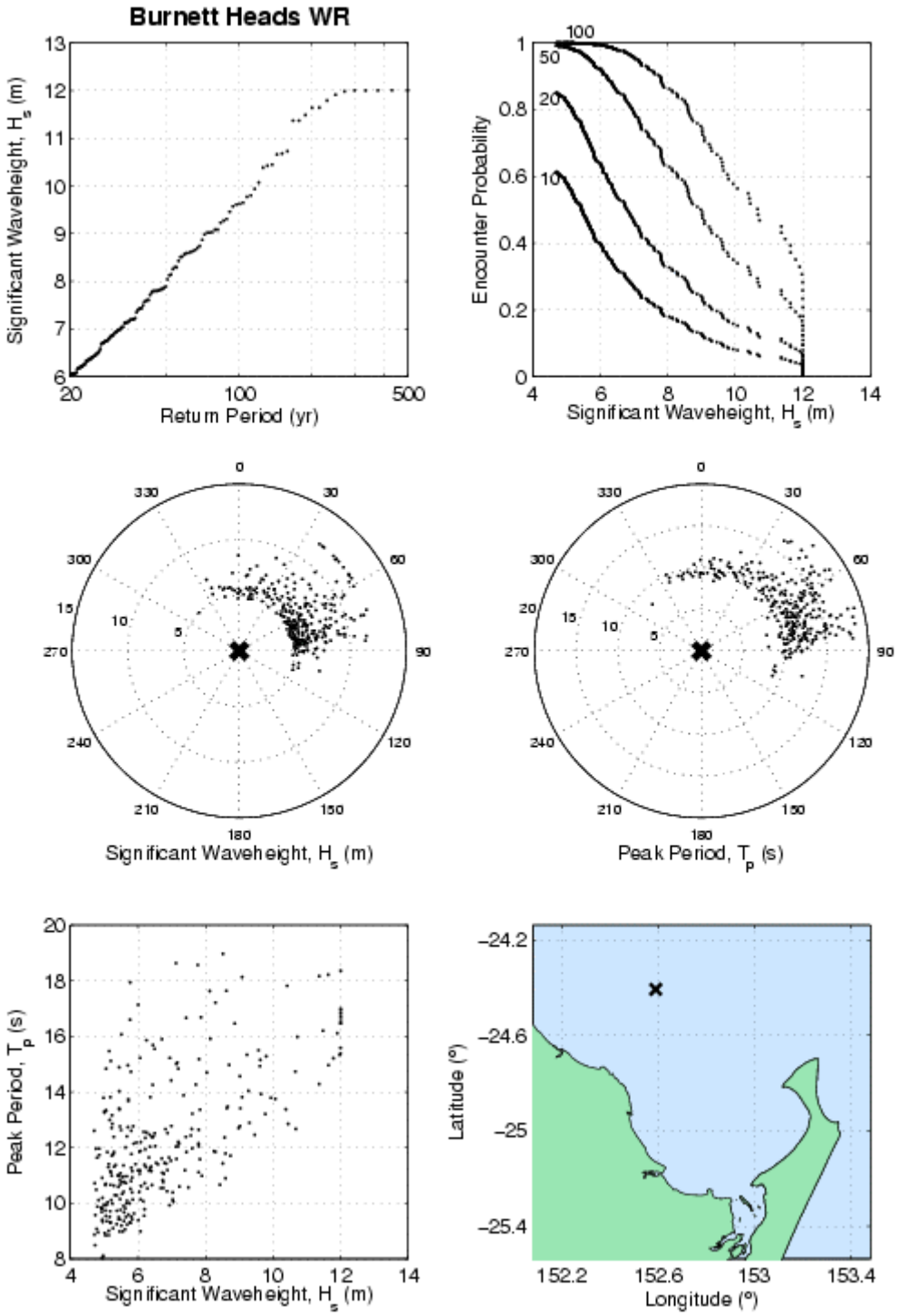

Figure C2. *Burnett Heads WR*. (a) return period of H_s, (b) encounter probability of H_s for L = 10, 20, 50 and 100 years (c) polar plot of H_s as a function of direction, (d) polar plot of T_p as a function of direction, (e) scatter plot of H_s vs T_p, (f) location map.

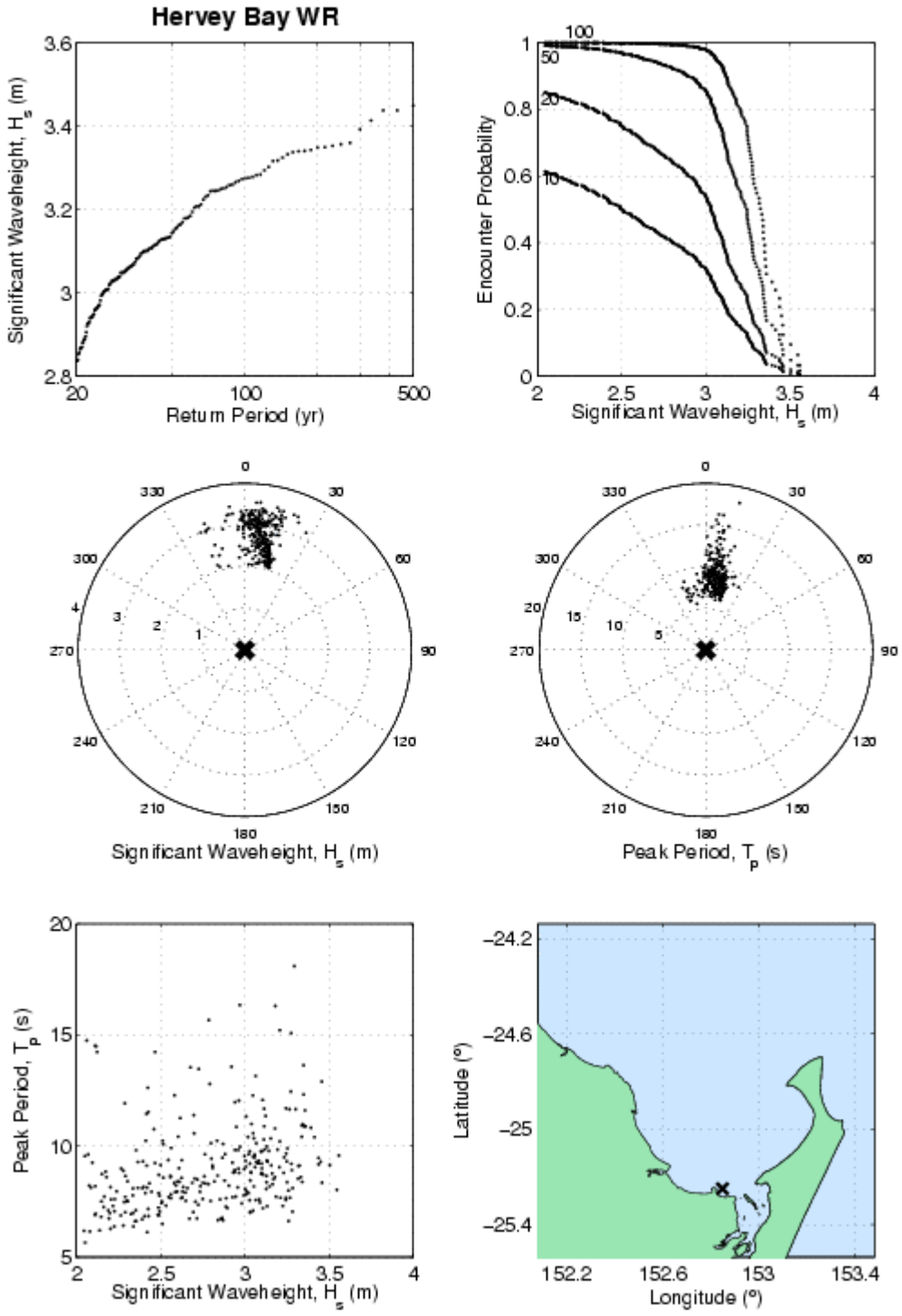

Figure C3. *Hervey Bay WR*. (a) return period of H_s, (b) encounter probability of H_s for L = 10, 20, 50 and 100 years (c) polar plot of H_s as a function of direction, (d) polar plot of T_p as a function of direction, (e) scatter plot of H_s vs T_p, (f) location map.

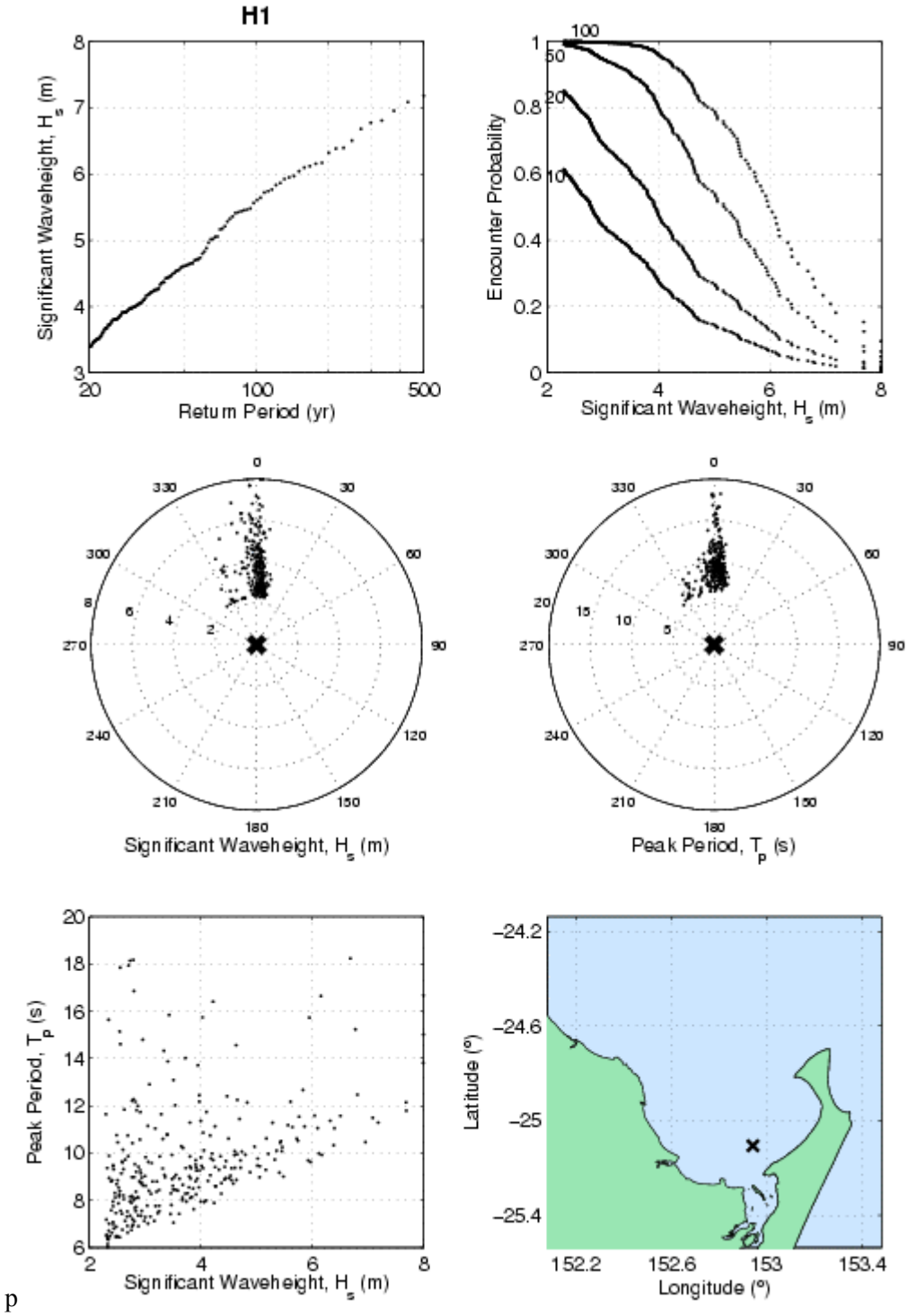

p

Figure C4. *H1*. (a) return period of H_s, (b) encounter probability of H_s for L = 10, 20, 50 and 100 years, (c) polar plot of H_s as a function of direction, (d) polar plot of T_p as a function of direction, (e) scatter plot of H_s vs T_p, (f) location map.

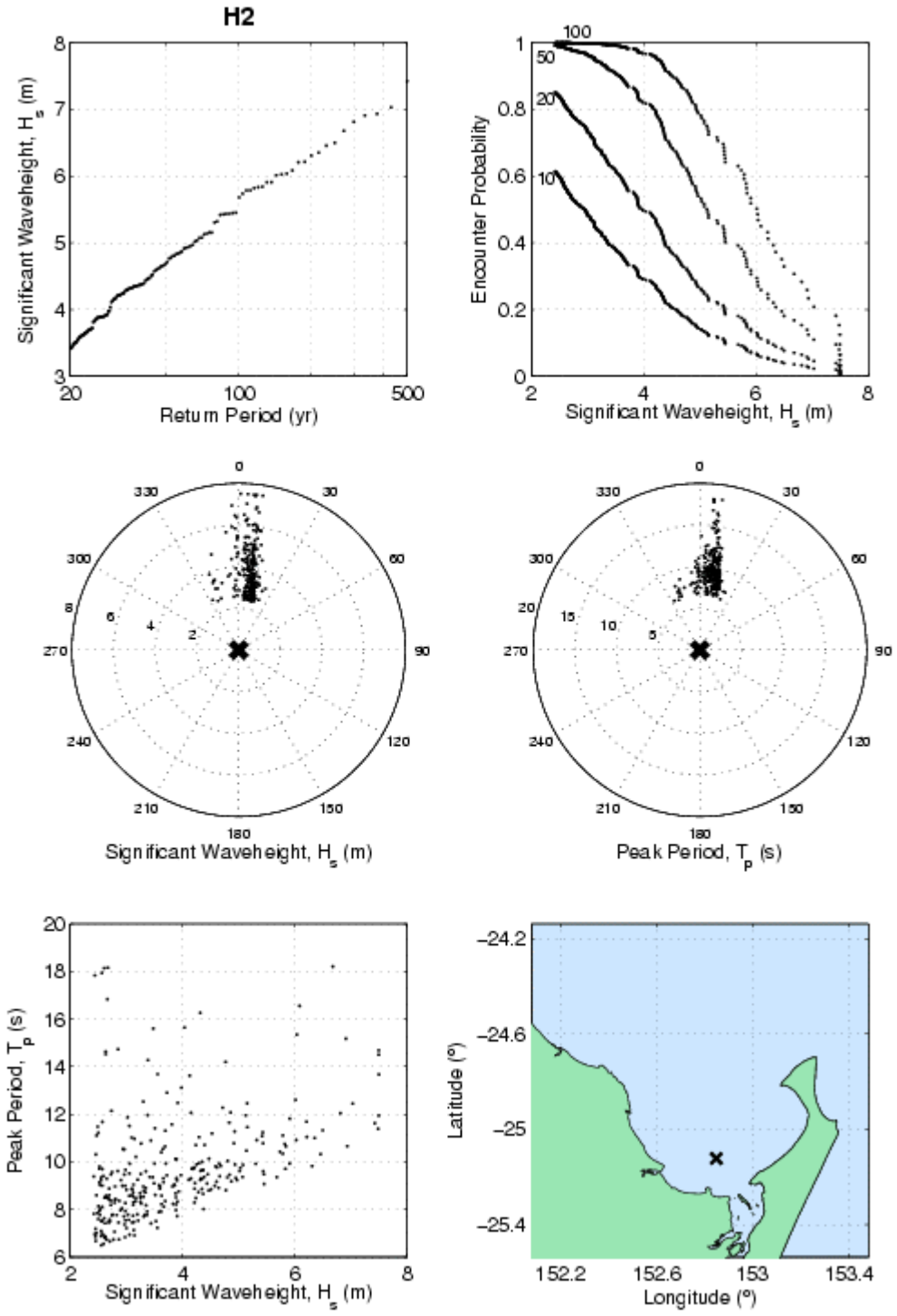

Figure C5. *H2*. (a) return period of H_s, (b) encounter probability of H_s for L = 10, 20, 50 and 100 years, (c) polar plot of H_s as a function of direction, (d) polar plot of T_p as a function of direction, (e) scatter plot of H_s vs T_p, (f) location map.

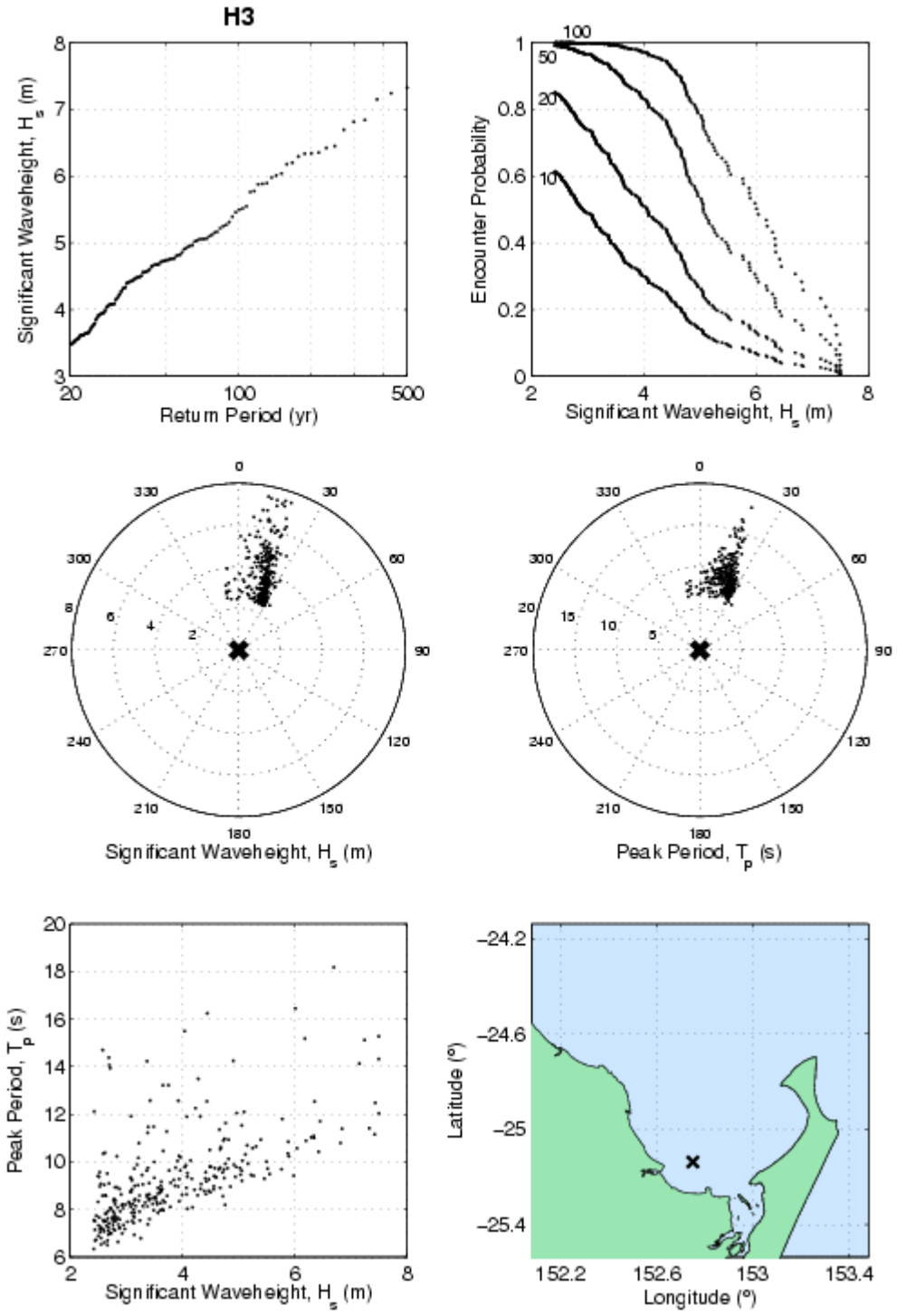

Figure C6. *H3*. (a) return period of H_s, (b) encounter probability of H_s for L = 10, 20, 50 and 100 years, (c) polar plot of H_s as a function of direction, (d) polar plot of T_p as a function of direction, (e) scatter plot of H_s vs T_p, (f) location map.

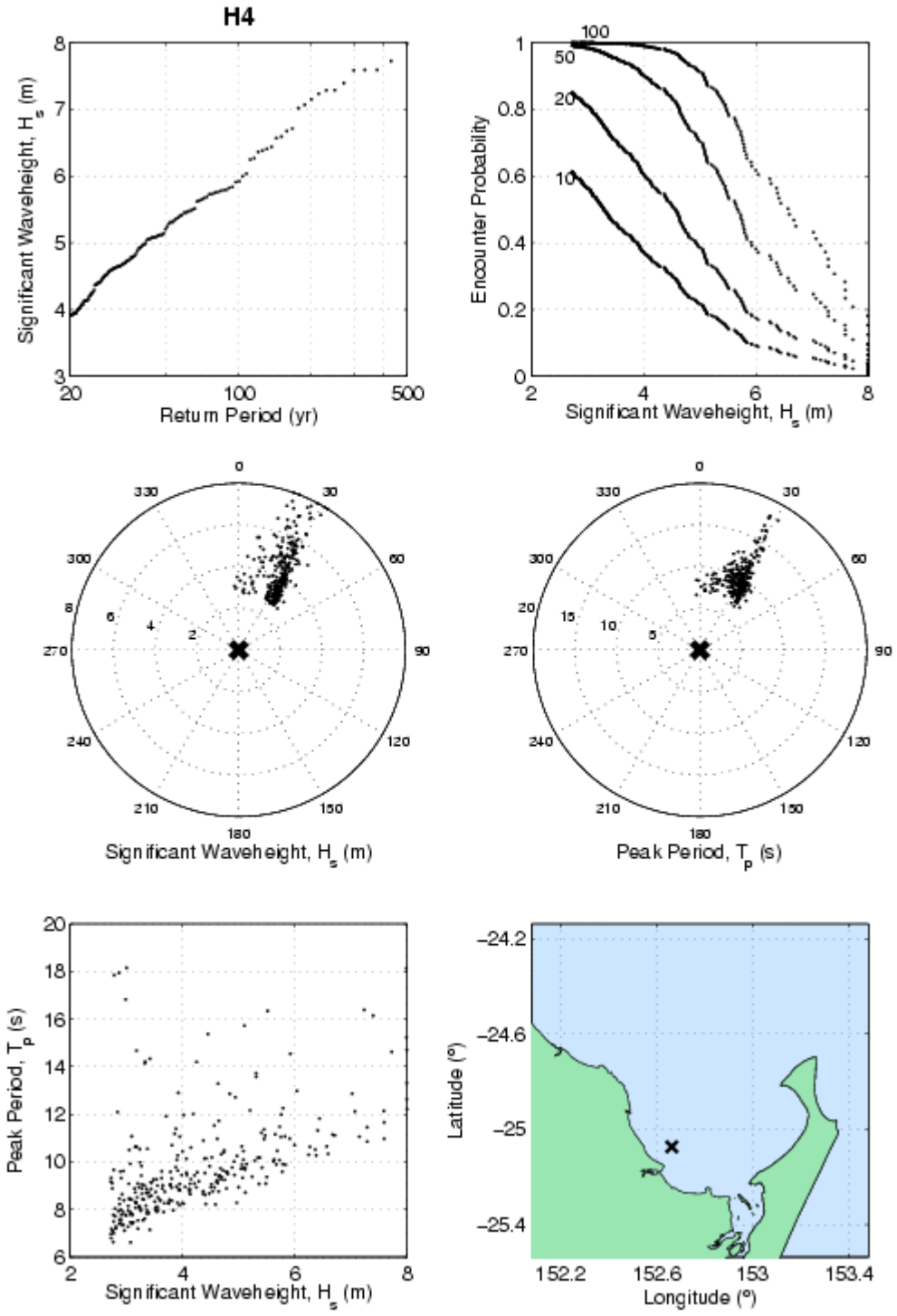

Figure C7. *H4*. (a) return period of H_s, (b) encounter probability of H_s for L = 10, 20, 50 and 100 years, (c) polar plot of H_s as a function of direction, (d) polar plot of T_p as a function of direction, (e) scatter plot of H_s vs T_p, (f) location map.

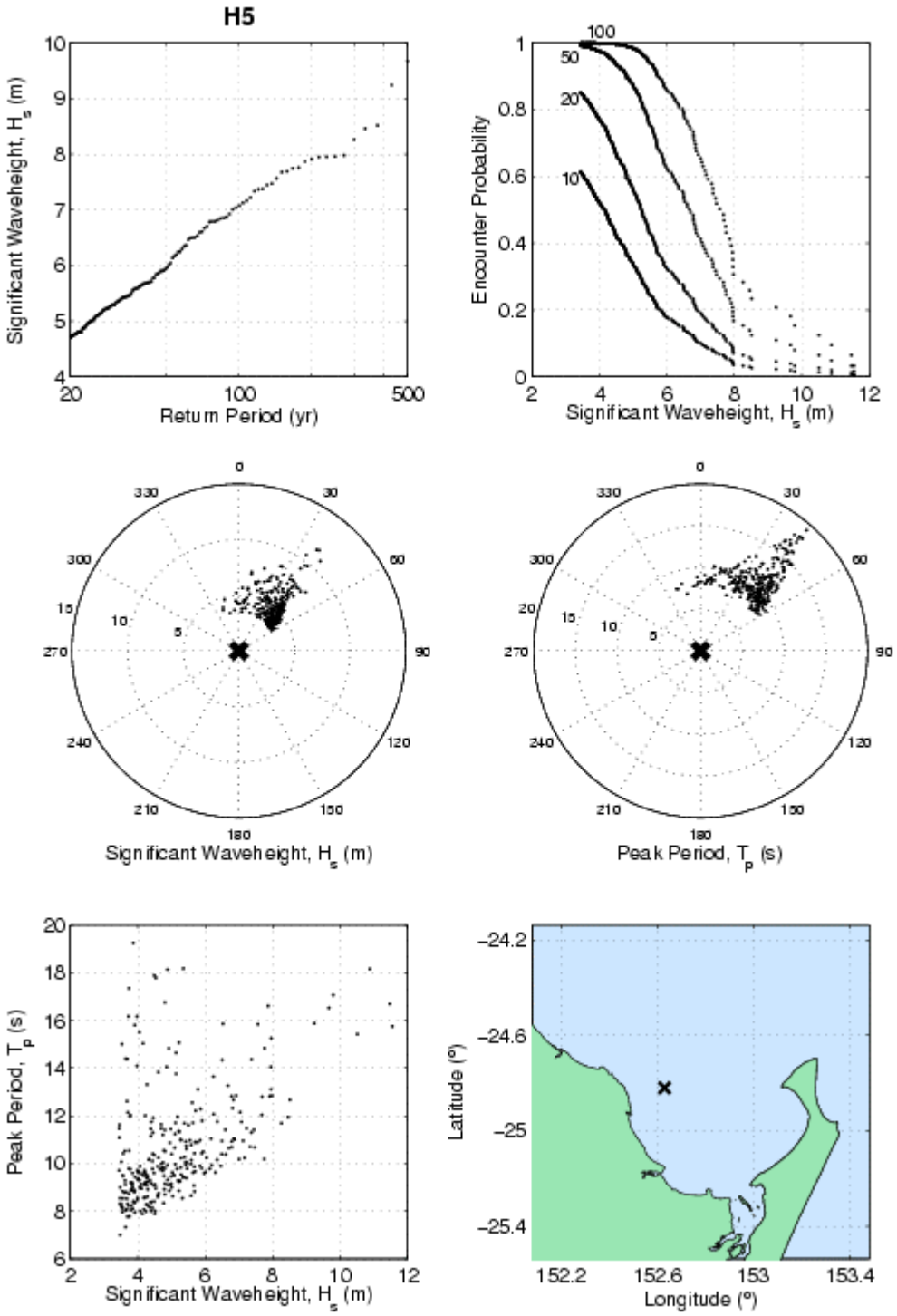

Figure C8. *H5*. (a) return period of H_s, (b) encounter probability of H_s for L = 10, 20, 50 and 100 years, (c) polar plot of H_s as a function of direction, (d) polar plot of T_p as a function of direction, (e) scatter plot of H_s vs T_p, (f) location map.

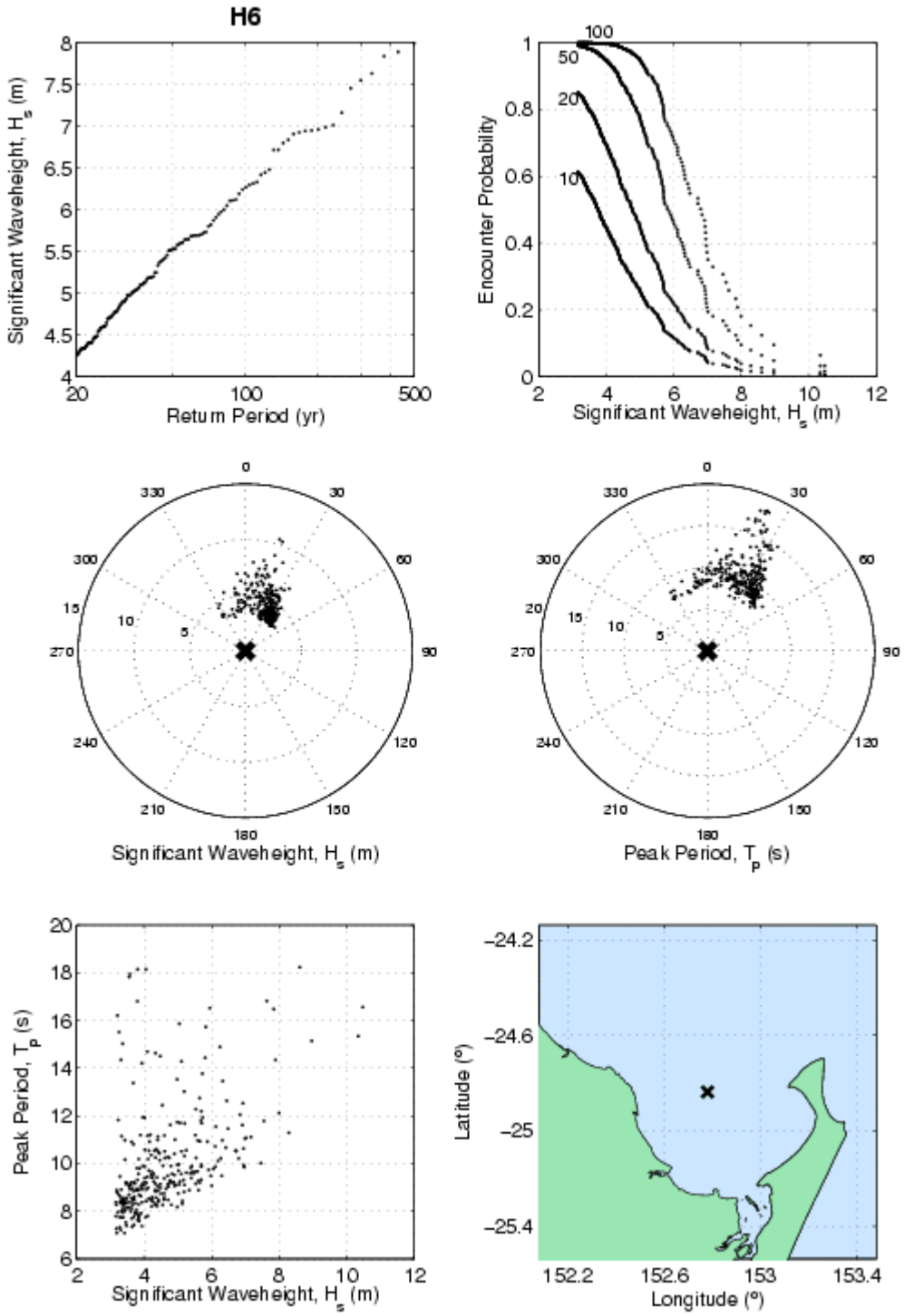

Figure C9. *H6*. (a) return period of H_s, (b) encounter probability of H_s for L = 10, 20, 50 and 100 years, (c) polar plot of H_s as a function of direction, (d) polar plot of T_p as a function of direction, (e) scatter plot of H_s vs T_p, (f) location map.

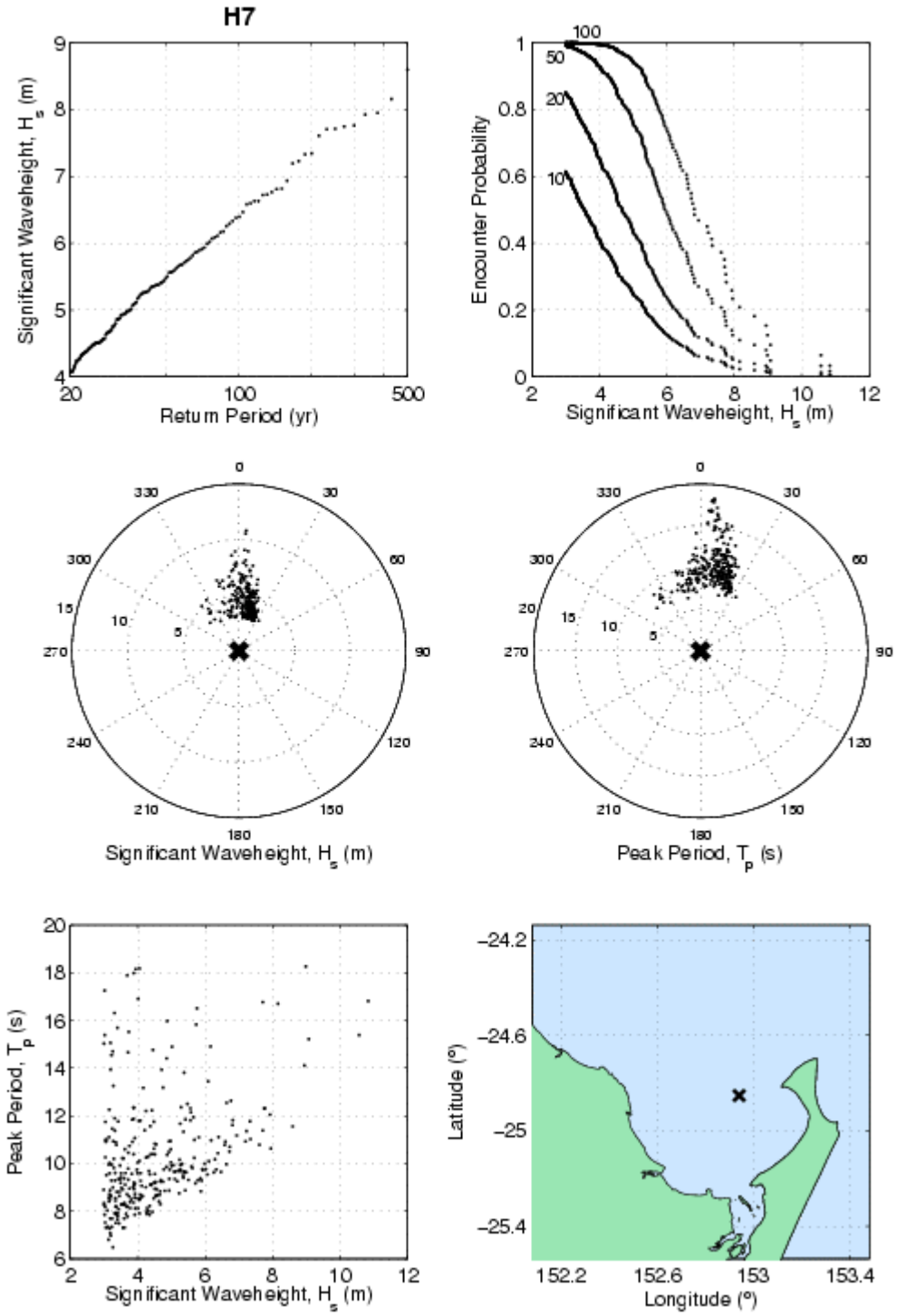

Figure C10. *H7*. (a) return period of H_s, (b) encounter probability of H_s for L = 10, 20, 50 and 100 years, (c) polar plot of H_s as a function of direction, (d) polar plot of T_p as a function of direction, (e) scatter plot of H_s vs T_p, (f) location map.

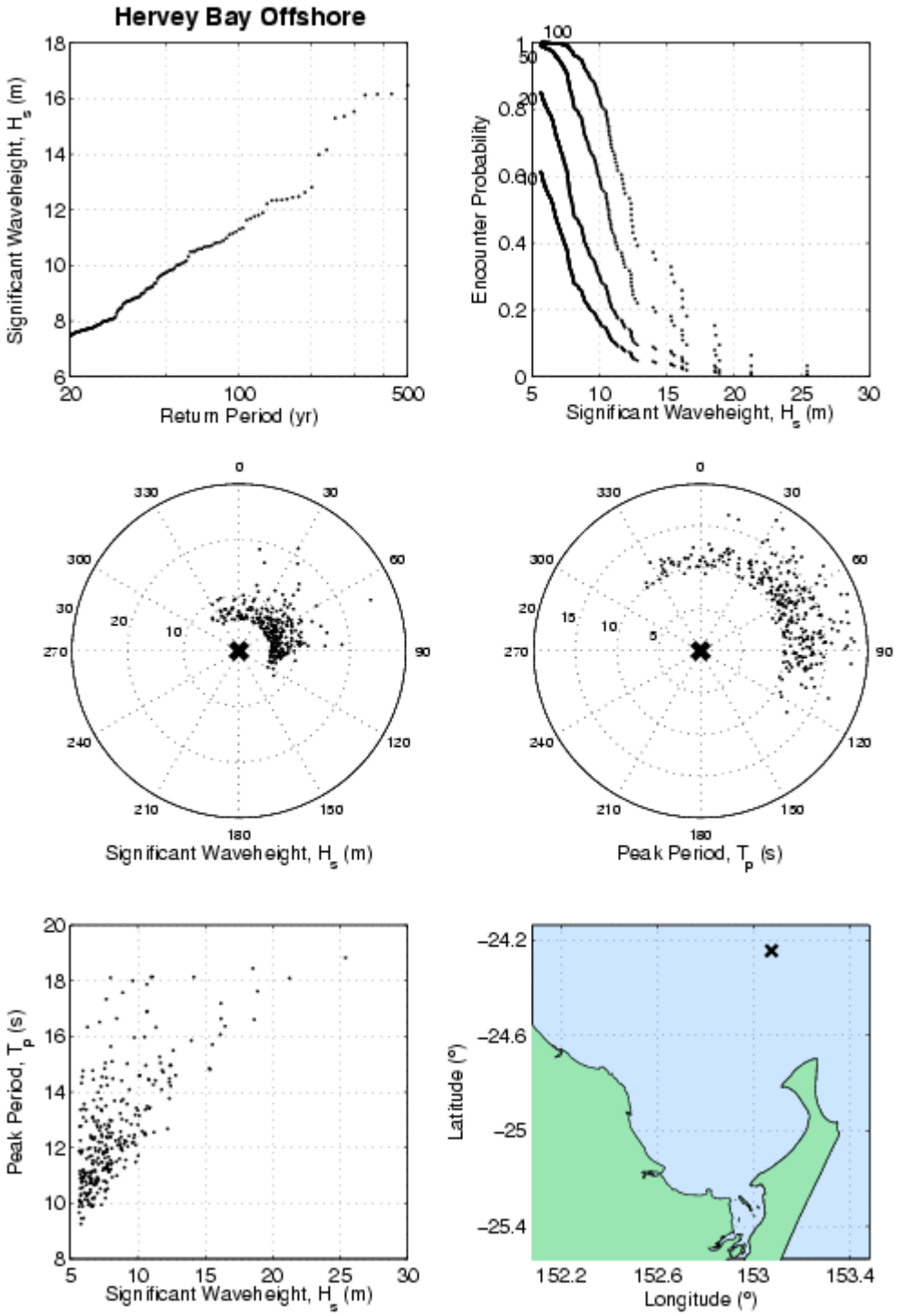

Figure C11. *Hervey Bay Offshore*. (a) return period of H_s, (b) encounter probability of H_s for L = 10, 20, 50 and 100 years (c) polar plot of H_s as a function of direction, (d) polar plot of T_p as a function of direction, (e) scatter plot of H_s vs T_p, (f) location map.

APPENDIX D

WAVE DATA SHEETS: SUNSHINE COAST

Wave data sheets, a sample of which was presented and discussed in the main body of the report (Figure 21), are presented here for Sunshine Coast.

These data are valid for waves produced during tropical cyclones. Extra-topical storms and other meteorological and oceanic causes of water level change (not modelled here) will contribute waves at lower return periods.

The following data sheets are for the locations indicated in Figure D1.

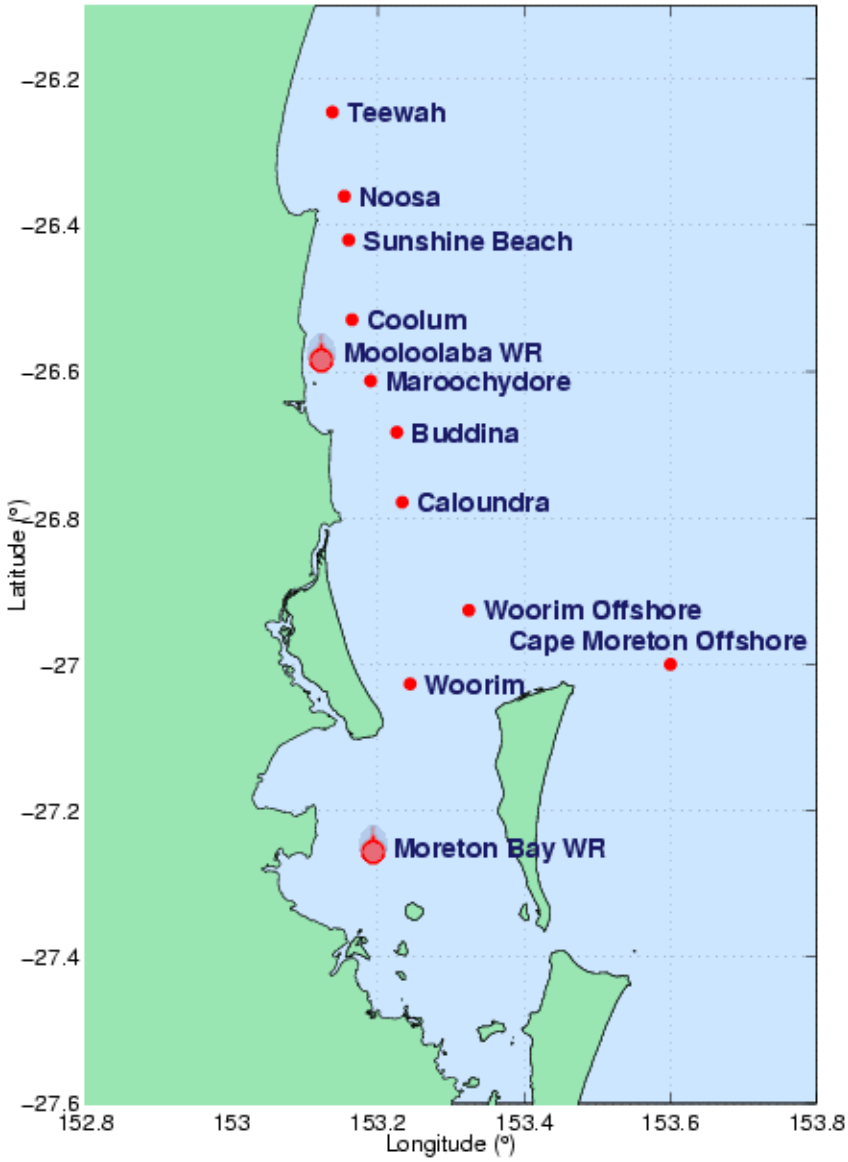

Figure D1. Locations for wave information: Sunshine Coast

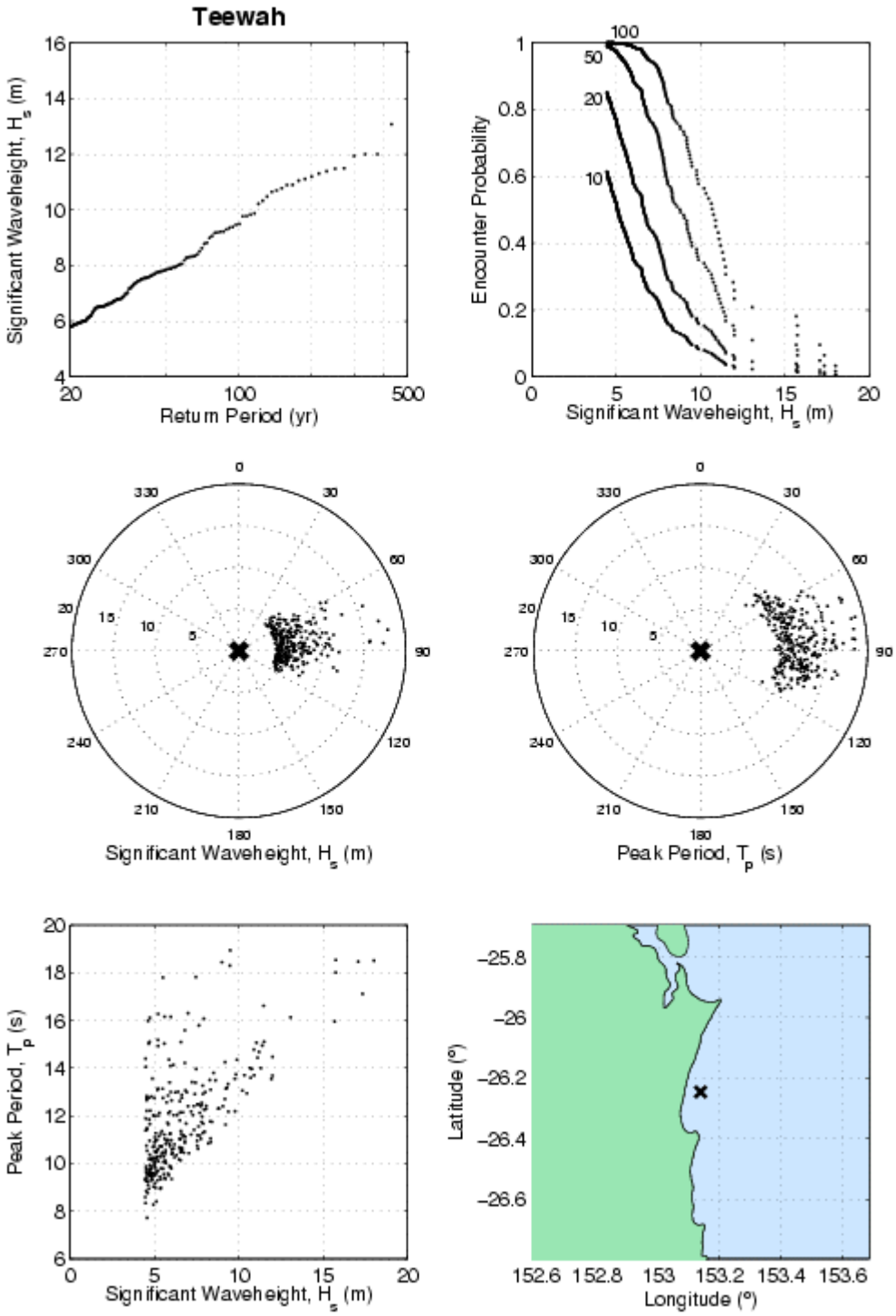

Figure D2. *Teewah*. Data sheet for wave modelling output. (a) return period of H_s, (b) encounter probability of H_s for L = 10, 20, 50 and 100 years, (c) polar plot of H_s as a function of direction, (d) polar plot of T_p as a function of direction, (e) scatter plot of H_s vs T_p, (f) location map.

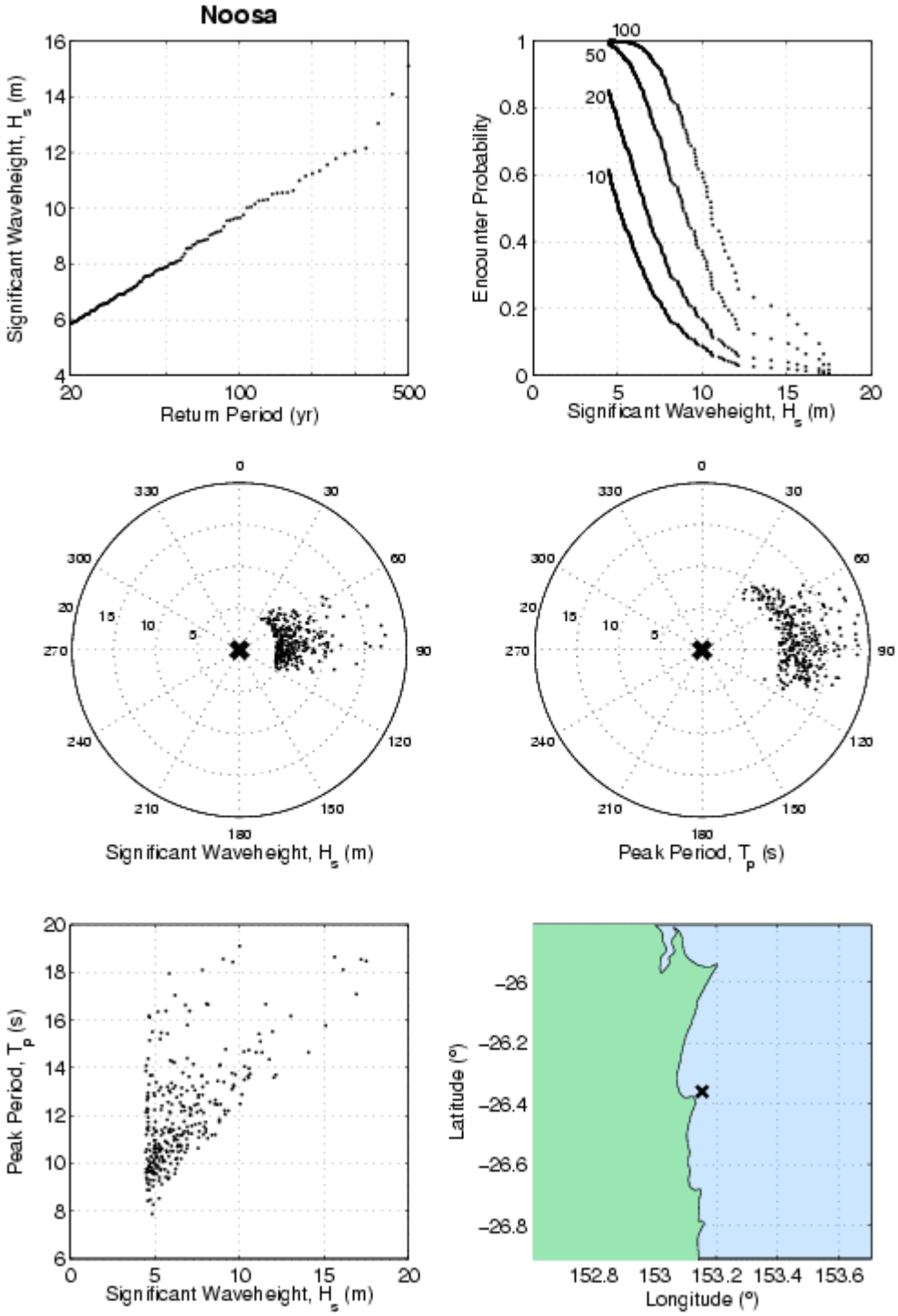

Figure D3. *Noosa*. Data sheet for wave modelling output. (a) return period of H_s, (b) encounter probability of H_s for L = 10, 20, 50 and 100 years, (c) polar plot of H_s as a function of direction, (d) polar plot of T_p as a function of direction, (e) scatter plot of H_s vs T_p, (f) location map.

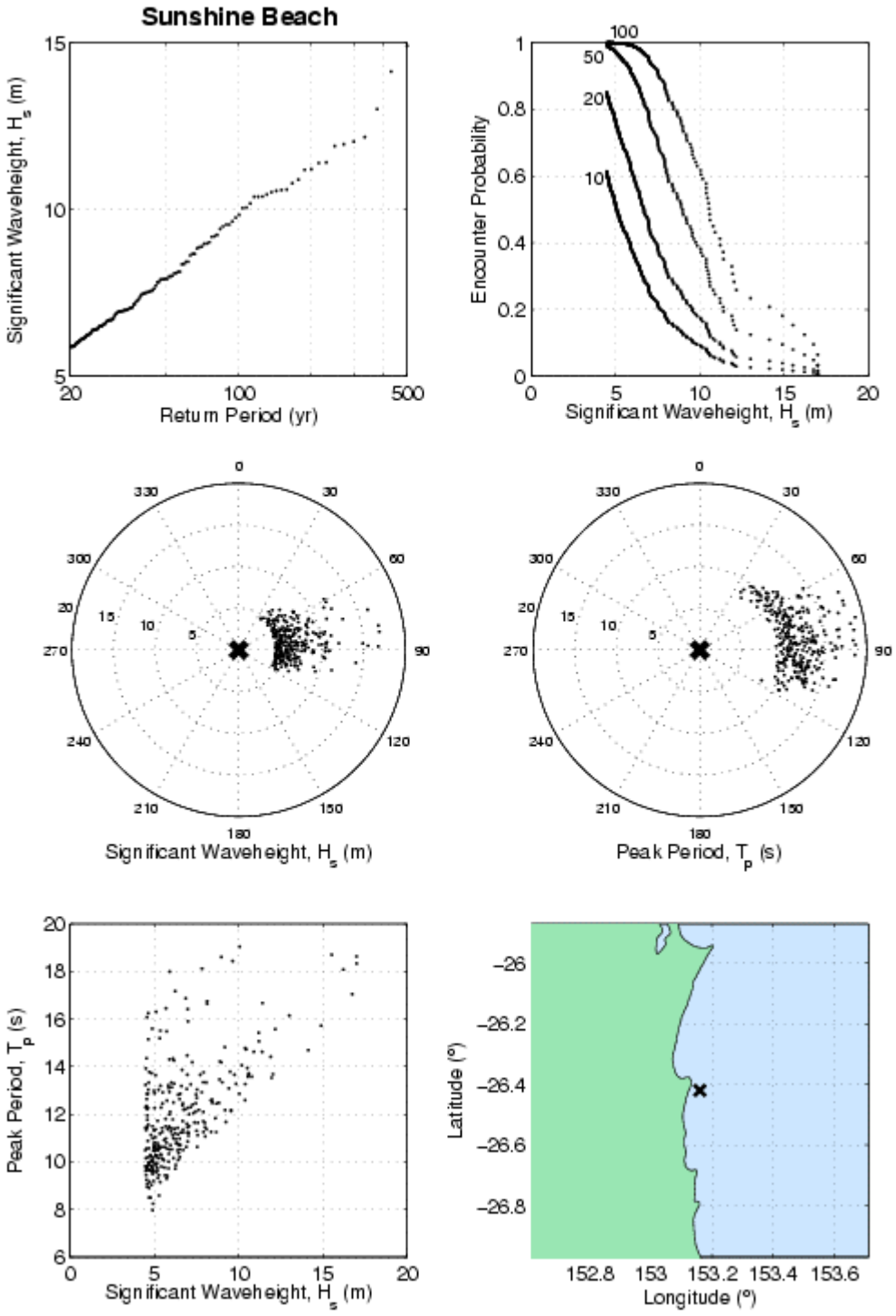

Figure D4. *Sunshine Beach*. Data sheet for wave modelling output. (a) return period of H_s, (b) encounter probability of H_s for L = 10, 20, 50 and 100 years, (c) polar plot of H_s as a function of direction, (d) polar plot of T_p as a function of direction, (e) scatter plot of H_s vs T_p, (f) location map.

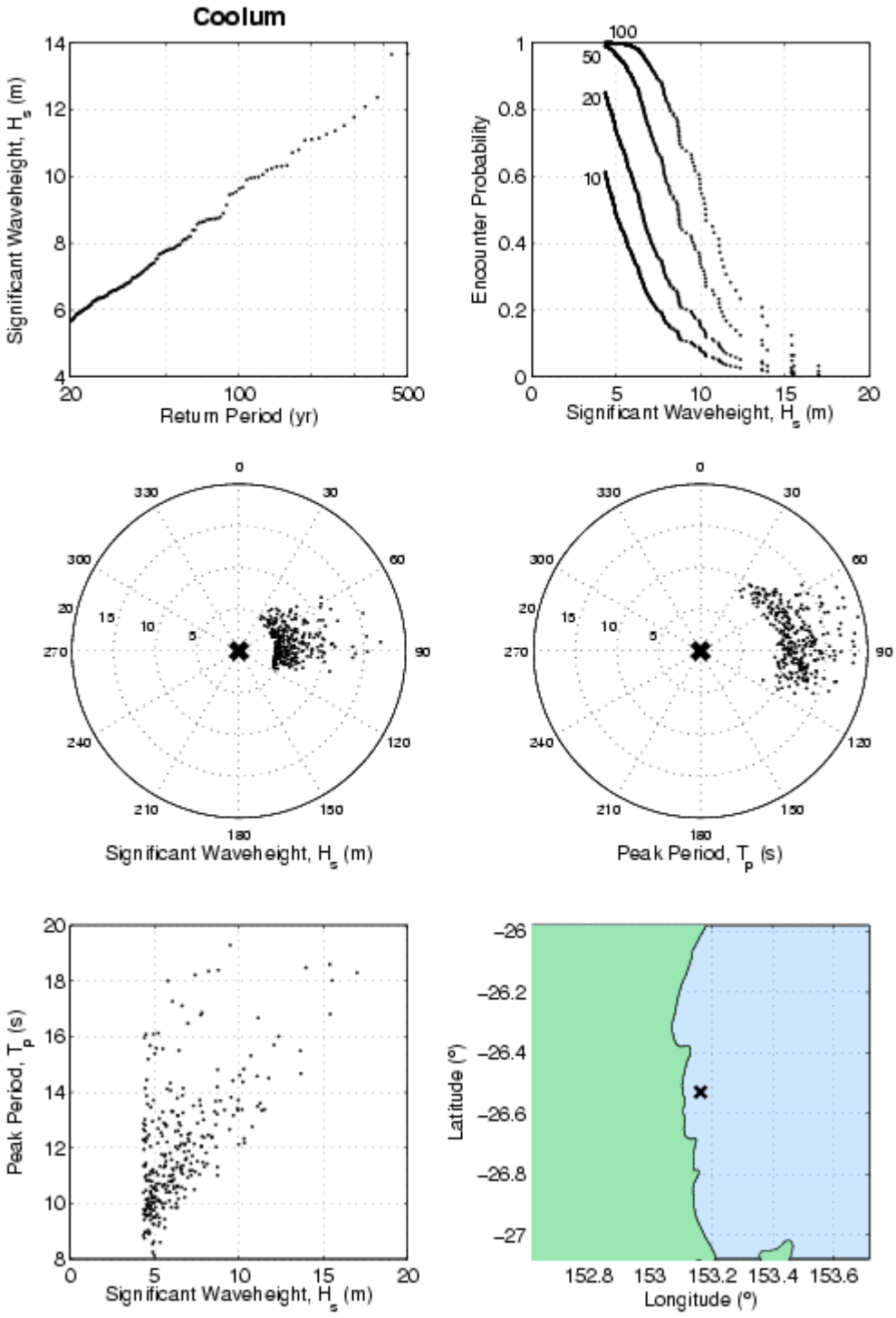

Figure D5. *Coolum*. Data sheet for wave modelling output. (a) return period of H_s, (b) encounter probability of H_s for L = 10, 20, 50 and 100 years, (c) polar plot of H_s as a function of direction, (d) polar plot of T_p as a function of direction, (e) scatter plot of H_s vs T_p, (f) location map.

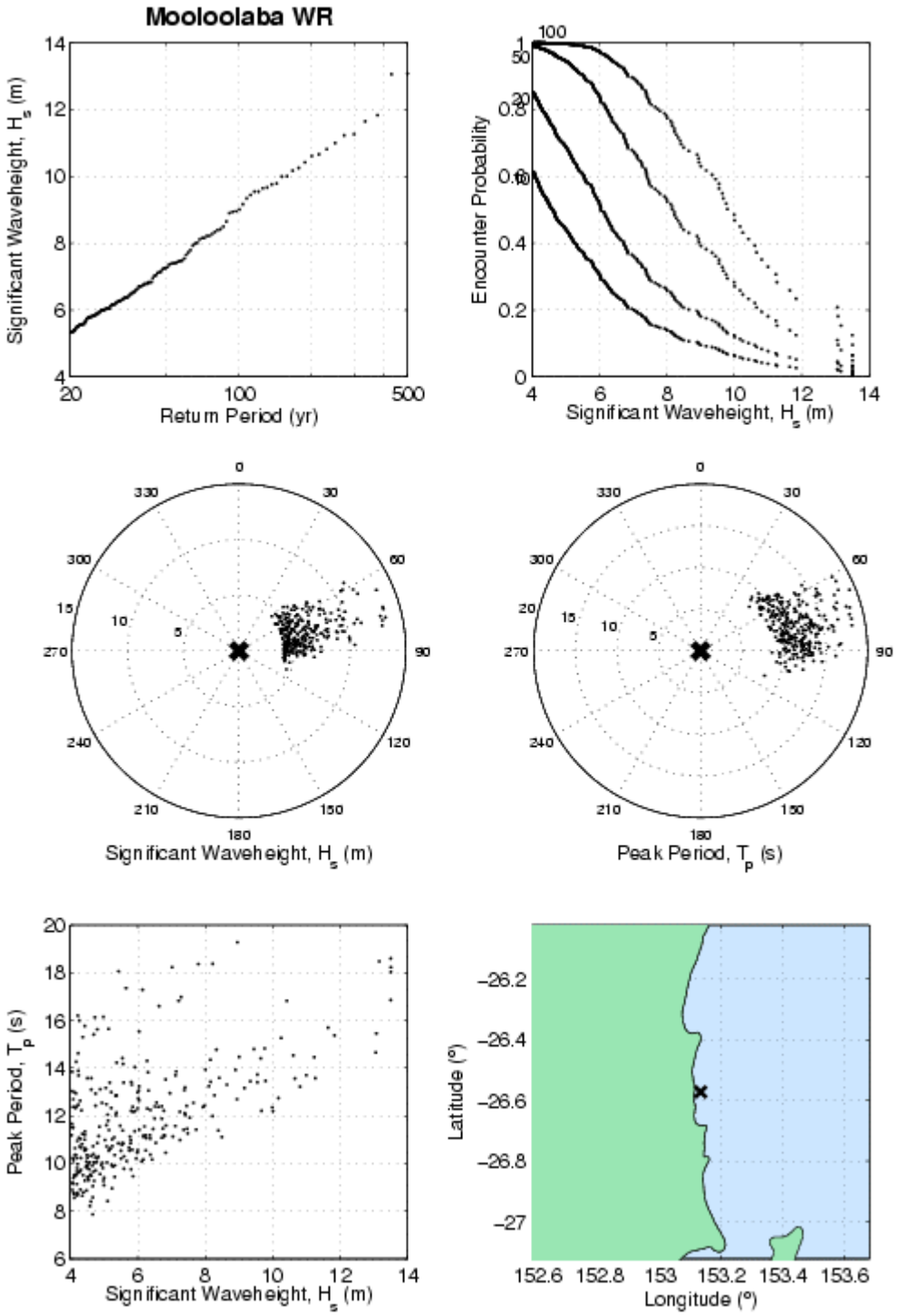

Figure D6. *Mooloolaba WR*. Data sheet for wave modelling output. (a) return period of H_s, (b) encounter probability of H_s for L = 10, 20, 50 and 100 years, (c) polar plot of H_s as a function of direction, (d) polar plot of T_p as a function of direction, (e) scatter plot of H_s vs T_p, (f) location map.

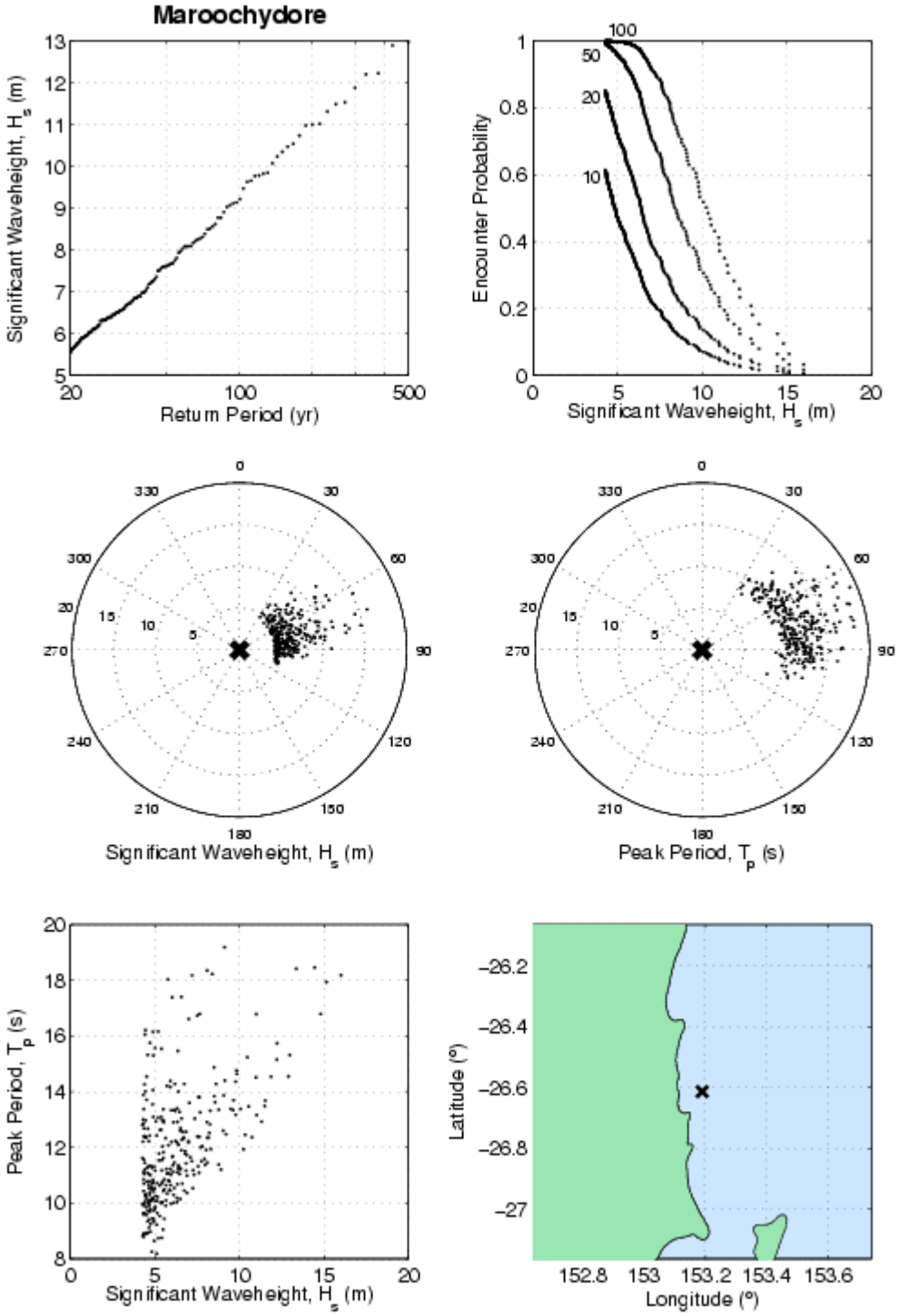

Figure D7. *Maroochydore*. Data sheet for wave modelling output. (a) return period of H_s, (b) encounter probability of H_s for L = 10, 20, 50 and 100 years, (c) polar plot of H_s as a function of direction, (d) polar plot of T_p as a function of direction, (e) scatter plot of H_s vs T_p, (f) location map.

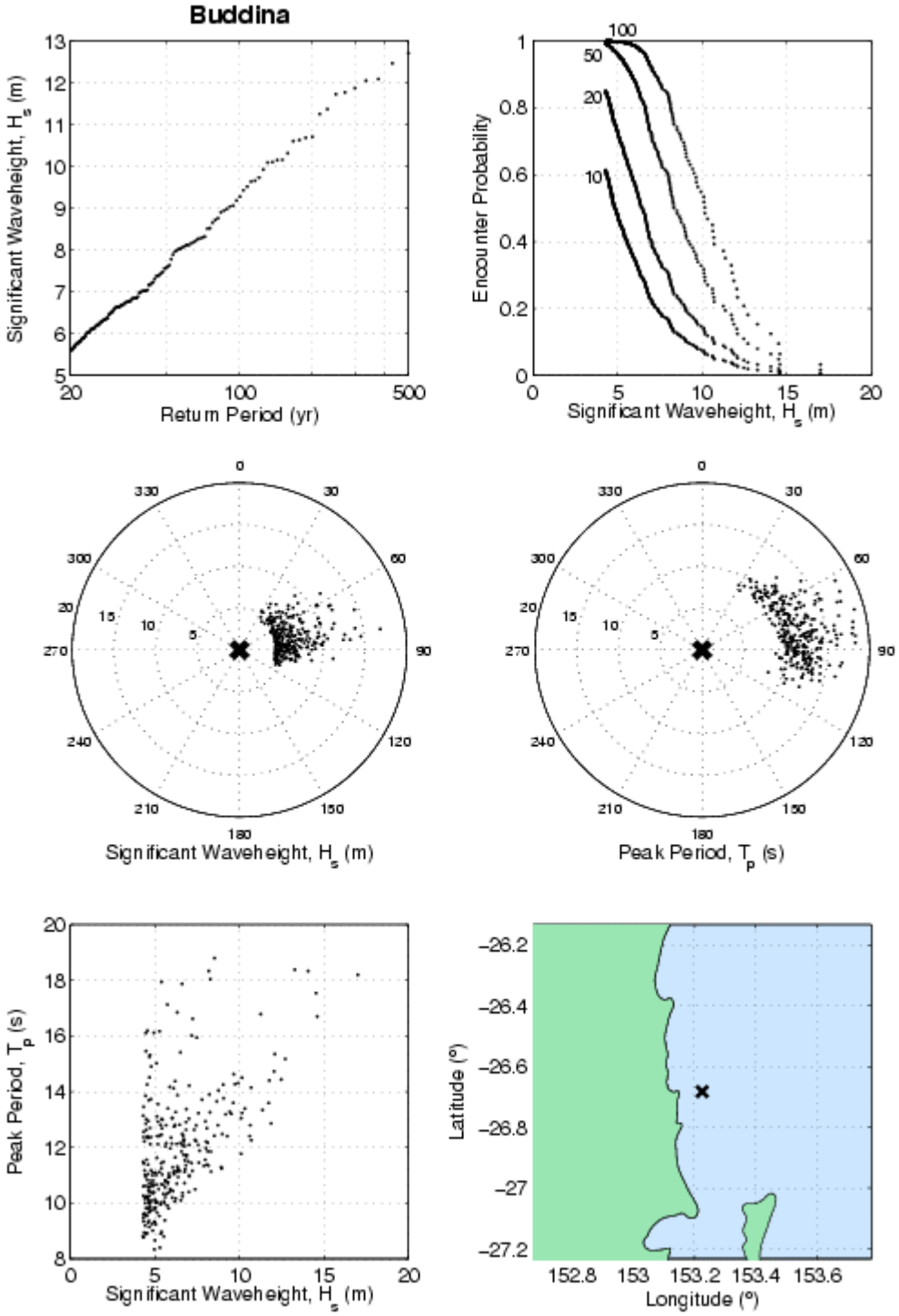

Figure D8. *Buddina*. Data sheet for wave modelling output. (a) return period of H_s, (b) encounter probability of H_s for L = 10, 20, 50 and 100 years, (c) polar plot of H_s as a function of direction, (d) polar plot of T_p as a function of direction, (e) scatter plot of H_s vs T_p, (f) location map.

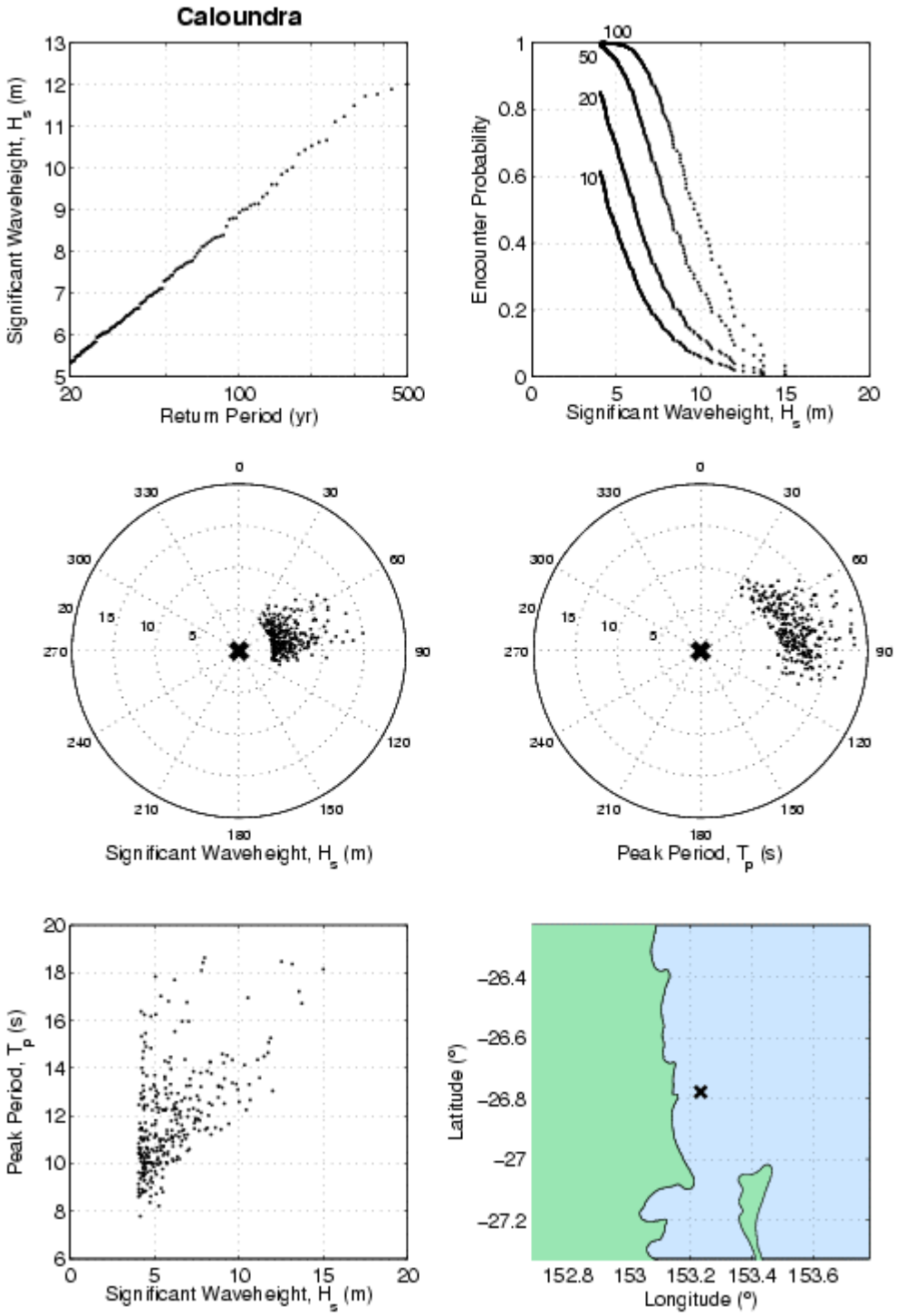

Figure D9. *Caloundra*. Data sheet for wave modelling output. (a) return period of H_s, (b) encounter probability of H_s for L = 10, 20, 50 and 100 years, (c) polar plot of H_s as a function of direction, (d) polar plot of T_p as a function of direction, (e) scatter plot of H_s vs T_p, (f) location map.

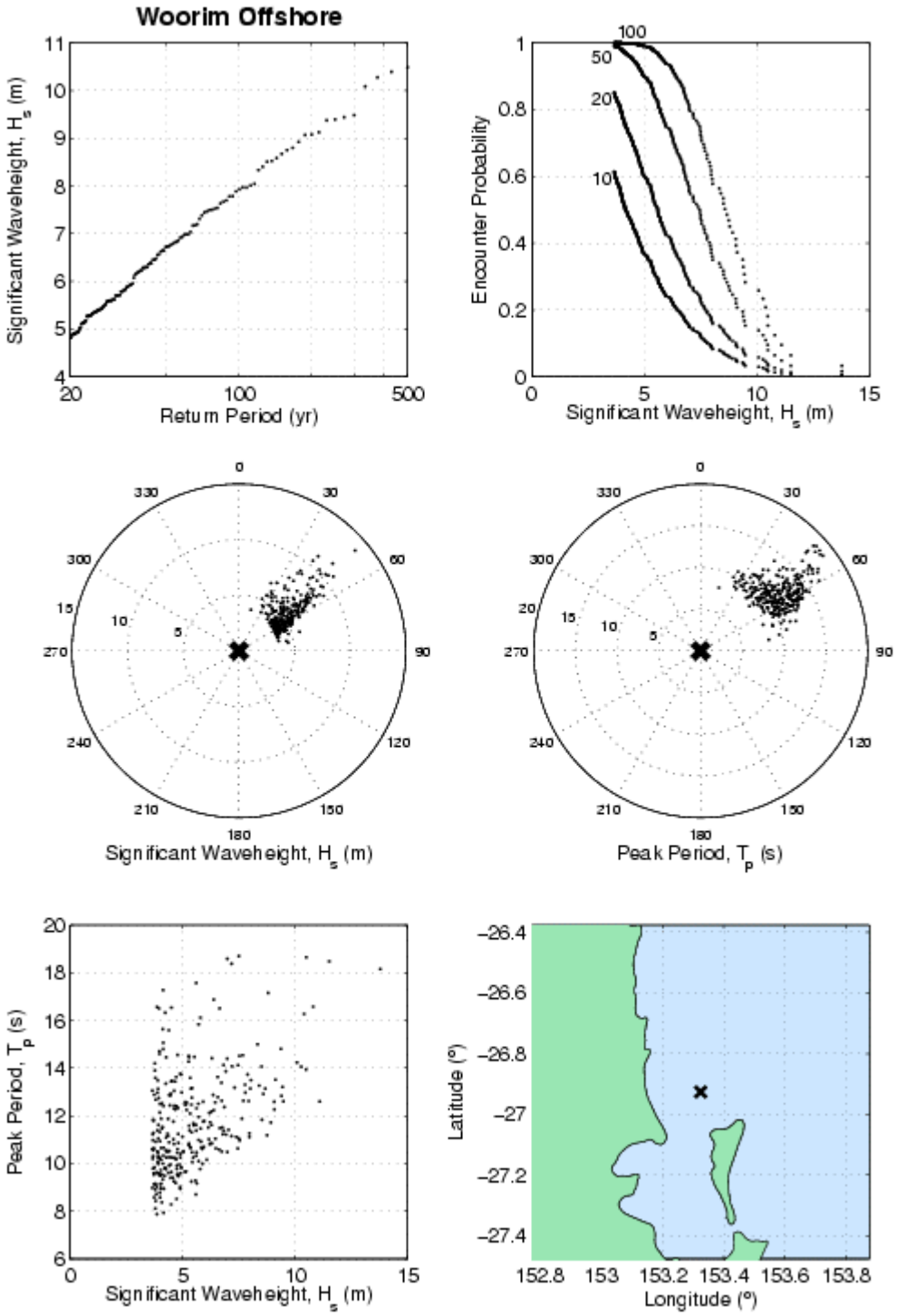

Figure D10. *Woorim Offshore*. Data sheet for wave modelling output. (a) return period of H_s, (b) encounter probability of H_s for L = 10, 20, 50 and 100 years, (c) polar plot of H_s as a function of direction, (d) polar plot of T_p as a function of direction, (e) scatter plot of H_s vs T_p, (f) location map.

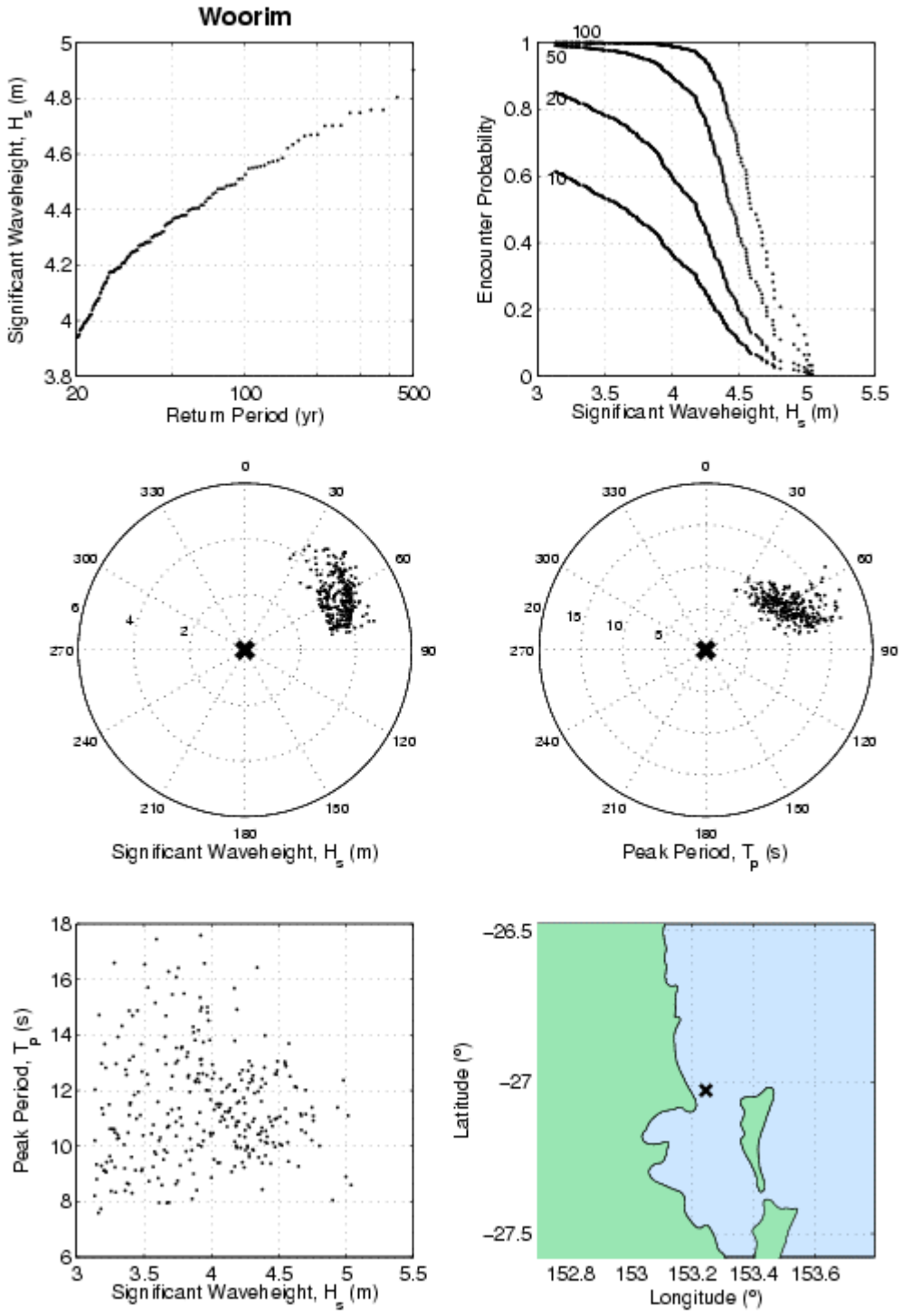

Figure D11. *Woorim*. Data sheet for wave modelling output. (a) return period of H_s, (b) encounter probability of H_s for L = 10, 20, 50 and 100 years, (c) polar plot of H_s as a function of direction, (d) polar plot of T_p as a function of direction, (e) scatter plot of H_s vs T_p, (f) location map.

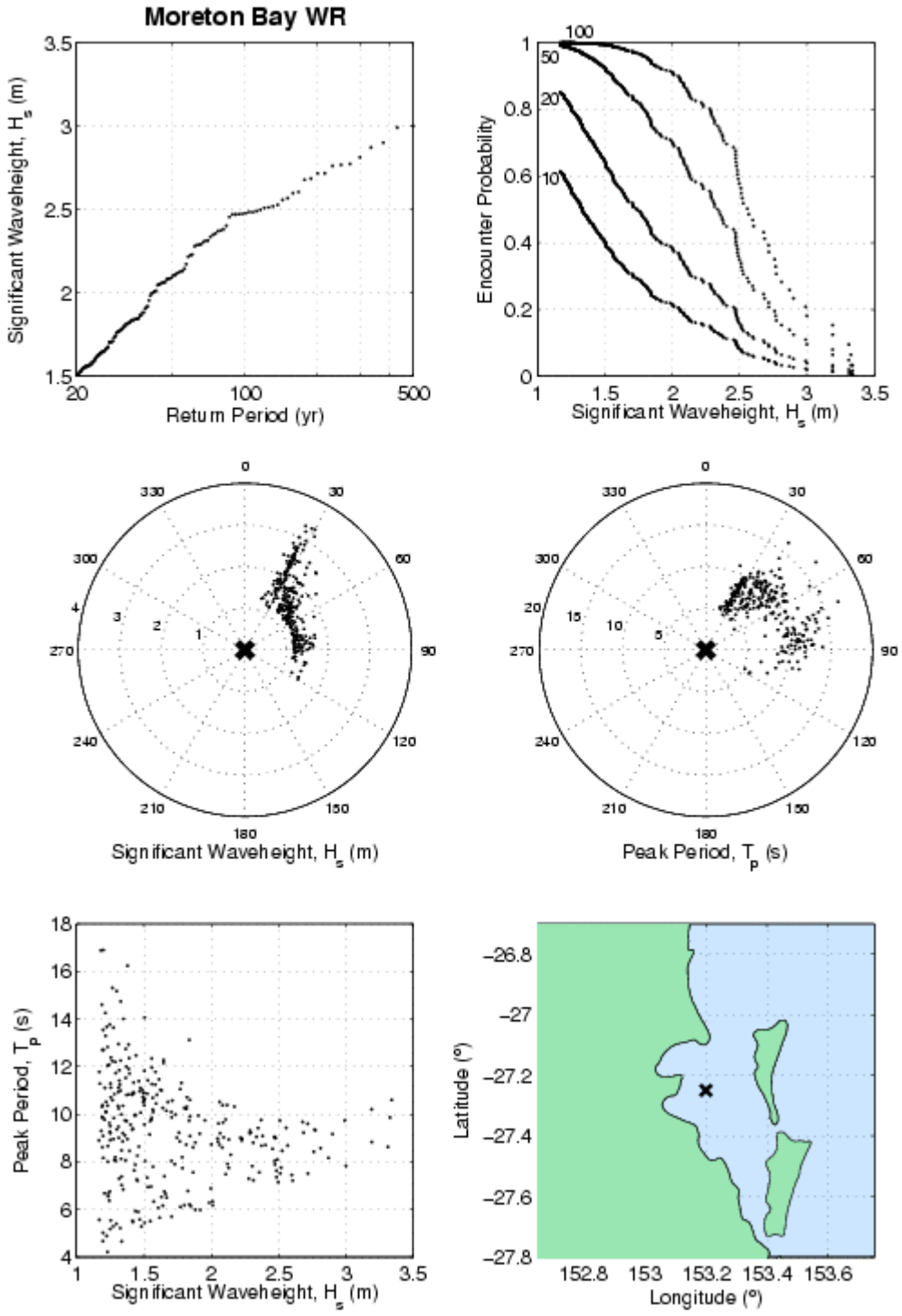

Figure D12. *Moreton Bay WR*. Data sheet for wave modelling output. (a) return period of H_s, (b) encounter probability of H_s for L = 10, 20, 50 and 100 years, (c) polar plot of H_s as a function of direction, (d) polar plot of T_p as a function of direction, (e) scatter plot of H_s vs T_p, (f) location map.

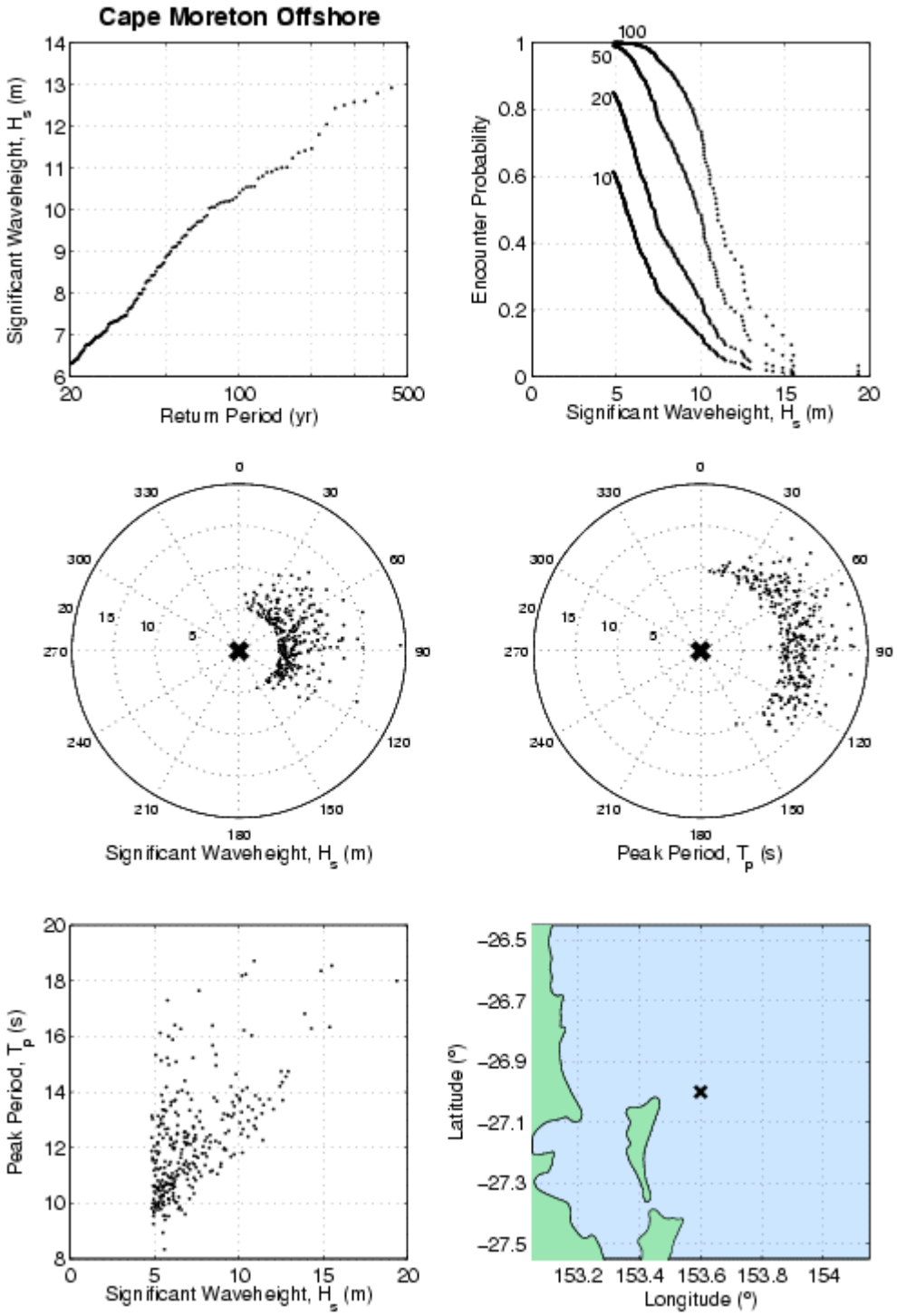

Figure D13. *Cape Moreton Offshore*. Data sheet for wave modelling output. (a) return period of H_s, (b) encounter probability of H_s for L = 10, 20, 50 and 100 years (c) polar plot of H_s as a function of direction, (d) polar plot of T_p as a function of direction, (e) scatter plot of H_s vs T_p, (f) location map.

APPENDIX E

GREENHOUSE: STORM TIDE RETURN PERIOD CURVES: HERVEY BAY

Return Period curves for storm tide, surge plus tide, surge and wave setup, including the effects of three greenhouse scenarios, for the output points in Hervey Bay (Figure E1) are presented. These same curves are also displayed in the *Atlas of Physical Processes in the Great Barrier Reef World Heritage Area* which is located on the *MMU* web site (http://mmu.jcu.edu.au).

These curves are valid for water levels produced during tropical cyclones. Extra-topical storms and other meteorological and oceanic causes of water level change (not modelled here) will contribute to the return period of water levels at lower return periods.

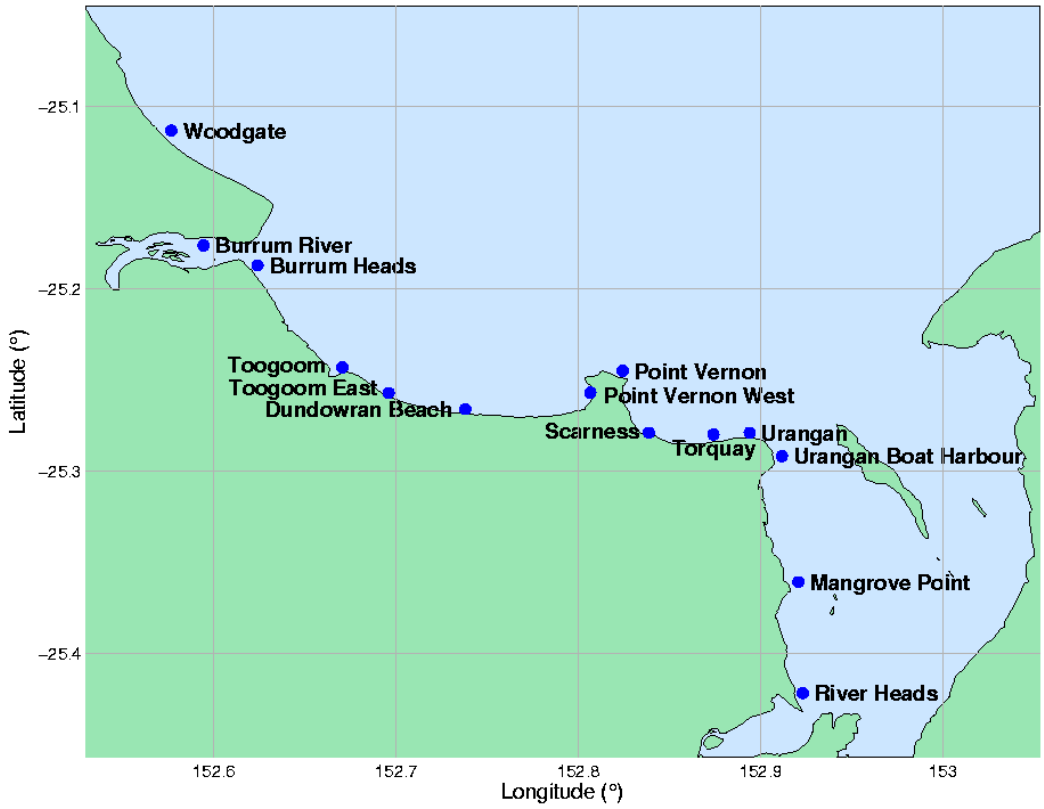

Figure E1. Hervey Bay study area and water level reporting locations

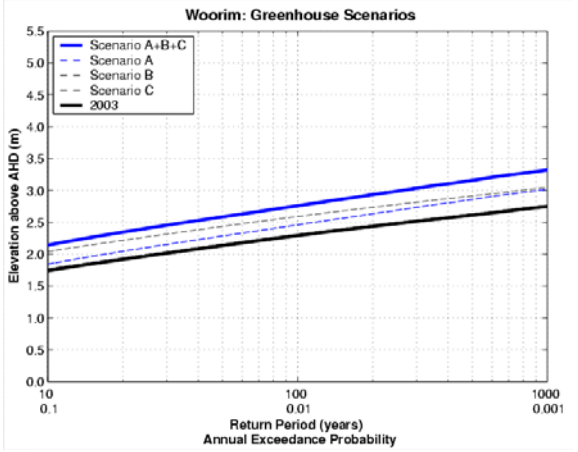

Figure E2. Water level frequency: *Woodgate*

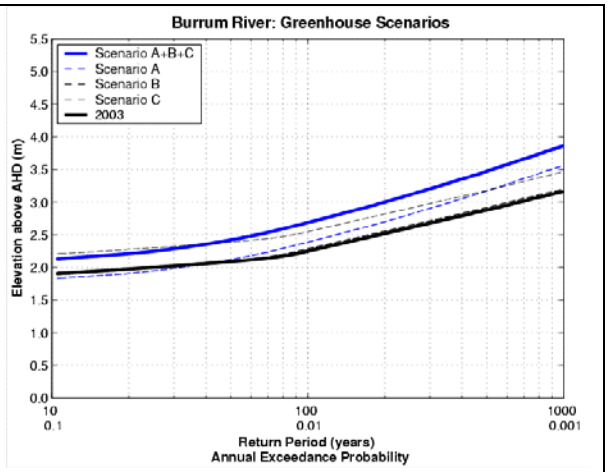

Figure E3. Water level frequency: *Burrum River*

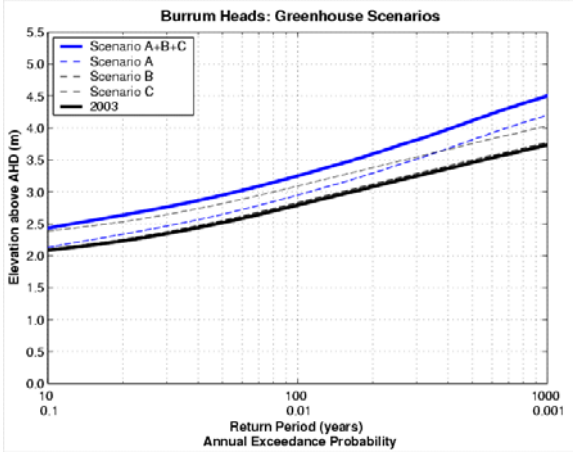

Figure E4. Water level frequency: *Burrum Heads*

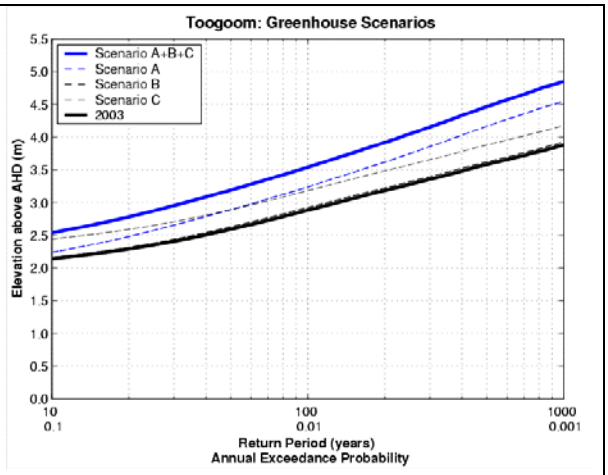

Figure E5. Water level frequency: *Toogoom*

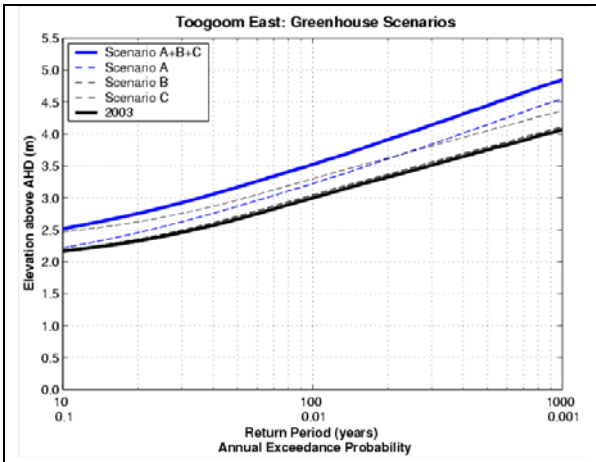

Figure E6. Water level frequency: *Toogoom East*

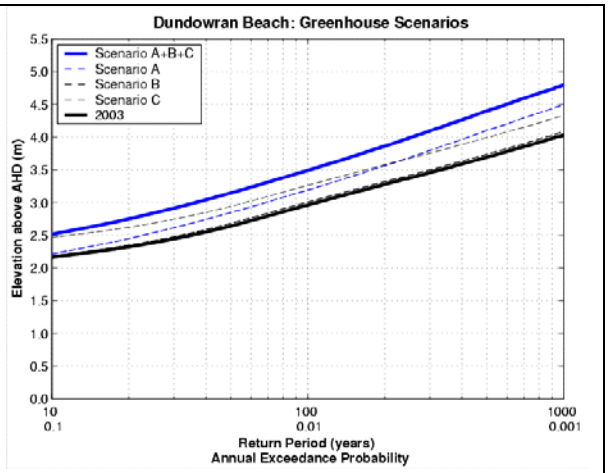

Figure E7. Water level frequency: *Dundowran Beach*

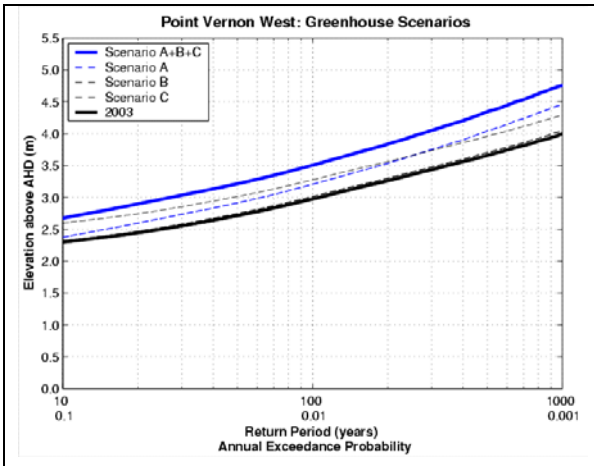

Figure E8. Water level frequency*: Point Vernon West*

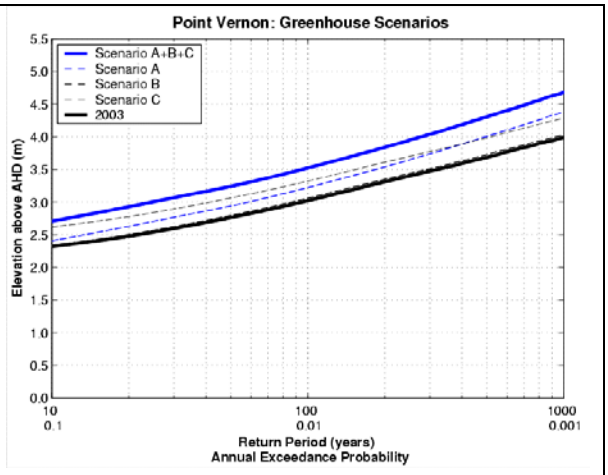

Figure E9. Water level frequency: *Point Vernon*

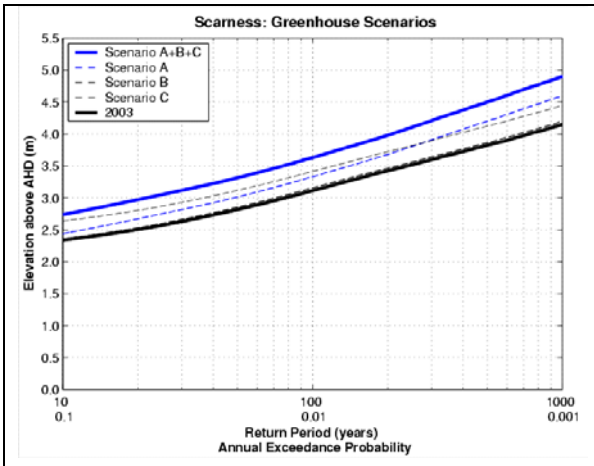

Figure E10. Water level frequency: *Scarness*

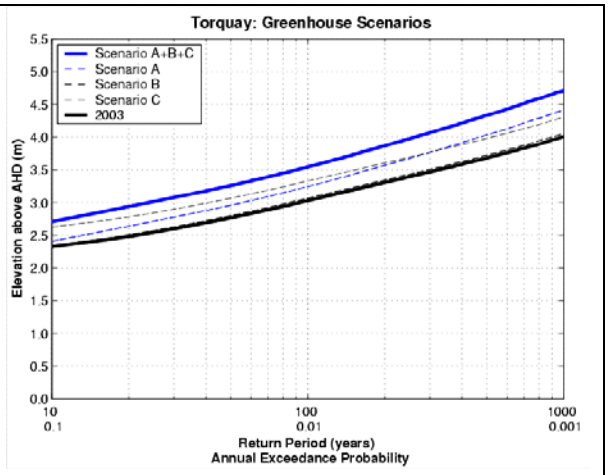

Figure E11. Water level frequency: *Torquay*

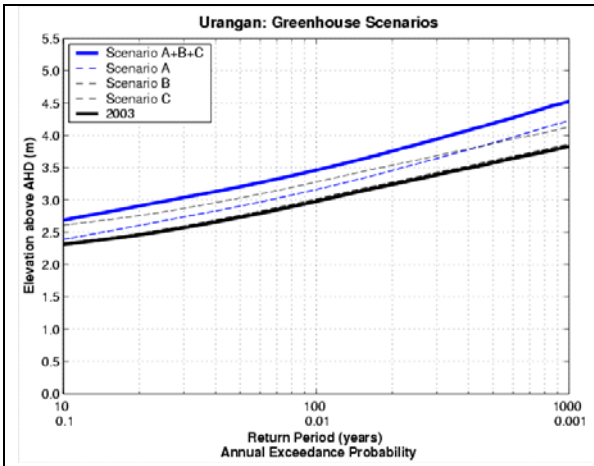

Figure E12. Water level frequency: *Urangan*

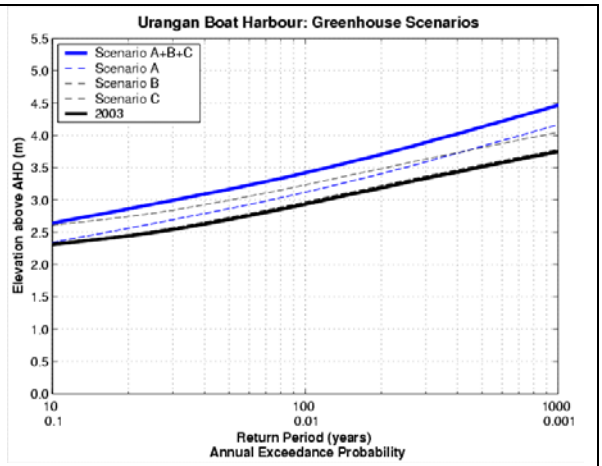

Figure E13. Water level frequency: *Urangan Boat Hr.*

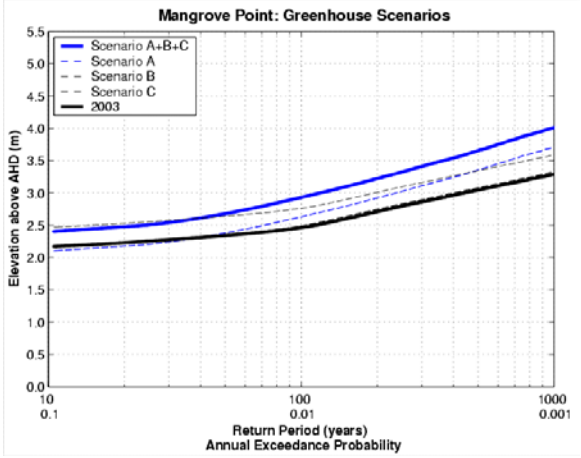

Figure E14. Water level frequency*: Mangrove Point*

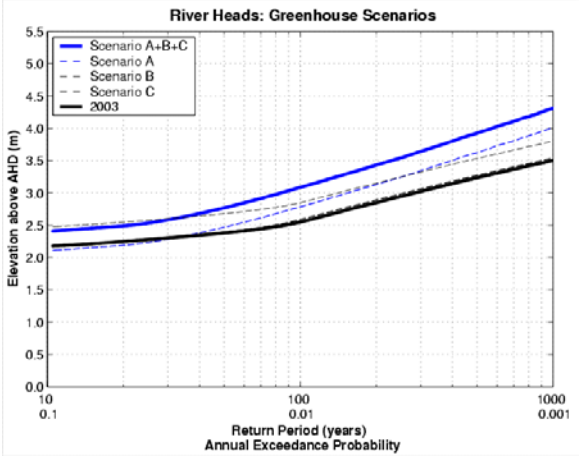

Figure E15. Water level frequency: *River Heads*

APPENDIX F

GREENHOUSE: STORM TIDE RETURN PERIOD CURVES: SUNSHINE COAST

Return Period curves for storm surge, surge plus tide, surge and wave setup, including the effects of three greenhouse scenarios, for the output points at Sunshine Coast (Figure F1) are presented. These same curves are also displayed in the *Atlas of Physical Processes in the Great Barrier Reef World Heritage Area* which is located on the *MMU* web site (http://mmu.jcu.edu.au).

These curves are valid for water levels produced during tropical cyclones. Extra-topical storms and other meteorological and oceanic causes of water level change (not modelled here) will contribute to the return period of water levels at lower return periods.

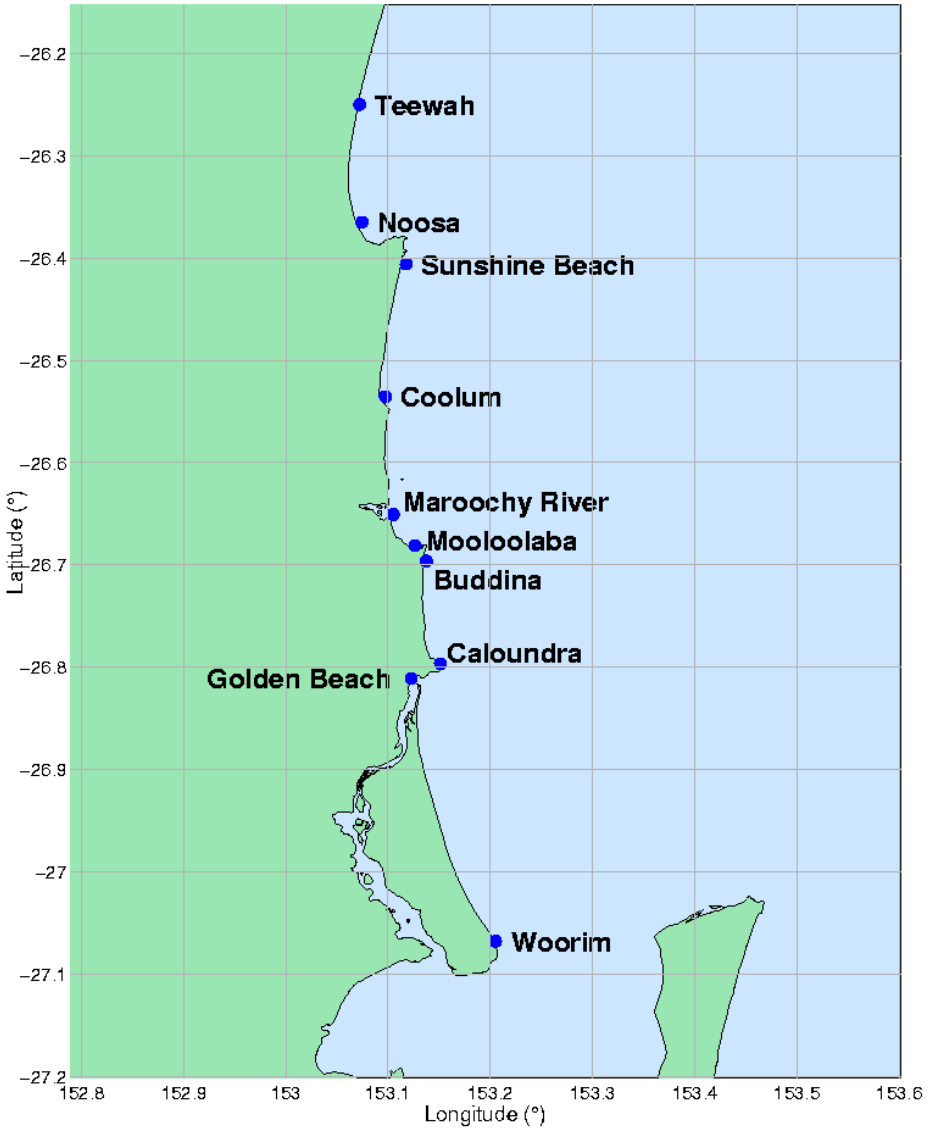

Figure F1. Sunshine Coast study area and water level reporting locations

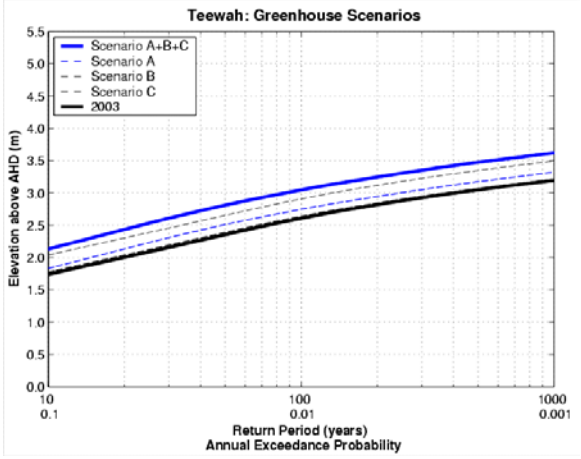

Figure F2. Water level frequency: *Teewah*

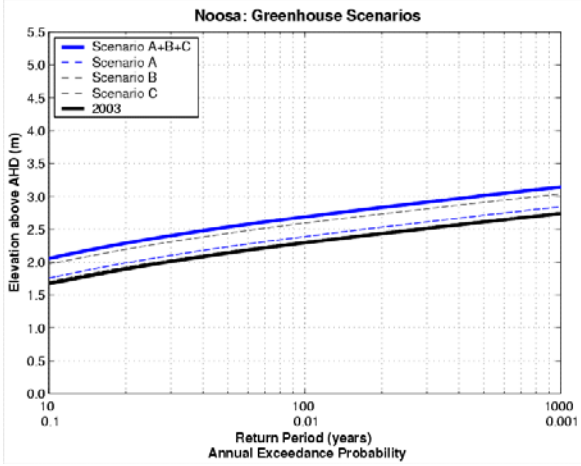

Figure F3. Water level frequency: *Noosa*

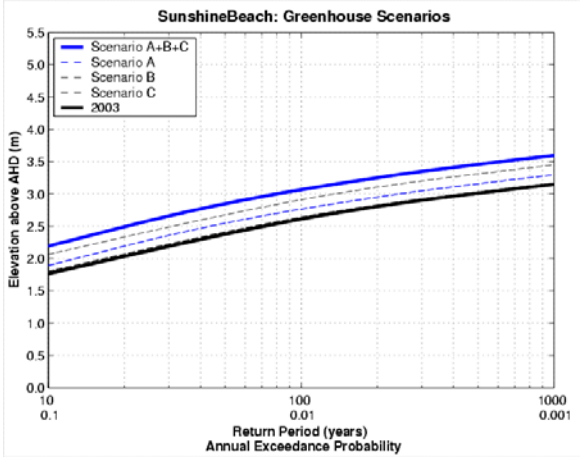

Figure F4. Water level frequency: *Sunshine Beach*

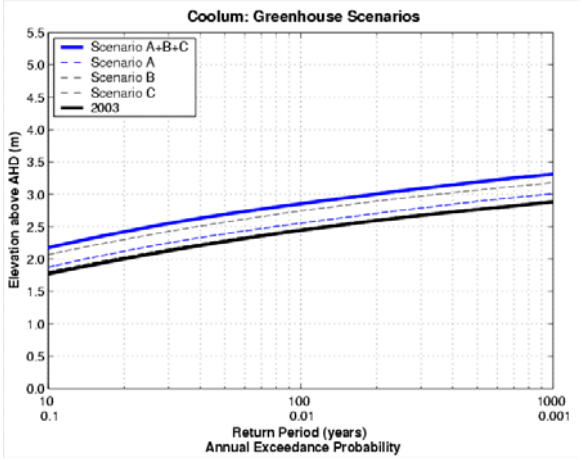

Figure F5. Water level frequency: *Coolum*

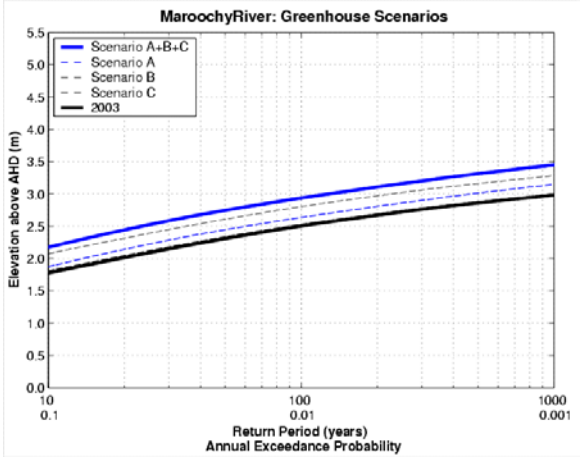

Figure F6. Water level frequency: *Maroochy River*

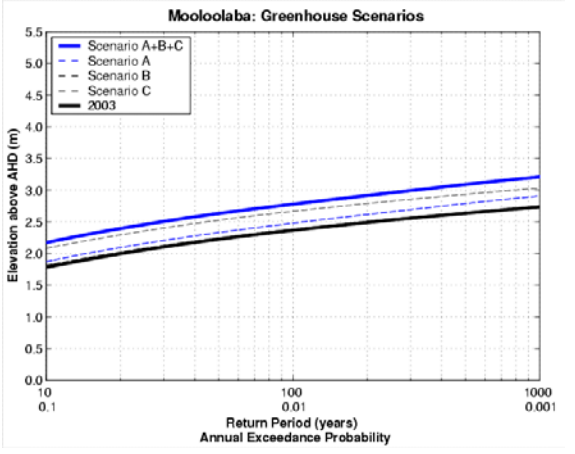

Figure F7. Water level frequency: *Mooloolaba*

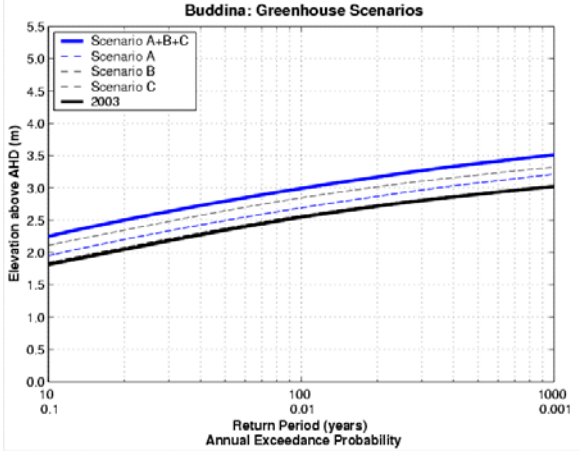

Figure F8. Water level frequency: *Buddina*

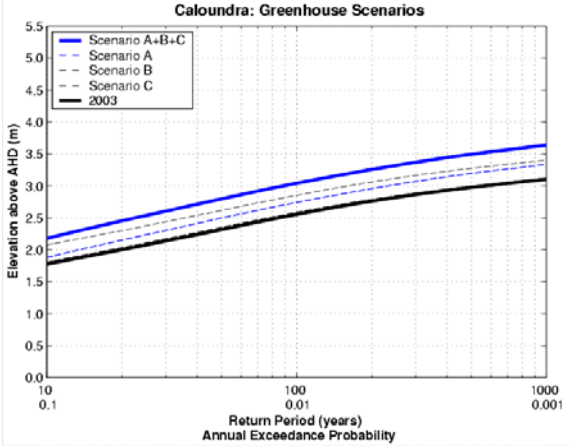

Figure F9. Water level frequency: *Caloundra*

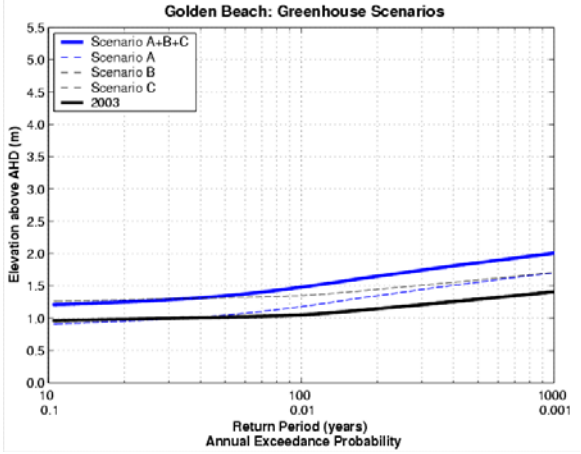

Figure F10. Water level frequency: *Golden Beach*

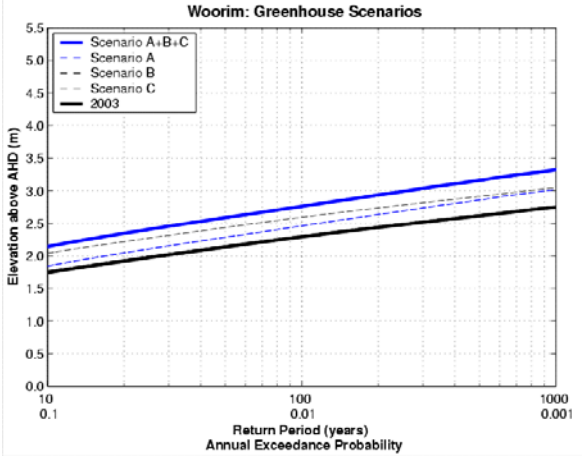

Figure F11. Water level frequency: *Woorim*

APPENDIX G
PARAMETRIC MODEL OF TROPICAL CYLONE WAVES

James Cook University
School of Engineering
Marine Modelling Unit

Queensland Climate Change and Community Vulnerability to Tropical Cyclones: Ocean Hazards Assessment - Stage 2

Parametric Tropical Cyclone Wave Model for Hervey Bay and Gold Coast

DRAFT

November 2002

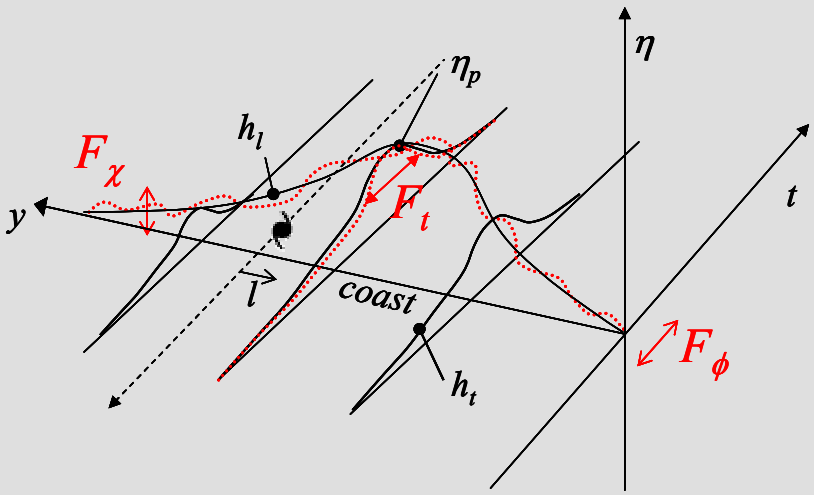

Numerical Modelling and Risk Assessment

ABN 65 073 544 439

7 Mercury Court
Bridgeman Downs
Qld 4035

J0202-PR001A

Table of Contents

1 Introduction

The parametric wave model has been proposed under the Ocean Hazards Assessment project (Harper 2001) to permit very fast estimation of site specific wave conditions likely to be experienced during tropical cyclones that can be used in either forecast scenario situations or for use in Monte Carlo simulation studies to assist planning and design.

The parametric model is developed from a series of detailed numerical model simulations, where the results are systematically analysed to extract the basic forms of the spatial and temporal variations in wave conditions at specific sites. The accuracy of the parametric model is firstly dependent on the number of specific scenarios that are provided to it and secondly on the degree of smoothing and approximation applied during the analysis.

The following development is based on the work undertaken as part of the Ocean Hazards Assessment Stage 1 surge model development (BoM 2001), partly paralleling the development of the parametric storm surge model. Additional parameters are included here to account for wave period and direction.

2 Basis of the Tropical Cyclone Parametric Wave Model

2.1 Premise

The wave response η at any coastal site (x,y) can be represented by a combination of the incident tropical cyclone parameters $\{TC\}$ and the characteristics of the coastal basin $\{Basin\}$, viz

$$\eta = \boldsymbol{f}\,[\ \{TC\}\ ,\ \{Basin\}\ ]$$

where

$$\{TC\} \quad = \boldsymbol{f}\,[\ \Delta p\ ,\ R\ ,\ B,\ V_{fm}\ ,\ \theta_{fm}\ ]$$

with Δp = the central pressure deficit (hPa)
R = the radius of maximum winds (km)
B = the windfield peakedness after Holland (1980)
V_{fm} = the speed of forward motion (ms^{-1})
θ_{fm} = the bearing of movement (°)

$$\{Basin\} \quad = \boldsymbol{f}\,[\ l\ ,\ \chi_b\ ,\ \chi_c\ ]$$

and l = perpendicular distance from the storm track centreline to (x,y)
χ_b = the *global basin* characteristics, e.g. depths, shelf width, slope, reefs etc
χ_c = the *local coastal* influences, e.g. bays, capes etc

This is illustrated by considering a hypothetical straightline coast basin with invariant shelf and slope characteristics. In Figure 2.1, the location (x_i,y_i) is any coastal location of interest in the schematic $\{Basin\}$, situated a distance l perpendicular from the (assumed straightline) track of a tropical cyclone with characteristics $\{TC\}$, which makes landfall at location (x_l,y_l).

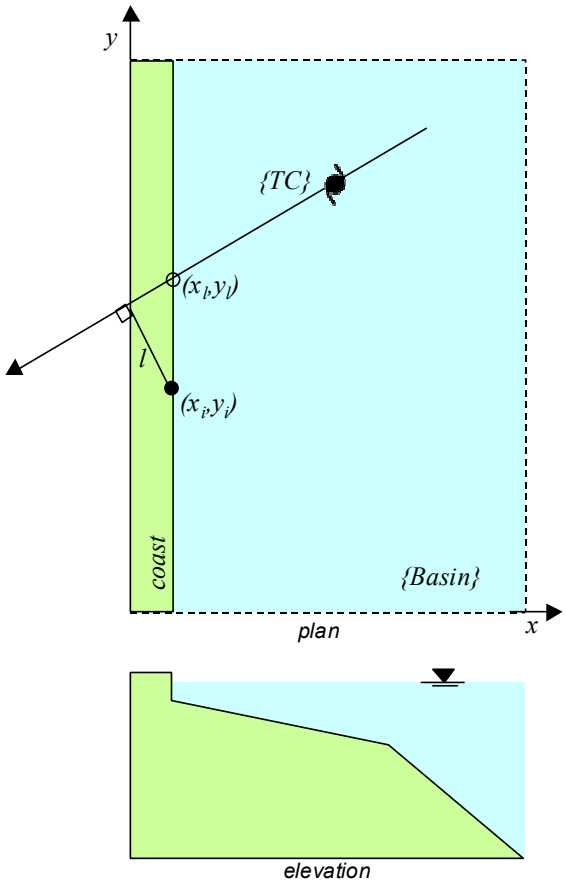

Figure 2.1 Schematic of a tropical cyclone impinging on a hypothetical straightline uniform basin.

The expected shape of the time history of wave height $\eta(t)$ at (x_i,y_i) is illustrated in Figure 2.2 as a single-peaked response.

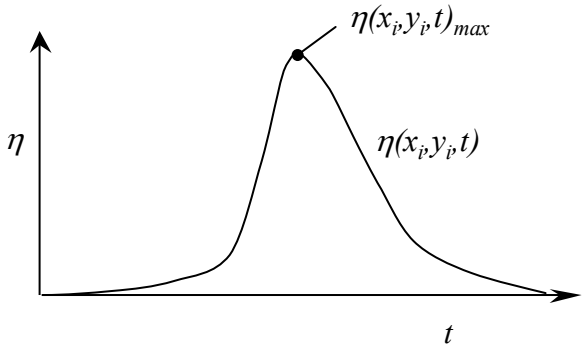

Figure 2.2 Wave height time history at any coastal location.

In a real-world basin the coastline is irregular and the offshore bathymetry varies, such that χ_c is not constant, and

$$\eta(x_i,y_i,t)_{max} = \boldsymbol{f}\,[\,\{TC\},\ \chi_b\ ,\ l\ ,\ \chi_c\,]$$

However, for the schematic uniform basin, it matters not where the point of interest lies but only the relative distance between the point and the storm track. In that case χ_c is constant, hence

$$\eta(x_i,y_i,t)_{max} = \boldsymbol{f}\,[\,\{TC\},\ \chi_b\ ,\ l\ \,]$$

Now consider the maximum envelope of wave height throughout the schematic basin after a tropical cyclone event has occurred, where the peak "open coast" wave height (not affected by χ_c) is η_p. as shown in Figure 2.3.

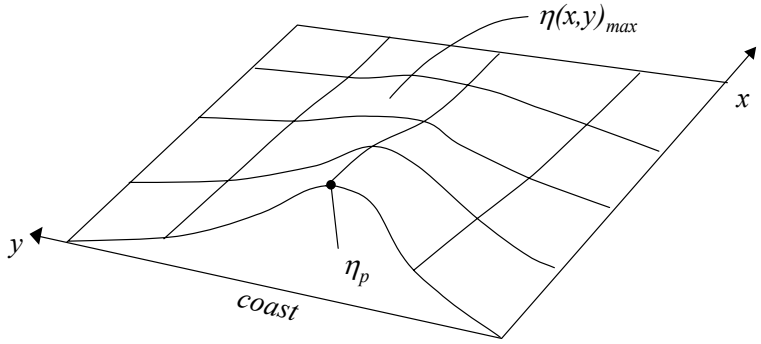

Figure 2.3 Maximum envelope of wave height.

It is then assumed that η_p within any specific basin will, to first order accuracy, be a joint function of storm intensity and track; viz

$$\eta_p = \boldsymbol{O_1}\,[\,\Delta p \mid \theta_{fm} \mid \chi_b\,]$$

However, θ_{fm} *and* χ_b may be essentially combined because of the interaction between storm track and line of coastline, with χ_b essentially being bound to that result, hence

$$\eta_p = \boldsymbol{O_1}\,[\,\Delta p \mid \theta_{fm}\,]$$

The remaining parameters are then assumed to be second-order and independent, i.e.

$$\eta_p = \boldsymbol{O_1}\,[\,\Delta p \mid \theta_{fm}\,] \;+\; \boldsymbol{O_2}\,[\,R\ ,\ B\ ,\ V_{fm}\,]$$

This is then evaluated numerically as follows:

$$\eta_p = h_p\,(\,\Delta p\ ,\ \theta_{fm}\,) \times F_R \times F_B \times F_{Vfm}$$

where h_p is a joint response function of Δp and θ_{fm} based on a set of reference values for R, B and V_{fm} which yields the peak open coast wave magnitude.

F_R , F_B , and F_{Vfm} are then dimensionless open coast response scaling factors or multipliers, relative to the adopted reference value for each parameter in the h_p function, e.g.

$F_R = [h_p]_{R=R'} / [h_p]_{R=R^*}$

Where $R = R^*$ is the reference value for R used in the definition of the h_p function (selected from mean climatology) and R' is the actual value required.

Hence, in summary

$h_p = \boldsymbol{f}(\Delta p , \theta_{fm})_{R=R^*, B=B^*, Vfm=Vfm^*}$

which is obtained via numerical experimentation to yield, e.g.

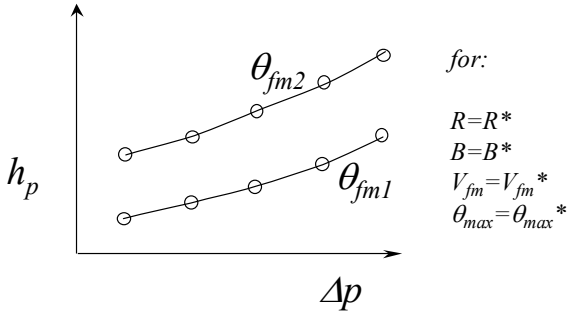

Figure 2.4 Construction of the base peak wave response function h_p.

2.2 Spatial Distribution of Open Coast Wave Magnitude

The spatial distribution of the open coast wave magnitude is then assumed to be a joint function of the following variables:

$h_l = \boldsymbol{f} [l \mid R \mid \theta_{fm}]$

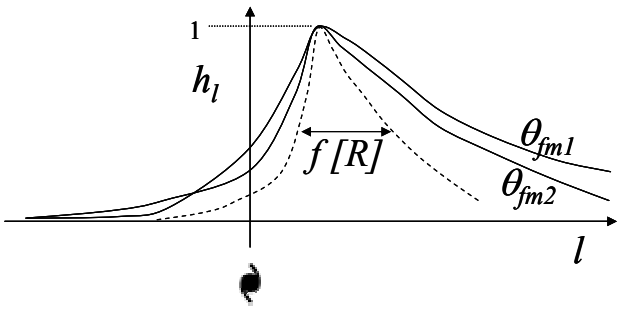

and expressed as a normalised function, as illustrated schematically in Figure 2.5 below.

Figure 2.5 Alongshore open coast wave magnitude distribution h_l.

It is argued that R, being the essential horizontal scale parameter of the tropical cyclone, will likewise scale the alongshore "width" of the wave magnitude.

This is achieved by converting the alongshore distance l into a non-dimensional form using R^*, where

$$l^* = \frac{l}{R^*} \qquad \text{which yields} \quad h_l = \boldsymbol{f}\,[\, l^*,\ \theta_{fm}]$$

2.3 Temporal Variation in Open Coast Wave Magnitude

The temporal distribution of the open coast wave magnitude is then assumed to be a joint function of the following variables:

$$h_t = \boldsymbol{f}\,[\, t \mid V_{fm} \mid \theta_{fm}]$$

and expressed as a normalised function, as illustrated schematically in Figure 2.6 below.

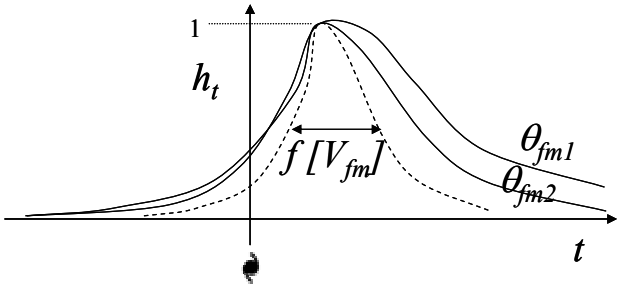

Figure 2.6 Temporal variation in open coast wave magnitude h_t.

It is argued that V_{fm}, being the essential scale parameter of the tropical cyclone movement, will likewise scale the temporal "width" of the wave hydrograph.

This is achieved by converting the time base t to a non-dimensional form using the time to travel R^* at V_{fm}^*, where[1]

$$t^* = \frac{t}{t_{R^*,\ V_{fm}^*}} \qquad \text{which yields} \quad h_t = \boldsymbol{f}\,[\, t^*,\ \theta_{fm}]$$

2.4 Local Coastal Influences

The site specific coastal influences χ_c are then assumed to act locally in modifying the open coast wave magnitude and timing, whereby

F_χ = a dimensionless wave magnitude multiplier; and

F_ϕ = a relative peak wave magnitude phase shift value in hours; and

F_t = a dimensionless time history shape factor.

with the expected variation in each of these being schematised as a function of the alongshore position y. From experiment, these are best represented as a local function of l but are represented schematically in Figure 2.7 by their mean values.

[1] Any suitable spatial scale can be used and a fixed value of 20 km has been used in practice.

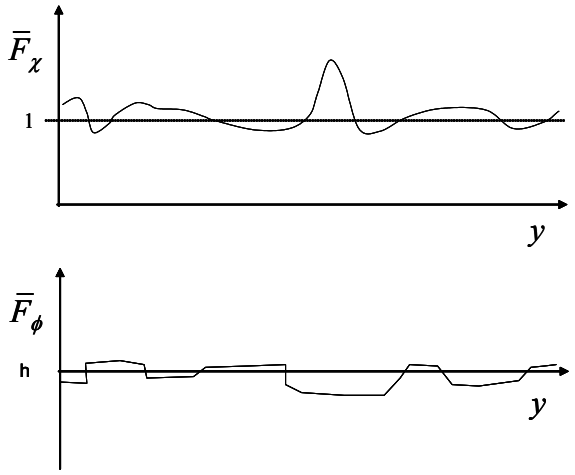

Figure 2.7 Localised open coast wave magnitude and phase modification.

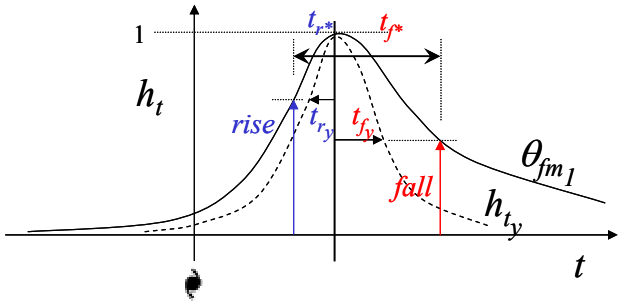

Figure 2.8 Localised open coast time history shape modification.

The time history shape factor F_t is determined by the relative "width" of the time history response at each site *y* compared with the equivalent width for the open coast time history. This is evaluated at separate *rising* and *falling* stages of the wave hydrograph, relative to the time of the peak wave. The parameters *rise* and *fall* are proportions of the normalised peak wave height and have been fixed for all sites at 0.8 and 0.4 respectively[2].

The site specific shape factors are, from Figure 2.8 then:

$$\overline{F}_{t_{rise\,y}} = \frac{t_{r^*}}{t_{r_y}} \quad \text{and} \quad \overline{F}_{t_{fall\,y}} = \frac{t_{f^*}}{t_{f_y}}$$

2.5 Combined Tropical Cyclone Wave Response

The combined wave time history at any coastal location *(y)* can then be expressed in terms of a combination of each component, as illustrated in Figure 2.9:

$$\eta(y,t) = \eta_p \times h_l(l, R, \theta_{fm}) \times h_t(t + \phi_\chi(y, l, \theta_{fm})) \cdot F_t(y, l, \theta_{fm}) \times F_\chi(y, l, \theta_{fm})$$

[2] These are taken from the surge modelling experience where it was found that the rising leg fitted better with a higher proportion, the falling leg with a low proportion. Optimisation could be used to determine the best overall combination for wave modelling.

where

$\eta_p = h_p(\Delta p, \theta_{fm}) \times F_R \,.\, F_B \times F_{Vfm}$

$F_R = f(\Delta p, R, \theta_{fm})$

$F_B = f(\Delta p, B, \theta_{fm})$

$F_{Vfm} = f(\Delta p, V_{fm}, \theta_{fm})$

with $l = l^* R^*$ and $t = t^* t_{R^*, Vfm^*}$

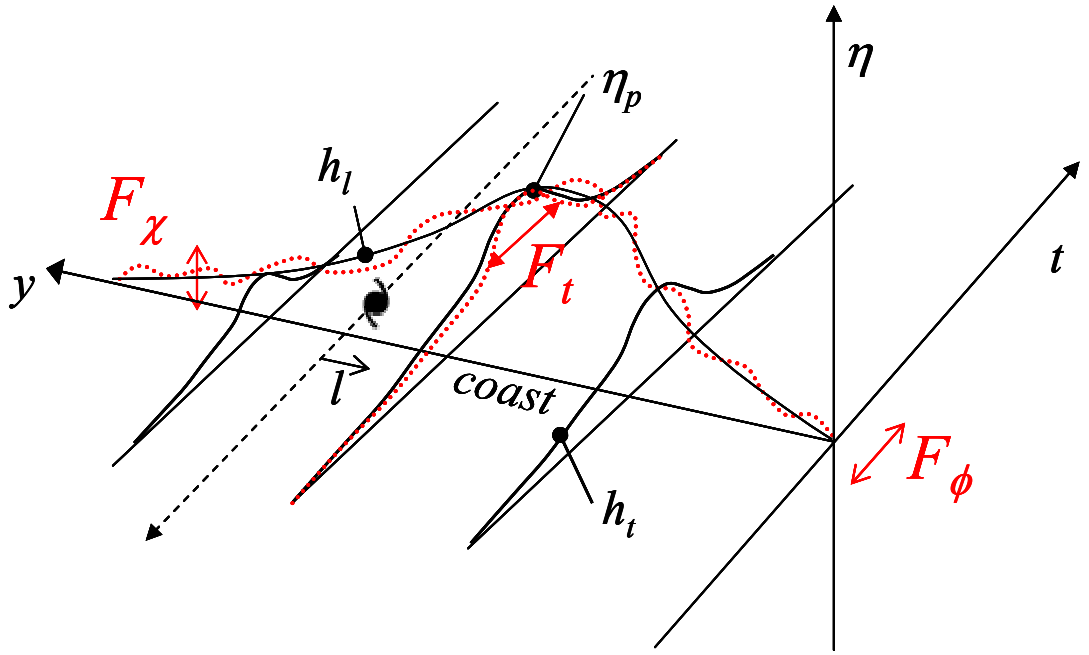

Figure 2.9 Combined wave response including local coastal effects.

The above formulation is applied specifically to the significant wave height H_s and is repeated in respect of the associated values of peak spectral period T_p and mean wave direction θ. The peak values of the associated variables are those at the time of the peak H_s. In the case of θ, the analysis is carried out separately on the x and y components of the wave direction vector, i.e. θ_x and θ_y. These are recombined in the final step to reconstitute the estimated value of θ.

It should be noted that references to specific sites is henceforth via the y index, which is simply each site's positional rank rather than a spatial offset within the model grid. Spatial offsets l are then retained for each site relative to each storm track during parameterisation and later calculated based on the landfall position during reconstruction.

3 Extraction of Parametric Forms

3.1 General Approach

Construction of a parametric wave model for any given {Basin} then proceeds as follows:

- Establish optimum tropical cyclone parameter ranges for the region
- Create numerical model domains of required extent and resolution
- Devise sequence of numerical experiments
- Perform the numerical modelling
- Analyse the results systematically to extract the parametric forms

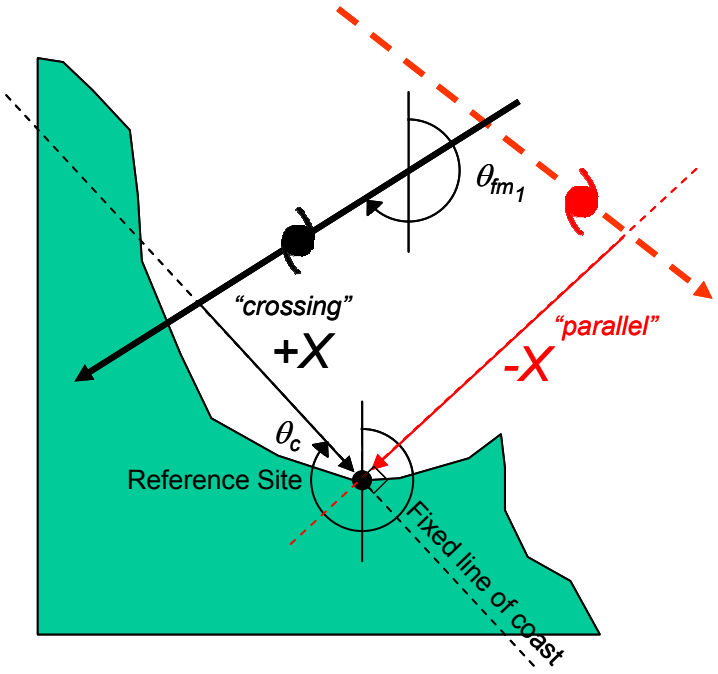

Figure 3.1 Coordinate system.

A coordinate reference system is needed to establish the geometry for the parameterisation. Figure **3.1** shows the coordinate system adopted for the present study[3], whereby a nominal coastal reference site is chosen together with an assumed "line of coast" θ_c. The line of coast is used simply to provide a baseline for the definition of the storm track landfall locations along the coast, whereby X is the distance from the track intersection with the line of coast to the reference site for "crossing" tracks. X is positive to the LHS of the track. The time of storm landfall at the actual coastline is also required to provide a common time reference for the parameterisation. In the case of "parallel" tracks, which do not cross the line of coast, the reference distance X is then taken perpendicular to the line of coast and the equivalent time of "landfall" is the time of closest approach to the reference site. The sign convention for X remains as positive when the reference site is to the LHS of the track.

The aim is to first examine the wave response variation over the range of sites of interest (i.e. y), for a range of θ_{fm} track classes, for a range of intensities Δp, but with fixed storm reference

[3] BoM (2001) uses a different coordinate system but this has no bearing on the ultimate parameterisation.

parameters R^* , B^*, V_{fm}^*. To this end a series of arbitrarily (ideally closely and equally) spaced storm tracks (defined by X) are devised for the region and the coastal sites are used initially as sampling points for determining the alongshore profile of peak wave height. To facilitate the interpolation of results, it is critical that each track class adopts exactly the same number and values of Δp. Also, each track class must have the same *number* of tracks (X), although each track class may have different X values if desired (e.g. parallel to coast versus crossing the coast).

3.2 Determining the Peak Alongshore Response Profile

This consists of assembling all $\eta(x,y,t)_{max}$ for the case of $x=x_1, x_2, x_3 \ldots x_n$ and $y=y_1, y_2, y_3 \ldots y_n$ being those points defining the contiguous open coastline (but excluding islands or inlets, channels and the like for the moment) and at the time of the local maximum value of η. To assist in schematising the results, the (x,y) spatial references are firstly converted to the storm landfall reference l (refer Figure 2.1). Because of this spatial transformation, which interacts with the storm track angle and the actual coastline shape, it is possible that l will not be unique and not monotonically increasing. Accordingly, the alongshore series is sorted in l and the maximum envelope is sampled on the basis of a defined resolution interval δl and the mean η_{max} is found within the interval. This is illustrated in Figure 3.2 below.

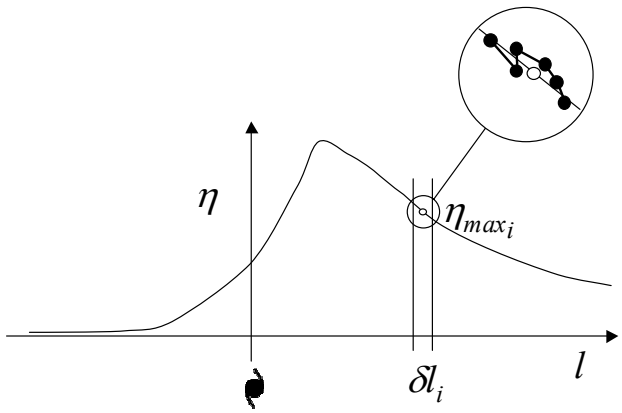

Figure 3.2 Sampled alongshore maximum wave envelope for a single storm event.

Multiple instances of the alongshore profiles are then combined from all of the closely spaced storm tracks (for each X) by aligning the responses on the basis of l. These are also averaged within each interval δl to form a *mean alongshore maximum envelope* as shown in Figure 3.3. This is considered to represent the "open coast response" for the basin for this combination of Δp , R^* , B^*, V_{fm}^* and θ_{fm}. The peak wave magnitude for this case is then stored as $h_p(\Delta p, \theta_{fm})$.

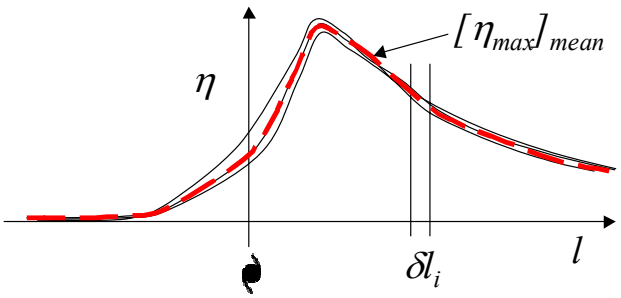

Figure 3.3 Mean alongshore maximum wave envelope formed from multiple tracks with same Δp.

This step is repeated for all Δp variants of the present θ_{fm} track set and the alongshore profiles are normalised in each case by the respective peak $h_p(\Delta p, \theta_{fm})$. The set of normalised alongshore profiles is then averaged to remove central pressure as a dependent variable. This is done as a weighted average according to h_p so that the model result will be biased towards the higher wave height cases.

Because the alongshore spacing of the wave model runs is likely to be relatively sparse, a spline curve is fitted to the final averaged profile to provide additional smoothing so that the next step in the processing will provide more gradually varying responses.

3.3 Local Site Specific Alongshore Factors

The residual difference between the mean alongshore maximum profile for this θ_{fm} track set of R^*, B^*, V_{fm}^* and the local (x,y) site maximum is then deemed to represent the influence of the local point-specific coastal effects $F\chi$.

Referring to Figure 3.4:

$$F\chi_i = (\delta\eta_i + \eta_i) / \eta_i$$

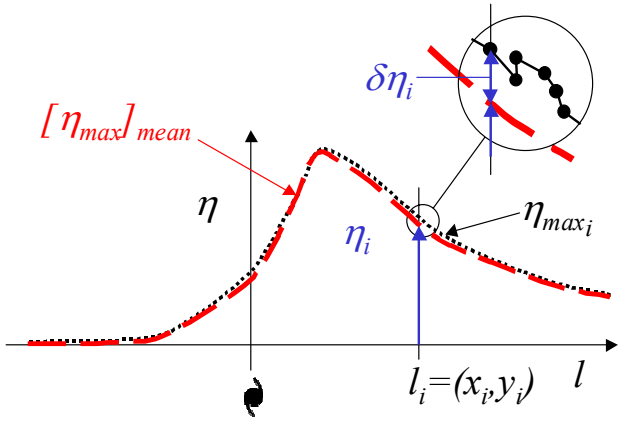

Figure 3.4 Derivation of local alongshore coastal response factors.

$F\chi_i$ was found to be best retained as a local function of l, with a typical site specific response function as shown in Figure 3.5.

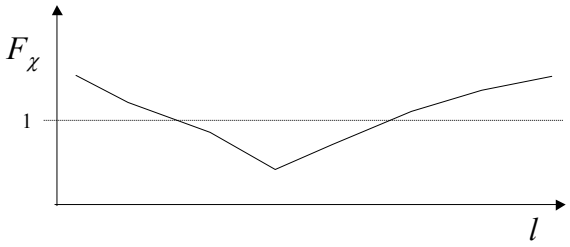

Figure 3.5 Typical alongshore local response factor.

3.4 Parallel Track Offshore Profiles

The case of the parallel track is treated differently in that, as per Figure **3.1**, the spatial profile of interest is in a plane perpendicular to the track direction rather than along the track. Figure 3.6 illustrates the arrangement, whereby the offshore profile is constructed by finding the $\eta(l)_{max}$ for each θ_{fm} track set.

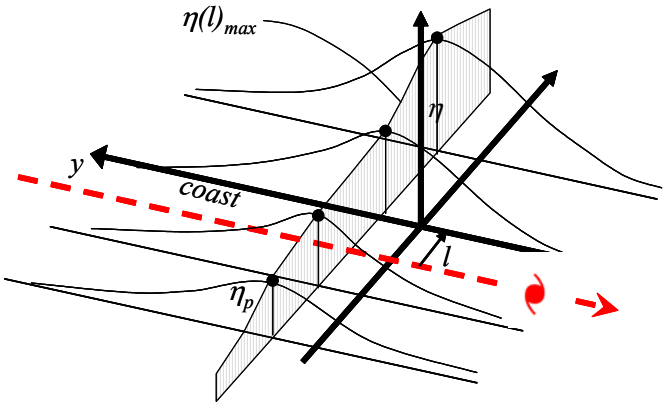

Figure 3.6 Mean offshore maximum wave envelope for the parallel track case.

3.5 Time History Response Profiles

This analysis is somewhat analogous to the alongshore spatial case but carried out in the time domain for each coastal point of interest. The starting context is many storms, each with a constant track θ_{fm} and constant intensity Δp but different coast crossing points X.

Firstly, the time response at each coastal point for each storm is normalised by its individual peak wave magnitude to give $h_t(l,t)_i$. Then the relative timing F_ϕ of the peak wave at each point i is retained and used to time shift its normalised time profile to the same zero time position and the mean time profile $h_t(l,t)_{mean}$ is calculated for each δl slice along the coast (refer Figure 3.7)[4]. The averaged phase offsets $F_\phi(l)_{mean}$ of each averaged peak are also retained at this point. The above is repeated for each Δp variant and a final weighted mean time history profile is established for each θ_{fm} track set. The parallel track case is treated analogously.

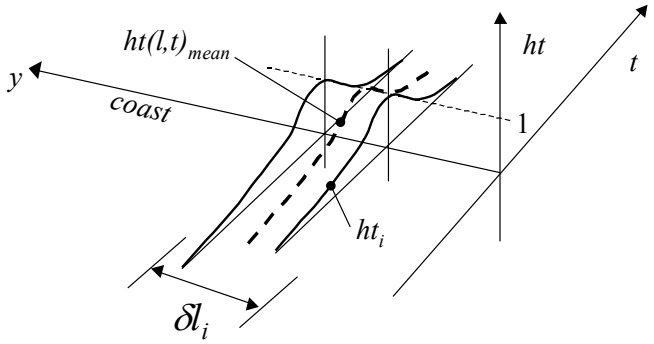

Figure 3.7 Mean time history curve formed from many tracks at δl resolution.

[4] The δl sampling of the time history profiles was not used in the present wave model development.

3.6 Site Specific Time History Profile Shape Factors

These are determined as per Figure 2.8, whereby the rising and falling wave hydrograph widths (for H_s only at this time) are calculated for each site and the ratio of those widths to the mean profile shape is retained as the shape factor $F_t\ (y, l, \theta_{fm})$. The use of H_s only in this process is believed to be a source of inaccuracy in regard to the estimation of T_p and θ away from the time of landfall and could be improved by including different shape factors for each variable.

3.7 Forward Speed Factors

The effect of forward speed is included by storing the base parameter time history profile results (i.e. using R^*, B^*, V_{fm}^*) in a non-dimensional time format. The actual forward speed is then used to re-dimensionalise the time profile in the predictive mode. However, because the forward speed can also have a strong influence on the absolute value of the peak wave condition, an F_{Vfm} factor is calculated from a separate (equivalent) set of model results where a range of V_{fm} values is used to complement the base value of V_{fm}^*. All other parameter values are held constant at the base values. This yields a set of h_p factors relative to the base V_{fm}^* value.

3.8 Radius to Maximum Wind Factors

These are assembled in an analogous manner to V_{fm}. The effect of radius is included by storing the base parameter peak alongshore profile results (i.e. using R^*, B^*, V_{fm}^*) in a non-dimensional spatial format. The actual radius R is then used to re-dimensionalise the spatial profile in the predictive mode. The radius can also have a strong influence on the absolute value of the peak wave condition, and so an F_R factor is calculated from a separate (equivalent) set of model results where a range of R values is used to complement the base value of R^*. All other parameter values are held constant at the base values. This yields a set of h_p factors relative to the base R^* value.

3.9 Windfield Peakedness Factors

These have not been included in the present model formulation due to the extra overheads originally envisaged in performing the regional WAM model simulations. It is believed that the effect of B will be similar to that for R, i.e. principally a spatial scaling effect but with additional impact on the absolute scale of the wave magnitude.

3.10 Regional and Local Parameters

Of the above parameters, the model separates those that apply in a regional sense from those that are site-specific. This allows better control over site-specific factors, for example, allowing particular sites to be grouped to improve their prediction accuracy. It also allows sites to be included that have been excluded from the regional analysis, e.g. offshore islands and the like. Accordingly, h_p , h_l , F_R , F_B , F_{Vfm}, are deemed *regional* parameters, while h_t , ϕ_χ , F_t , F_χ are *local* parameters.

4 Hervey Bay Implementation

The parent study (JCU 2002) utilised three nested numerical wave model grids (*A, B, C*; detailed elsewhere) and the WAMGBR spectral wave model (Hardy *et al* 2001). Of interest to the parametric model development is that the *regional* analysis should be based on a numerical grid which adequately samples the spatial extent of the tropical cyclone wave response. Typically, this would be satisfied by a domain of the order of ± 300 km (i.e. ± 10 *R*) at a nominal resolution of 5 km. The *B* grid satisfied these requirements.

4.1 Regional Site Selection

This was limited initially to all *B* grid sites south from Port Clinton but was restricted further after some experimentation to a lesser number of sites, as shown in Figure 4.1 . Restricting the number of sites was initially due to the need to remove the localised influences of Hervey Bay on the determination of the open coast alongshore profile. Accordingly, the regional sites were limited to those forming a more representative open coast sample.

After testing, problems with localised "noise" from some sites near Rockhampton necessitated their removal also. This manifested as fairly erratic responses at several of these sites, which was interfering with the smoothing of the alongshore profile. If many more *X* tracks had been possible, this issue would probably not have arisen.

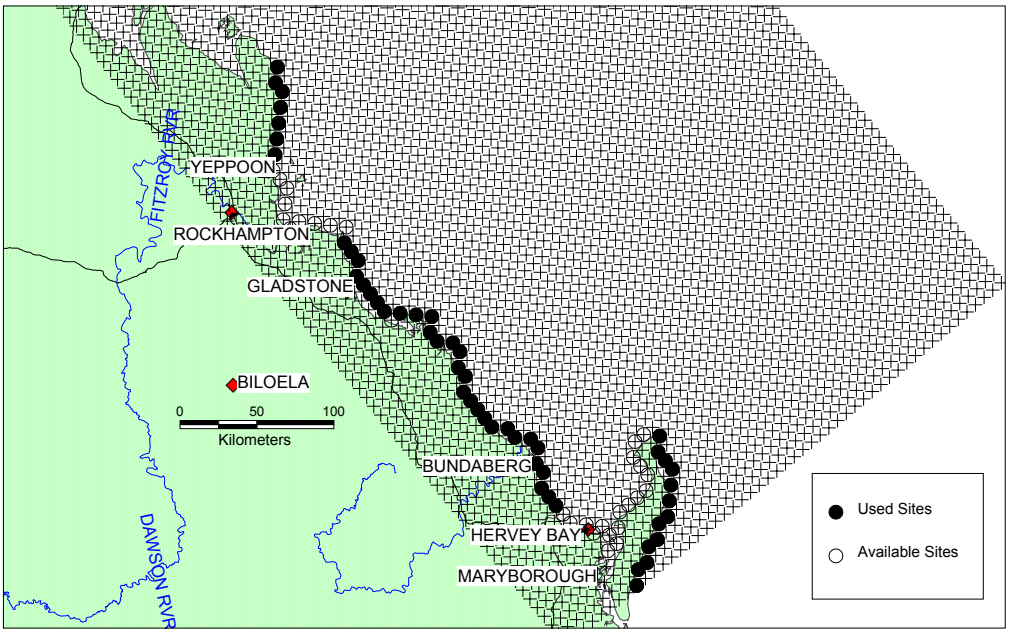

Figure 4.1 Open coast *B* grid sites selected for the Hervey Bay regional parametric model.

4.2 Storm Track Selection

The chosen reference site was near Urangan (-25.29°, 152.89°), with an assumed line of coast θ_c of 320°, as shown in Figure 4.2. The sites on this figure are identified by their alongshore (north to south) sequence order from the *B* grid. The selected site order differs due to the previously discussed omission of some sites. The circled sites are used for illustration of the model performance in later sections and are labelled by their parametric model site sequence.

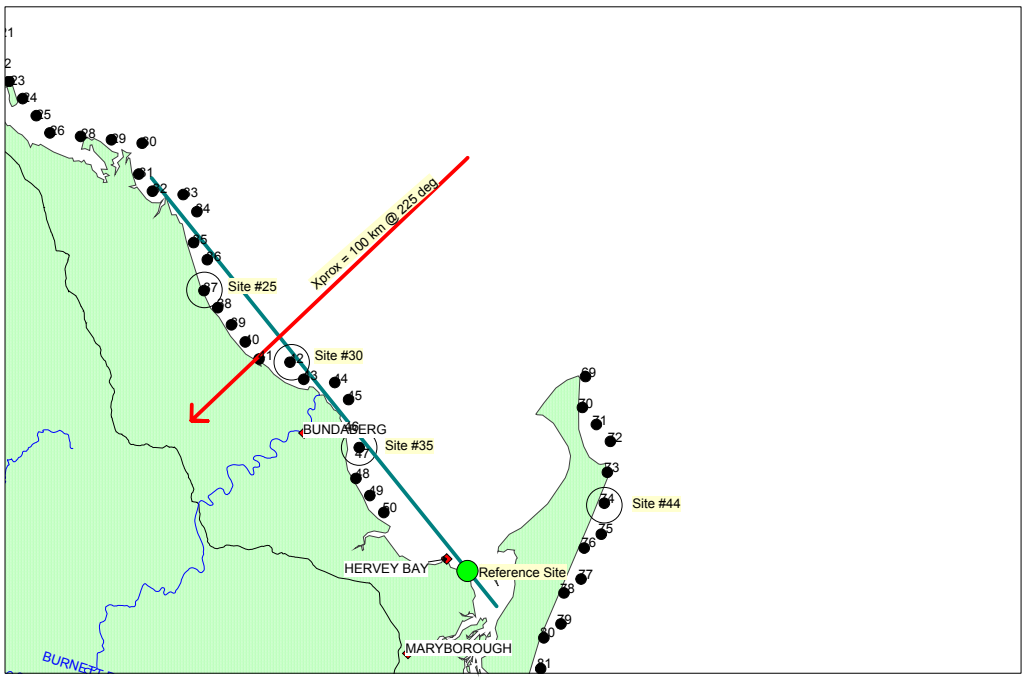

Figure 4.2 Reference geometry for Hervey Bay with example track.

Rather than evenly distributing track landfall positions equally along the coast (say every 20km), it was decided to target the limited number of tracks immediately near the Hervey Bay region. This was due to the expectation that the effect of the large scale bay could create some high gradients in wave conditions depending on the exact track landfall position. Accordingly, only six track landfall positions were simulated. These are shown below in Figure 4.3 for a landfalling case and in Figure 4.4 for the parallel track case, summarised as:

Landfalling	Parallel
X (km)	X (km)
-100	-200
0	-100
+25	-50
+50	-25
+100	0
+200	+100

4.3 Storm Parameter Selection

This was made in a manner designed to minimise the number of WAMGBR model simulations, whilst still providing representative coverage of the likely regional storm parameter ranges. The parameter values used are summarised as follows:

θ_{fm}	=	140,	180,	225,	270	°
Δp	=	23,	48			hPa
R	=	**20**,	50			km
V_{fm}	=	2,	**4**,	6,	10	ms^{-1}
B_0	=	**7.1**[5]				

with the "base run" parameters R^* and V_{fm}^* (representing the regional modal values) above shown in **bold**.

[5] A constant B_0 was used in preference to a fixed B; where $B = B_0 + p_c/160$.

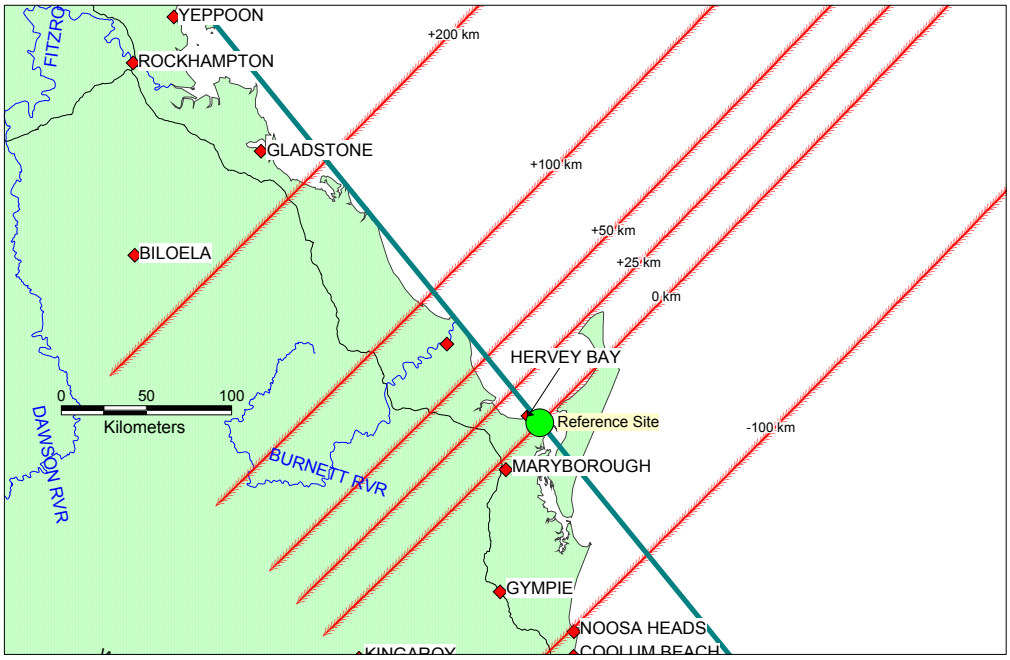

Figure 4.3 Modelled tracks for landfalling cases (225° case shown).

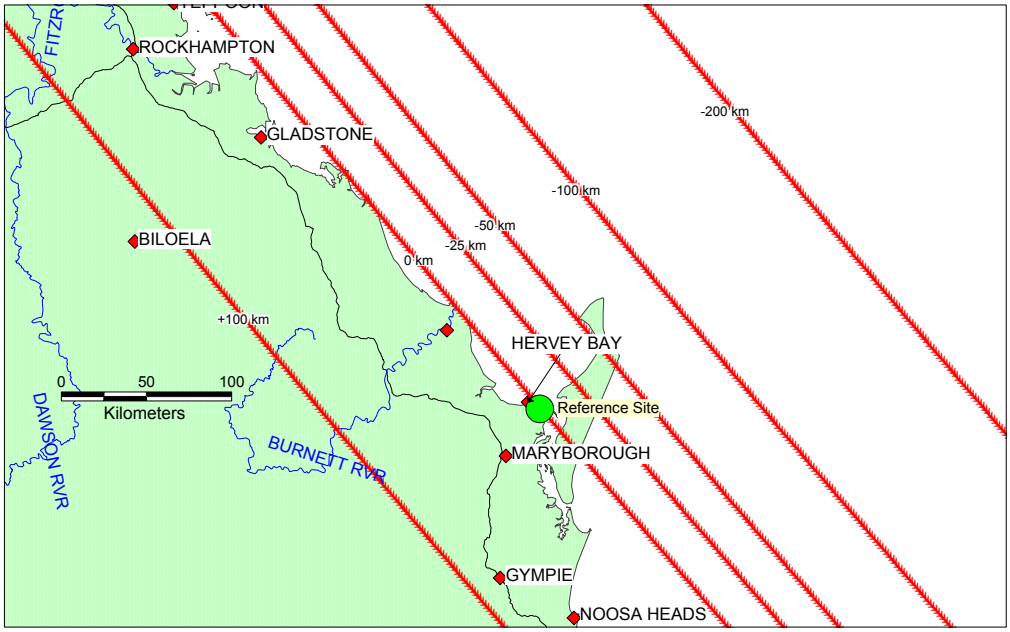

Figure 4.4 Modelled tracks for the single parallel case.

This parameter coverage required 64 separate WAMGBR storm simulations for each of the 6 track scenarios, totalling 384 runs over each of the three nested model grids. In addition, 2 special "anchor" runs were undertaken using Δp values of 10 and 90 hPa, but were applied only to a single θ_{fm} scenario of 225° and X of 25 km. These results were used to check the linearity of the wave response at values significantly above and below the standard range. The model allow "anchor" values to be used to provide an extrapolation capacity across the complete parameter range as a substitute for undertaking a larger number of simulations. The JCU MMU undertook the WAMGBR modelling and supplied the binary output files.

4.4 Local Site Selection

The finer scale *C* grid covering Hervey Bay itself was used to select a series of sites to be used for the *local* parametric model. These are shown below in Figure 4.5, with "Site 15" chosen for illustrative purposes in the following section.

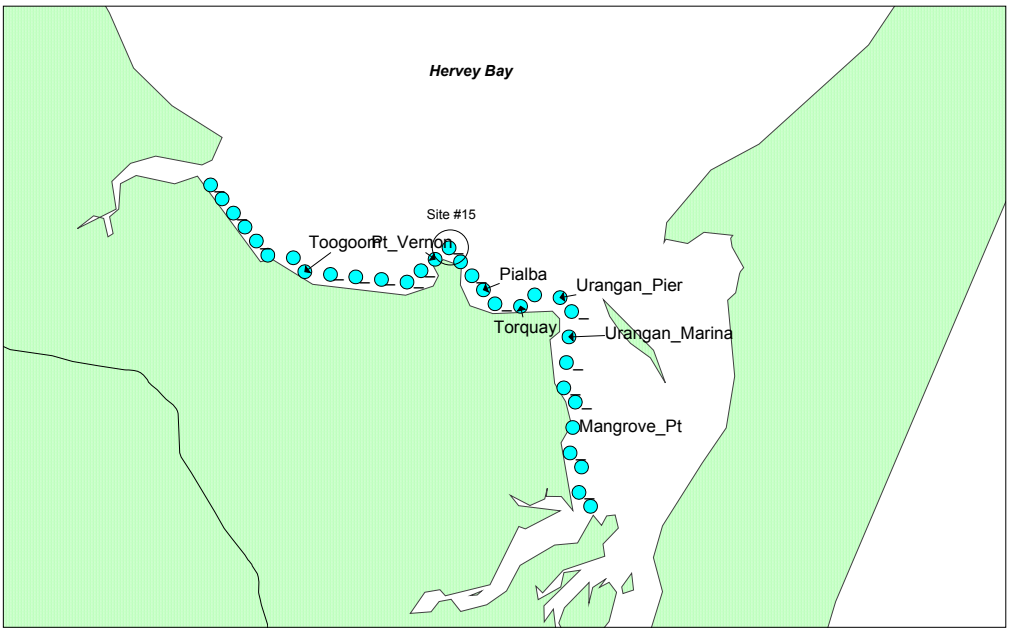

Figure 4.5 Nearshore *C* grid sites selected for the Hervey Bay local parametric model.

4.5 Parametric Model Performance

The parametric model is expected to be at its most accurate for the "base case" storms, where R is 20 km and V_{fm} is 4 ms^{-1}. During the data extraction process, the model maintains error statistics on the degree of approximation achieved. These show that the parameterisation of the peak wave conditions across all *B* grid sites is unbiased, with a mean RMS error for H_s of 0.20 m and for T_p of 0.45 s. The mean direction error, in component form, is 0.12 and 0.10 for N and E respectively. Maximum absolute errors may be higher for individual sites and also at times not near the time of the peak condition. Due to the high level of approximation, errors tend to increase beyond ±6 h of landfall.

Examples of the model performance are presented in Figure 4.6 to Figure 4.9 below for each of the *B* grid sites #25, #30, #35 and #44 for the θ_{fm} case of 225°, X of 100 km, with Δp value of 23 hPa. The corresponding error summaries are shown in Figure 4.10. A parallel example (θ_{fm} case of 140°) is given for *B* #35 in Figure 4.11 and the θ_{fm} case of 225° for *C* #15 is given in Figure 4.12.

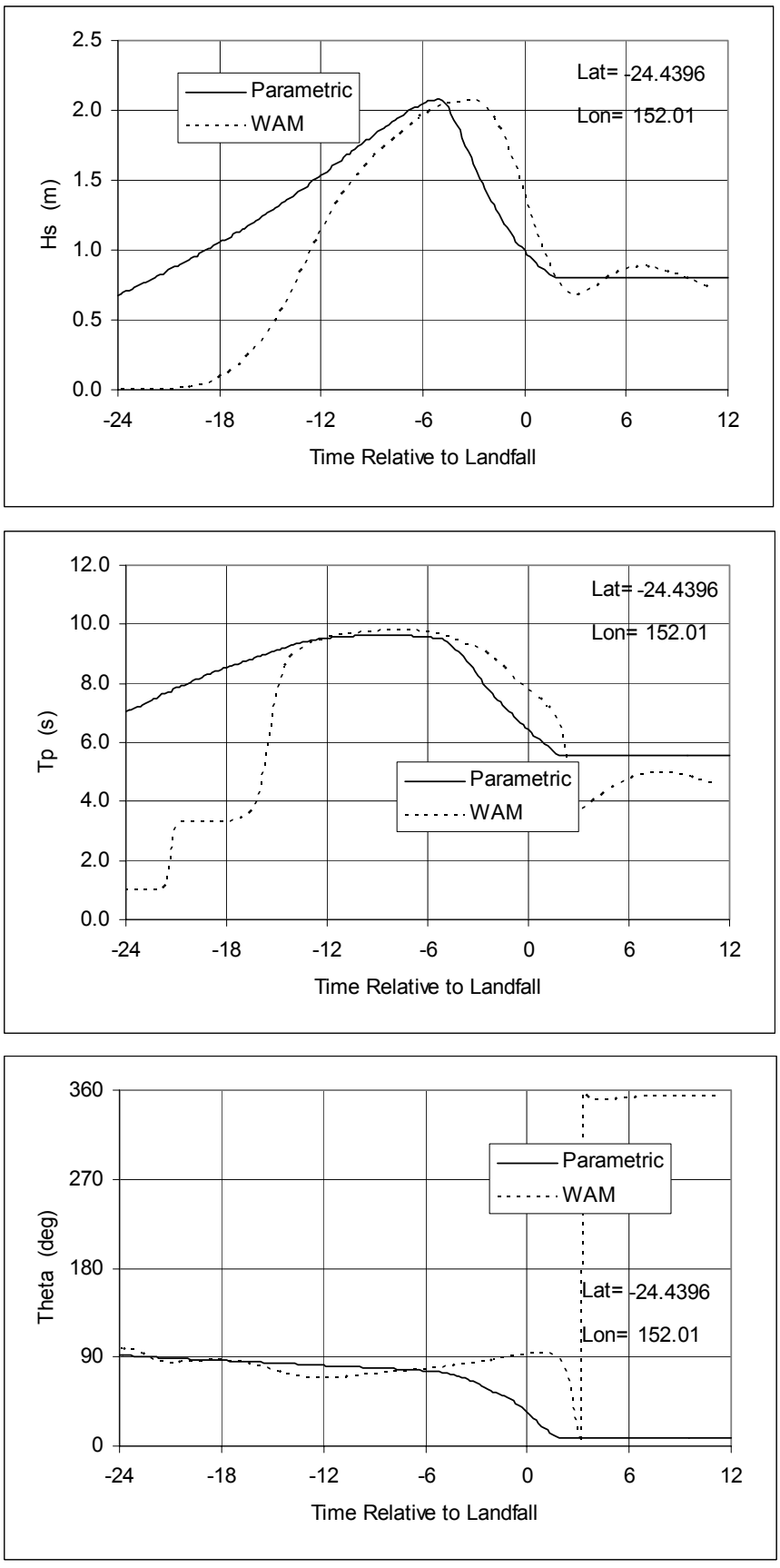

Figure 4.6 Parametric model result for *B* grid Site #25 (100 km, 225°, 23 hPa)

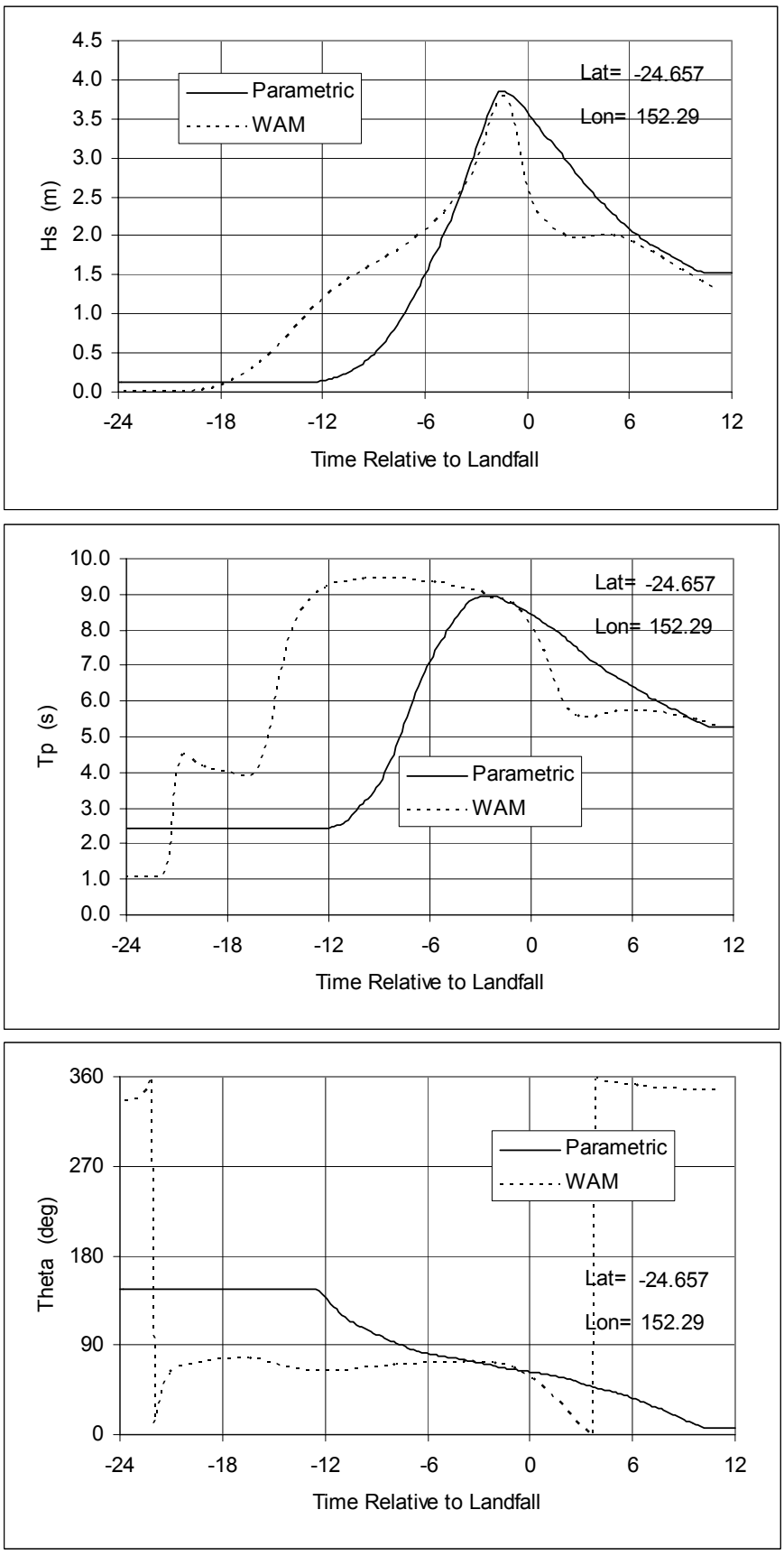

Figure 4.7 Parametric model result for *B* grid Site #30 (100 km, 225°, 23 hPa)

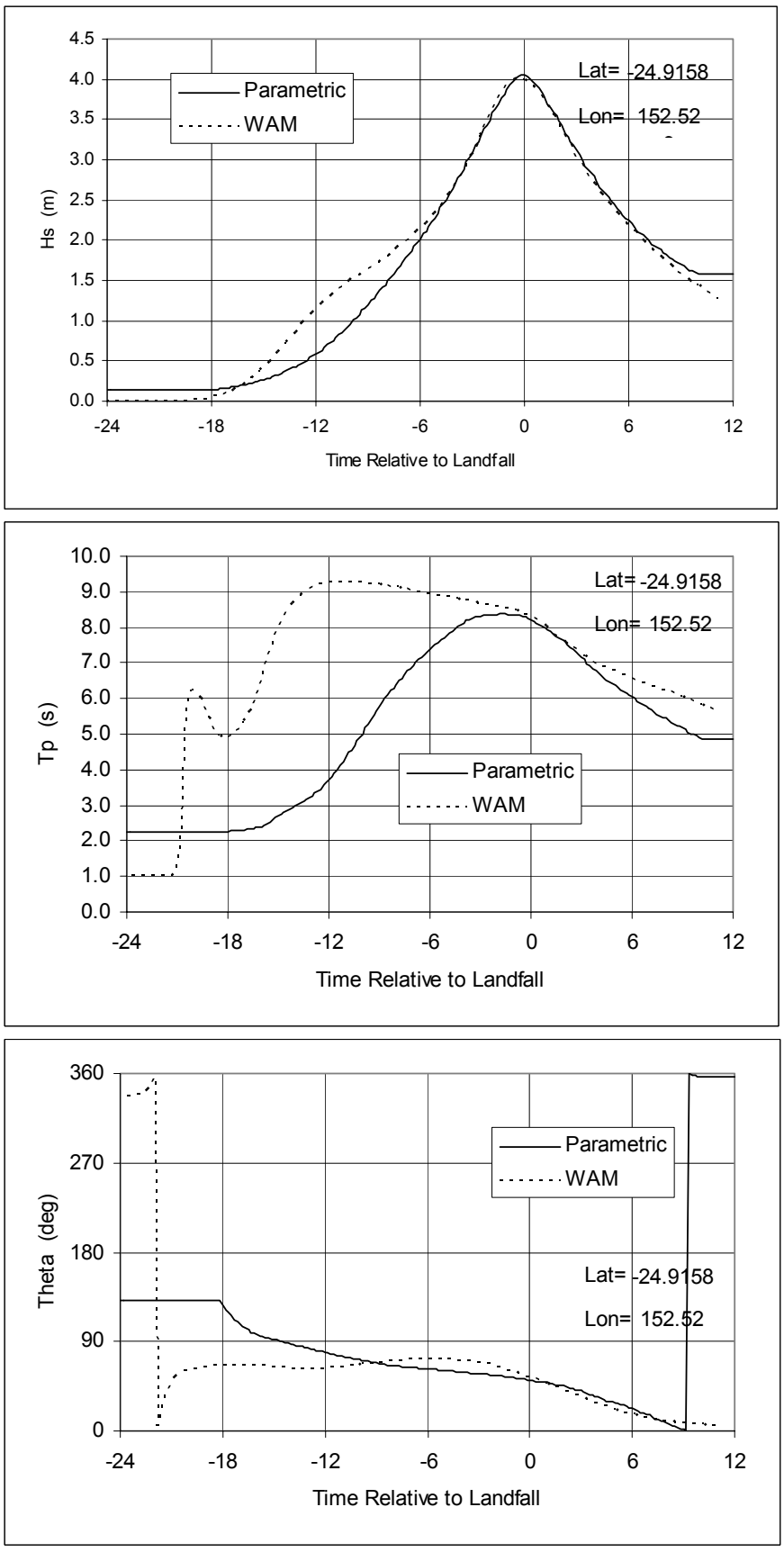

Figure 4.8 Parametric model result for *B* grid Site #35 (100 km, 225°, 23 hPa)

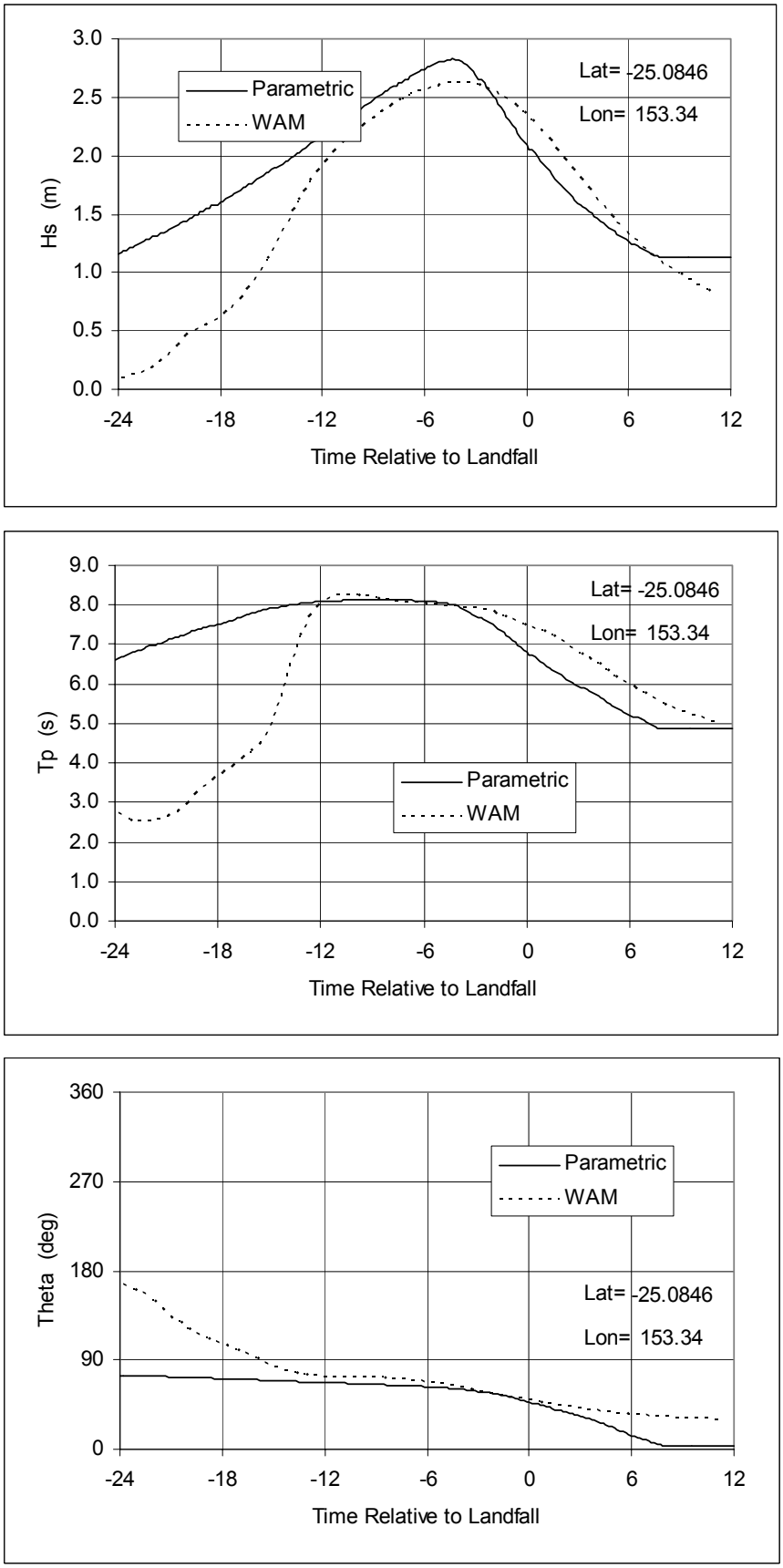

Figure 4.9 Parametric model result for *B* grid Site #44 (100 km, 225°, 23 hPa)

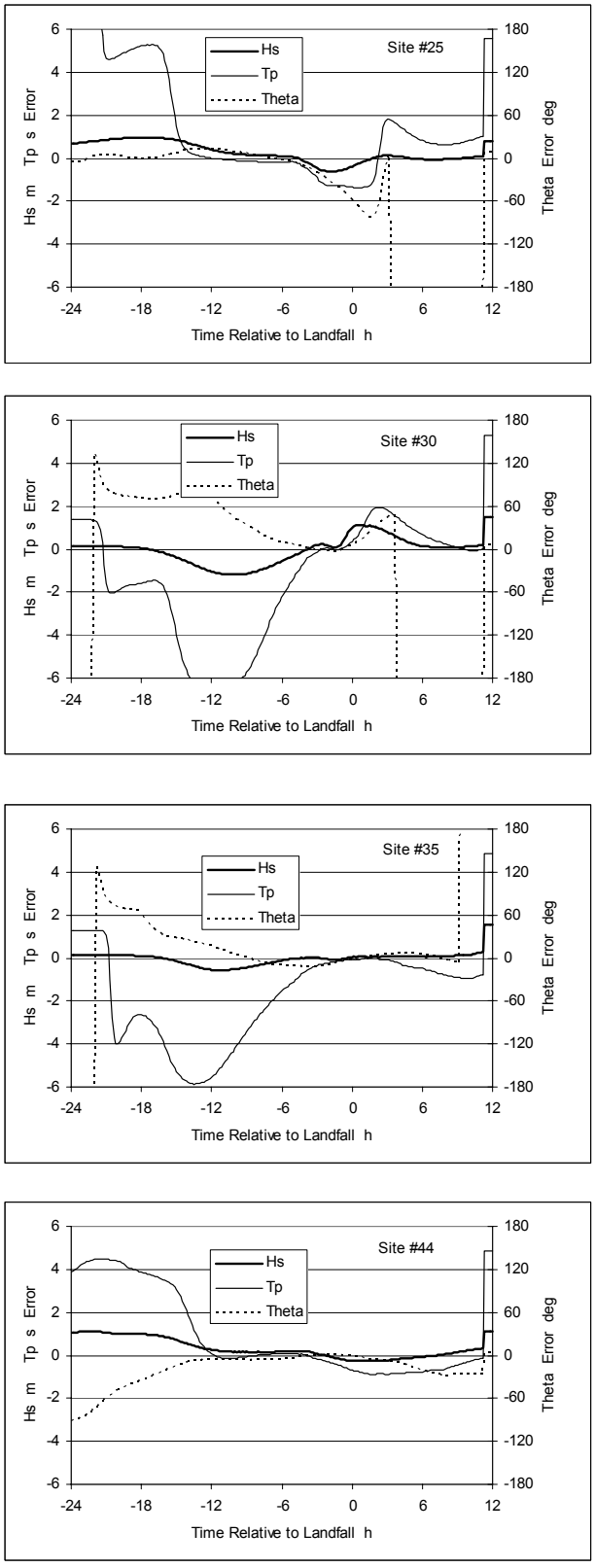

Figure 4.10 Parametric model errors for selected *B* grid Sites (100 km, 225°, 23 hPa)

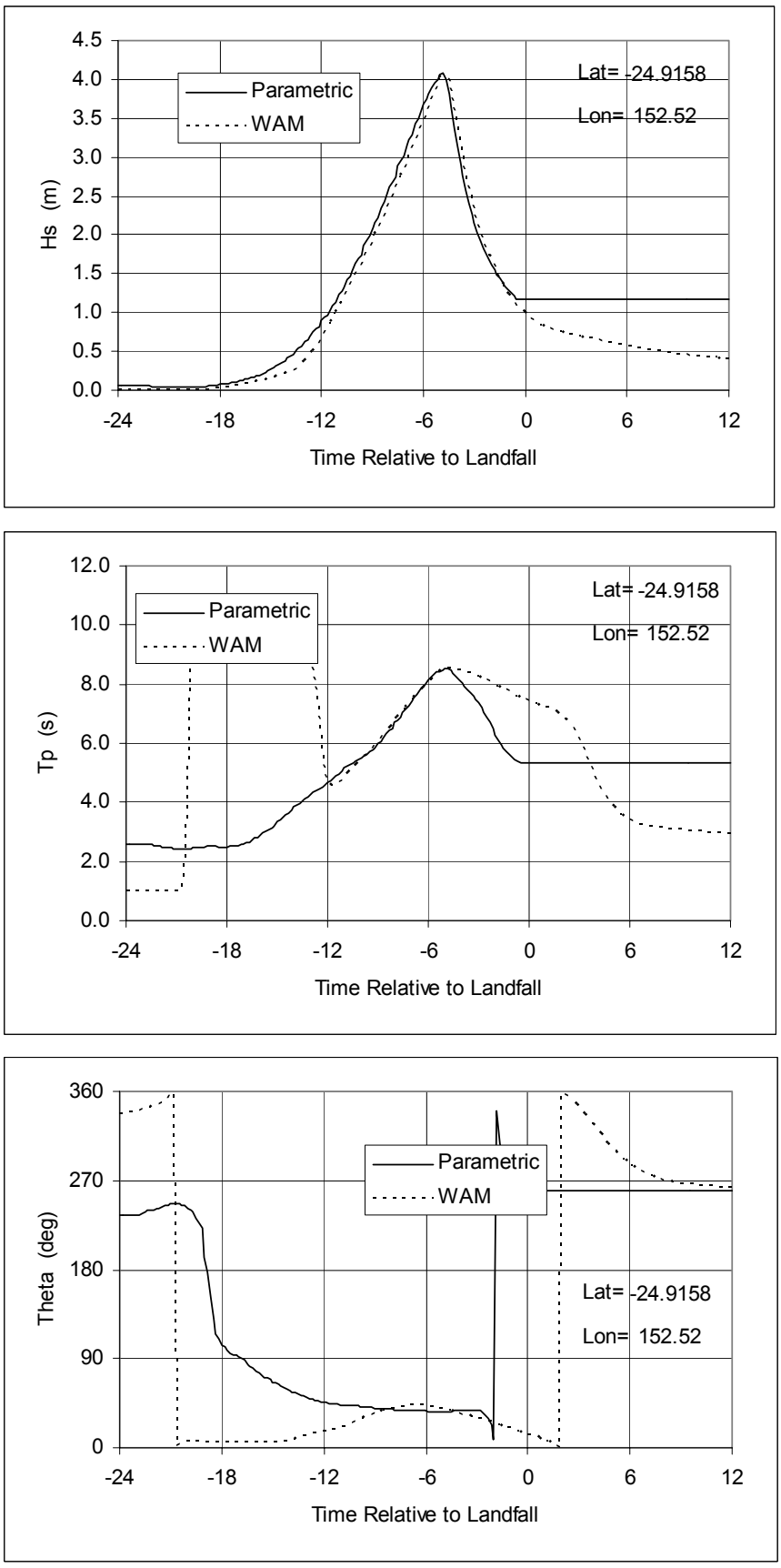

Figure 4.11 Parametric model result for *B* grid Site #35 (100 km, 140°, 23 hPa)

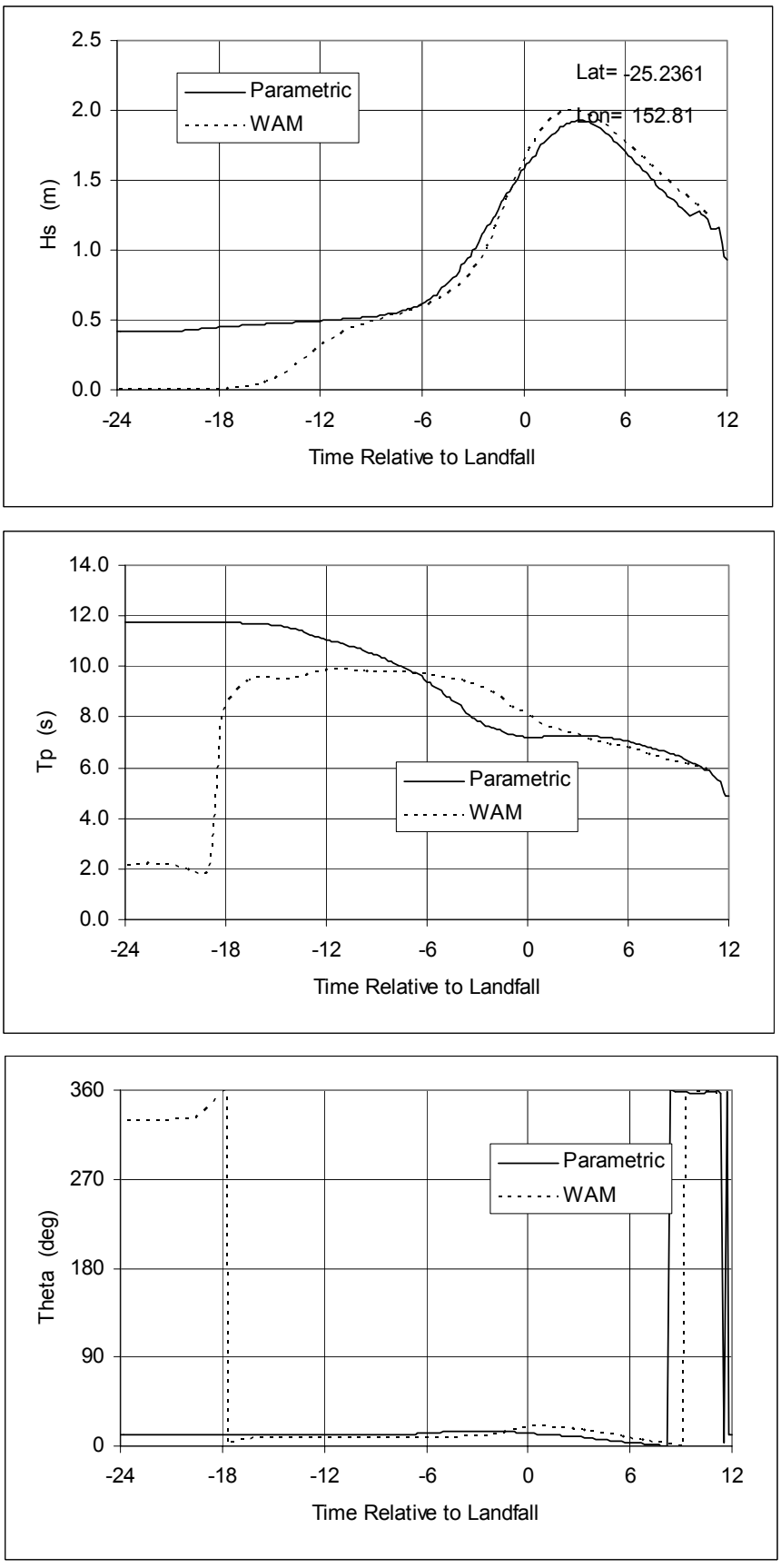

Figure 4.12 Parametric model result for *C* grid Site #15 (100 km, 225°, 23 hPa)

5 Conclusions

The tropical cyclone parametric wave model developed here appears sufficiently accurate to be used for both forecasting and planning purposes within the Hervey Bay region. It requires a data set less than 150KB in size and executable code of about twice that size. Execution time on a Pentium 4 1.9GHz in Windows XP is near-instantaneous.

The adopted parameterisation is similar to that proposed for BoM(2001) storm surge modelling but differs in aspects relating to the incorporation of V_{fm} and R effects.

The model accuracy can be improved by the addition of more track angles, R or B_0 values to either increase the resolution or to extend the range of coverage. There are also opportunities to improve the time history accuracy of T_p and possibly wave direction by further model enhancements.

6 References

BoM, 2001: MMUSURGE Modelling System – Operational Manual. Prepared by Systems Engineering Australia Pty Ltd for the Queensland Regional Office of the Bureau of Meteorology, Brisbane, Dec, SEA Doc J0103-PR001A.

Hardy, T.A., McConochie, J. and Mason, L.B., 2001: A wave model for the Great Barrier Reef. *Ocean Engineering* 28 (1), 45-70.

Harper B.A. (ed), 2001: Queensland Climate Change and Community Vulnerability to Tropical Cyclones: Stage 1 - Ocean Hazards, Queensland Government, March, 400pp.

Holland, G.J., 1980: An analytic model of the wind and pressure profiles in hurricanes. *Mon. Wea. Rev.,* 108, 1212-1218.

JCU, 2002: Queensland Climate Change and Community Vulnerability to Tropical Cyclones: Ocean Hazards Assessment – Stage 2. Hervey Bay and Gold Coast. Prepared by the Marine Modelling Unit, School of Engineering, James Cook University, for the Bureau of Meteorology, Qld.